

# Global warming in the pipeline

James E. Hansen,<sup>1</sup> Makiko Sato,<sup>1</sup> Leon Simons,<sup>2</sup> Larissa S. Nazarenko,<sup>3, 4</sup> Isabelle Sangha,<sup>1</sup> Karina von Schuckmann,<sup>5</sup> Norman G. Loeb,<sup>6</sup> Matthew B. Osman,<sup>7</sup> Qinjian Jin,<sup>8</sup> Pushker Kharecha,<sup>1</sup> George Tselioudis,<sup>3</sup> Eunbi Jeong,<sup>9</sup> Andrew Lacis,<sup>3</sup> Reto Ruedy,<sup>3,10</sup> Gary Russell,<sup>3</sup> Junji Cao,<sup>11</sup> Jing Li<sup>12</sup>

\*Correspondence: James E. Hansen <jeh1@columbia.edu>

---

## ABSTRACT

Improved knowledge of glacial-to-interglacial global temperature change implies that fast-feedback equilibrium climate sensitivity (ECS) is  $1.2 \pm 0.3^\circ\text{C}$  ( $2\sigma$ ) per  $\text{W}/\text{m}^2$ , which is  $4.8^\circ\text{C} \pm 1.2^\circ\text{C}$  for doubled  $\text{CO}_2$ . Consistent analysis of temperature over the full Cenozoic era – including “slow” feedbacks by ice sheets and trace gases – supports this ECS and implies that  $\text{CO}_2$  was 300-350 ppm in the Pliocene and about 450 ppm at transition to a nearly ice-free planet, thus exposing unrealistic lethargy of ice sheet models. Equilibrium global warming including slow feedbacks for today’s human-made greenhouse gas (GHG) climate forcing ( $4.1 \text{ W}/\text{m}^2$ ) is  $10^\circ\text{C}$ , reduced to  $8^\circ\text{C}$  by today’s aerosols. Decline of aerosol emissions since 2010 should increase the 1970-2010 global warming rate of  $0.18^\circ\text{C}$  per decade to a post-2010 rate of at least  $0.27^\circ\text{C}$  per decade. Under the current geopolitical approach to GHG emissions, global warming will likely pierce the  $1.5^\circ\text{C}$  ceiling in the 2020s and  $2^\circ\text{C}$  before 2050. Impacts on people and nature will accelerate as global warming pumps up hydrologic extremes. The enormity of consequences demands a return to Holocene-level global temperature. Required actions include: 1) a global increasing price on GHG emissions, 2) East-West cooperation in a way that accommodates developing world needs, and 3) intervention with Earth’s radiation imbalance to phase down today’s massive human-made “geo-transformation” of Earth’s climate. These changes will not happen with the current geopolitical approach, but current political crises present an opportunity for reset, especially if young people can grasp their situation.

---

<sup>1</sup> Climate Science, Awareness and Solutions, Columbia University Earth Institute, New York, NY, USA

<sup>2</sup> The Club of Rome Netherlands, ‘s-Hertogenbosch, The Netherlands

<sup>3</sup> NASA Goddard Institute for Space Studies, New York, NY, USA

<sup>4</sup> Center for Climate Systems Research, Columbia University Earth Institute, New York, NY, USA

<sup>5</sup> Mercator Ocean International, Ramonville St.-Agne, France

<sup>6</sup> NASA Langley Research Center, Hampton, VA, USA

<sup>7</sup> Department of Geosciences, University of Arizona, Tucson, AZ, USA

<sup>8</sup> Department of Geography and Atmospheric Science, University of Kansas, Lawrence, KS, USA

<sup>9</sup> CSAS KOREA, Goyang, Gyeonggi-do, South Korea

<sup>10</sup> Business Integra, Inc., New York, NY, USA

<sup>11</sup> Institute of Atmospheric Physics, Chinese Academy of Sciences, Beijing, China

<sup>12</sup> Department of Atmospheric and Oceanic Sciences, School of Physics, Peking University, Beijing, China

## 28 **1. BACKGROUND INFORMATION AND STRUCTURE OF PAPER**

29 It has been known since the 1800s that infrared-absorbing (greenhouse) gases (GHGs) warm  
30 Earth's surface and that the abundance of GHGs changes naturally as well as from human  
31 actions.<sup>1,2</sup> Roger Revelle wrote in 1965 that we are conducting a “vast geophysical experiment”  
32 by burning fossil fuels that accumulated in Earth's crust over hundreds of millions of years.<sup>3</sup>  
33 Carbon dioxide (CO<sub>2</sub>) in the air is now increasing and already has reached levels that have not  
34 existed for millions of years, with consequences that have yet to be determined. Jule Charney led  
35 a study in 1979 by the United States National Academy of Sciences that concluded that doubling  
36 of atmospheric CO<sub>2</sub> was likely to cause global warming of  $3 \pm 1.5^\circ\text{C}$ .<sup>4</sup> Charney added:  
37 “However, we believe it is quite possible that the capacity of the intermediate waters of the  
38 ocean to absorb heat could delay the estimated warming by several decades.”

39 After U.S. President Jimmy Carter signed the 1980 Energy Security Act, which included a focus  
40 on unconventional fossil fuels such as coal gasification and rock fracturing (“fracking”) to  
41 extract shale oil and tight gas, the U.S. Congress asked the National Academy of Sciences again  
42 to assess potential climate effects. Their massive *Changing Climate* report had a measured tone  
43 on energy policy – amounting to a call for research.<sup>5</sup> Was not enough known to caution  
44 lawmakers against taxpayer subsidy of the most carbon-intensive fossil fuels? Perhaps the  
45 equanimity was due in part to a major error: the report assumed that the delay of global warming  
46 caused by the ocean's thermal inertia is 15 years, independent of climate sensitivity. With that  
47 assumption, they concluded that climate sensitivity for  $2\times\text{CO}_2$  is near or below the low end of  
48 Charney's 1.5-4.5°C range. If climate sensitivity was low and the lag between emissions and  
49 climate response was only 15 years, climate change would not be nearly the threat that it is.

50 Simultaneous with preparation of *Changing Climate*, climate sensitivity was addressed at the  
51 1982 Ewing Symposium at the Lamont Doherty Geophysical Observatory of Columbia  
52 University on 25-27 October, with papers published in January 1984 as a monograph of the  
53 American Geophysical Union.<sup>6</sup> Paleoclimate data and global climate modeling together led to an  
54 inference that climate sensitivity is in the range 2.5-5°C for  $2\times\text{CO}_2$  and that climate response  
55 time to a forcing is of the order of a century, not 15 years.<sup>7</sup> Thus, the concept that a large amount  
56 of additional human-made warming is already “in the pipeline” was introduced. E.E. David, Jr.,  
57 President of Exxon Research and Engineering, in his keynote talk at the symposium insightfully  
58 noted<sup>8</sup>: “The critical problem is that the environmental impacts of the CO<sub>2</sub> buildup may be so  
59 long delayed. A look at the theory of feedback systems shows that where there is such a long  
60 delay, the system breaks down, unless there is anticipation built into the loop.”

61 Thus, the danger caused by climate's delayed response and the need for anticipatory action to  
62 alter the course of fossil fuel development was apparent to scientists and the fossil fuel industry  
63 40 years ago.<sup>9</sup> Yet industry chose to long deny the need to change energy course,<sup>10</sup> and now,  
64 while governments and financial interests connive, most industry adopts a “greenwash” approach  
65 that threatens to lock in perilous consequences for humanity. Scientists will share responsibility,  
66 if we allow governments to rely on goals for future global GHG levels, as if targets had meaning  
67 in the absence of policies required to achieve them.

68 The Intergovernmental Panel on Climate Change (IPCC) was established in 1988 to provide  
69 scientific assessments on the state of knowledge about climate change<sup>11</sup> and almost all nations  
70 agreed to the 1992 United Nations Framework Convention on Climate Change<sup>12</sup> with the  
71 objective to avert “dangerous anthropogenic interference with the climate system.” The current  
72 IPCC Working Group 1 report<sup>13</sup> provides a best estimate of 3°C for equilibrium global climate  
73 sensitivity to 2×CO<sub>2</sub> and describes shutdown of the overturning ocean circulations and large sea  
74 level rise on the century time scale as “high impact, low probability” even under extreme GHG  
75 growth scenarios. This contrasts with “high impact, high probability” assessments reached in a  
76 paper<sup>14</sup> – hereafter abbreviated *Ice Melt* – that several of us published in 2016. Recently, our  
77 paper’s first author (JEH) described a long-time effort to understand the effect of ocean mixing  
78 and aerosols on observed and projected climate change, which led to a conclusion that most  
79 climate models are unrealistically insensitive to freshwater injected by melting ice and that ice  
80 sheet models are unrealistically lethargic in the face of rapid, large climate change.<sup>15</sup>

81 Eelco Rohling, editor of Oxford Open Climate Change, invited a perspective article on these  
82 issues. Our principal motivation in this paper is concern that IPCC has underestimated climate  
83 sensitivity and understated the threat of large sea level rise and shutdown of ocean overturning  
84 circulations, but these issues, because of their complexity, must be addressed in two steps. Our  
85 present paper addresses climate sensitivity and warming in the pipeline, concluding that these  
86 exceed IPCC’s best estimates. Response of ocean circulation and ice sheet dynamics to global  
87 warming– already outlined in the *Ice Melt* paper – will be addressed further in a later paper.<sup>16</sup>

88 The structure of our present paper is as follows. Section 2 (Climate Sensitivity) makes a fresh  
89 evaluation of Charney’s equilibrium climate sensitivity (ECS) based on improved paleoclimate  
90 data and introduces Earth system sensitivity (ESS), which includes the feedbacks that Charney  
91 held fixed. Section 3 (Climate Response Time) explores the fast-feedback response time of  
92 Earth’s temperature and energy imbalance to an imposed forcing, concluding that cloud  
93 feedbacks buffer heat uptake by the ocean, thus increasing the delay in surface warming and  
94 making Earth’s energy imbalance an underestimate of the forcing reduction required to stabilize  
95 climate. Section 4 (Cenozoic Era) analyzes temperature change of the past 66 million years,  
96 tightens evaluation of climate sensitivity, and assesses the history of CO<sub>2</sub>, thus providing insights  
97 about climate change. Section 5 (Aerosols) addresses the absence of aerosol forcing data via  
98 inferences from paleo data and modern global temperature change, and we point out potential  
99 information in “the great inadvertent aerosol experiment” provided by recent restrictions on fuels  
100 in international shipping. Section 6 (Summary) discusses policy implications of high climate  
101 sensitivity and the delayed response of the climate system. Warming in the pipeline need not  
102 appear. We can take actions that slow and reverse global warming; indeed, we suggest that such  
103 actions are needed to avoid disastrous consequences for humanity and nature. Reduction of  
104 greenhouse gas emissions as rapidly as practical has highest priority, but that policy alone is now  
105 inadequate and must be complemented by additional actions to affect Earth’s energy balance.  
106 The world is still early in this “vast geophysical experiment” – as far as consequences are  
107 concerned – but time has run short for the “anticipation” that E.E. David recommended.

## 108 2. CLIMATE SENSITIVITY (ECS AND ESS)

109 This section gives a brief overview of the history of ECS estimates since the Charney report and  
110 uses glacial-to-interglacial climate change to infer an improved estimate of ECS. We discuss  
111 how ECS and the more general Earth system sensitivity (ESS) depend upon the climate state.

112 Charney defined ECS as the eventual global temperature change caused by doubled CO<sub>2</sub> if ice  
113 sheets, vegetation and long-lived GHGs are fixed (except the specified CO<sub>2</sub> doubling). Other  
114 quantities affecting Earth's energy balance – clouds, aerosols, water vapor, snow cover and sea  
115 ice – change rapidly in response to climate change. Thus, Charney's ECS is also called the “fast  
116 feedback” climate sensitivity. Feedbacks interact in many ways, so their changes are calculated  
117 in global climate models (GCMs) that simulate such interactions. Charney implicitly assumed  
118 that change of the ice sheets on Greenland and Antarctica – which we categorize as a “slow  
119 feedback” – was not important on time scales of most public interest.

120 ECS defined by Charney is a gedanken concept that helps us study the effect of human-made and  
121 natural climate forcings. If knowledge of ECS were based only on models, it would be difficult  
122 to narrow the range of estimated climate sensitivity – or have confidence in any range – because  
123 we do not know how well feedbacks are modeled or if the models include all significant real-  
124 world feedbacks. Cloud and aerosol interactions are complex, e.g., and even small cloud changes  
125 can have a large effect. Thus, data on Earth's paleoclimate history are essential, allowing us to  
126 compare different climate states, knowing that all feedbacks operated.

### 127 2.1. Climate sensitivity estimated at the 1982 Ewing Symposium

128 Climate sensitivity was addressed in our paper<sup>7</sup> for the Ewing Symposium monograph using the  
129 feedback framework implied by E.E. David and employed by electrical engineers.<sup>17</sup> The climate  
130 forcing caused by 2×CO<sub>2</sub> – the imposed perturbation of Earth's energy balance – is ~ 4 W/m<sup>2</sup>. If  
131 there were no climate feedbacks and Earth radiated energy to space as a perfect black surface,  
132 Earth's temperature would need to increase ~ 1.2°C to increase radiation to space 4 W/m<sup>2</sup> and  
133 restore energy balance. However, feedbacks occur in the real world and in GCMs. In our GCM  
134 the equilibrium response to 2×CO<sub>2</sub> was 4°C warming of Earth's surface. Thus, the fraction of  
135 equilibrium warming due directly to the CO<sub>2</sub> change was 0.3 (1.2°C/4°C) and the feedback  
136 “gain,” g, was 0.7 (2.8°C/4°C). Algebraically, ECS and feedback gain are related by

$$137 \text{ECS} = 1.2^\circ\text{C}/(1-g). \quad (1)$$

138 We evaluated contributions of individual feedback processes to g by inserting changes of water  
139 vapor, clouds, and surface albedo (reflectivity, literally whiteness, due to sea ice and snow  
140 changes) from the 2×CO<sub>2</sub> GCM simulation one-by-one into a one-dimensional radiative-  
141 convective model,<sup>18</sup> finding g<sub>wv</sub> = 0.4, g<sub>cl</sub> = 0.2, g<sub>sa</sub> = 0.1, where g<sub>wv</sub>, g<sub>cl</sub>, and g<sub>sa</sub> are the water  
142 vapor, cloud and surface albedo gains. The 0.2 cloud gain was about equally from a small  
143 increase in cloud top height and a small decrease in cloud cover. These feedbacks all seemed  
144 reasonable, but how could we verify their magnitudes or the net ECS due to all feedbacks?

145 We recognized the potential of emerging paleoclimate data. Early data from polar ice cores  
146 revealed that atmospheric CO<sub>2</sub> was much less during glacial periods and the CLIMAP project<sup>19</sup>

147 used proxy data to reconstruct global surface conditions during the Last Glacial Maximum  
148 (LGM), which peaked about 20,000 years ago. A powerful constraint was the fact that Earth had  
149 to be in energy balance averaged over the several millennia of the LGM. However, when we  
150 employed CLIMAP boundary conditions including sea surface temperatures (SSTs), Earth was  
151 out of energy balance, radiating  $2.1 \text{ W/m}^2$  to space., i.e., Earth was trying to cool off with an  
152 enormous energy imbalance, equivalent to half of  $2\times\text{CO}_2$  forcing.

153 Something was wrong with either assumed LGM conditions or our climate model. We tried  
154 CLIMAP's maximal land ice – this only reduced the energy imbalance from  $2.1$  to  $1.6 \text{ W/m}^2$ .  
155 Moreover, we had taken LGM  $\text{CO}_2$  as 200 ppm and did not know that  $\text{CH}_4$  and  $\text{N}_2\text{O}$  were less in  
156 the LGM than in the present interglacial period; accurate GHGs and CLIMAP SSTs produce a  
157 planetary energy imbalance close to  $3 \text{ W/m}^2$ . Most feedbacks in our model were set by CLIMAP.  
158 Sea ice is set by CLIMAP. Water vapor depends on surface temperature, which is set by  
159 CLIMAP SSTs. Cloud feedback is uncertain, but ECS smaller than  $2.4^\circ\text{C}$  for  $2\times\text{CO}_2$  would  
160 require a negative cloud gain.  $g_{\text{cl}} \sim 0.2$  from our GCM increases ECS from  $2.4^\circ\text{C}$  to  $4^\circ\text{C}$  (eq. 1)  
161 and accounts for almost the entire difference of sensitivities of our model ( $4^\circ\text{C}$  for  $2\times\text{CO}_2$ ) and  
162 the Manabe and Stouffer model<sup>20</sup> ( $2^\circ\text{C}$  for  $2\times\text{CO}_2$ ) that had fixed cloud cover and cloud height.  
163 Manabe suggested<sup>21</sup> that our higher ECS was due to a too-large sea ice and snow feedback, but  
164 we noted<sup>7</sup> that sea ice in our control run was less than observed, so we likely understated sea ice  
165 feedback. Amplifying feedback due to high clouds increasing in height with warming is expected  
166 and is found in observations, large-eddy simulations and GCMs.<sup>22</sup> Sherwood *et al.*<sup>23</sup> conclude  
167 that negative low-cloud feedback is “neither credibly suggested by any model, nor by physical  
168 principles, nor by observations.” Despite a wide spread among models, GCMs today show an  
169 amplifying cloud feedback due to increases in cloud height and decreases in cloud amount,  
170 despite increases in cloud albedo.<sup>24</sup> These cloud changes are found in all observed cloud regimes  
171 and locations, implying robust thermodynamic control.<sup>25</sup>

172 CLIMAP SSTs were a more likely cause of the planetary energy imbalance. Co-author D. Peteet  
173 used pollen data to infer LGM tropical and subtropical cooling  $2\text{-}3^\circ\text{C}$  greater than in a GCM  
174 forced by CLIMAP SSTs. D. Rind and Peteet found that montane LGM snowlines in the tropics  
175 descended 1 km in the LGM, inconsistent with climate constrained by CLIMAP SSTs. CLIMAP  
176 assumed that tiny shelled marine species migrate to stay in a temperature zone they inhabit  
177 today. But what if these species partly adapt over millennia to changing temperature? Based on  
178 the work of Rind and Peteet, later published,<sup>26</sup> we suspected but could not prove that CLIMAP  
179 SSTs were too warm.

180 Based on GCM simulations for  $2\times\text{CO}_2$ , on our feedback analysis for the LGM, and on observed  
181 global warming in the past century, we estimated that ECS was in the range  $2.5\text{-}5^\circ\text{C}$  for  $2\times\text{CO}_2$ .  
182 If CLIMAP SSTs were accurate, ECS was near the low end of that range. In contrast, our  
183 analysis implied that ECS for  $2\times\text{CO}_2$  was in the upper half of the  $2.5\text{-}5^\circ\text{C}$  range, but our analysis  
184 depended in part on our GCM, which had sensitivity  $4^\circ\text{C}$  for  $2\times\text{CO}_2$ . To resolve the matter, a  
185 paleo thermometer independent of biologic adaptation was needed. Several decades later, such a  
186 paleo thermometer and advanced analysis techniques exist. We will use recent studies to infer  
187 our present best estimates for ECS and ESS. First, however, we will comment on other estimates  
188 of climate sensitivity and clarify the definition of climate forcings that we employ.

## 189 2.2. IPCC and independent climate sensitivity estimates

190 Reviews of climate sensitivity are available, e.g., Rohling *et al.*,<sup>27</sup> which focuses on the physics  
191 of the climate system, and Sherwood *et al.*,<sup>23</sup> which adds emphasis on probabilistic combination  
192 of multiple uncertainties. Progress in narrowing the uncertainty in climate sensitivity was slow in  
193 the first five IPCC assessment reports. The fifth assessment report<sup>28</sup> (AR5) in 2014 concluded  
194 only – with 66% probability – that ECS was in the range 1.5-4.5°C, the same as Charney’s report  
195 35 years earlier. The broad spectrum of information on climate change – especially constraints  
196 imposed by paleoclimate data – at last affected AR6,<sup>13</sup> which concluded with 66% probability  
197 that ECS is 2.5-4°C, with 3°C as their best estimate (AR6 Fig. TS.6).

198 Sherwood *et al.*<sup>23</sup> combine three lines of evidence: climate feedback studies, historical climate  
199 change, and paleoclimate data, inferring  $S = 2.6-3.9^\circ\text{C}$  with 66% probability for  $2\times\text{CO}_2$ , where  $S$   
200 is an “effective sensitivity” relevant to a 150-year time scale. They find ECS only slightly larger:  
201 2.6-4.1°C with 66% probability. Climate feedback studies, inherently, cannot yield a sharp  
202 definition of ECS, as we showed in the cloud feedback discussion above. Earth’s climate system  
203 includes amplifying feedbacks that push the gain,  $g$ , closer to unity than zero, thus making ECS  
204 sensitive to uncertainty in any feedback; the resulting sensitivity of ECS to  $g$  prohibits precise  
205 evaluation from feedback analysis. Similarly, historical climate change cannot define ECS well  
206 because the aerosol climate forcing is unmeasured. Also, forced and unforced ocean dynamics  
207 give rise to a pattern effect:<sup>29</sup> the geographic pattern of transient and equilibrium temperature  
208 changes differ, which affects ECS inferred from transient climate change. These difficulties help  
209 explain how Sherwood *et al.*<sup>23</sup> could estimate ECS as only 6% larger than  $S$ , an implausible  
210 result in view of the ocean’s great thermal inertia. An intercomparison of GCMs run for  
211 millennial time scales, LongRunMIP,<sup>30</sup> includes 14 simulations of 9 GCMs with runs of 5,000  
212 years (or close enough for extrapolation to 5,000 years). Their global warmings at 5,000 years  
213 range from 30% to 80% larger than their 150-year responses.

214 Our approach is to compare glacial and interglacial equilibrium climate states. The change of  
215 atmospheric and surface forcings can be defined accurately, thus leading to a sharp evaluation of  
216 ECS for cases in which equilibrium response is assured. With this knowledge in hand, additional  
217 information can be extracted from historical and paleo climate changes.

## 218 2.3. Climate forcing definitions

219 Attention to climate forcing definitions is essential for quantitative analysis of climate change.  
220 However, readers uninterested in radiative forcings may skip this section with little penalty. We  
221 describe our climate forcing definition and compare our forcings with those of IPCC. Our total  
222 GHG forcing matches that of IPCC within a few percent, but this close fit hides larger  
223 differences in individual forcings that deserve attention.

224 Equilibrium global surface temperature change is related to ECS by

$$225 \Delta T_s \sim F \times \text{ECS} = F \times \lambda, \quad (2)$$

226 where  $\lambda$  is a widely used abbreviation of ECS,  $\Delta T_s$  is the global mean equilibrium surface  
227 temperature change in response to climate forcing  $F$ , which is measured in  $\text{W}/\text{m}^2$  averaged over  
228 the entire planetary surface. There are alternative ways to define  $F$ , as discussed in Chapter 8<sup>31</sup> of

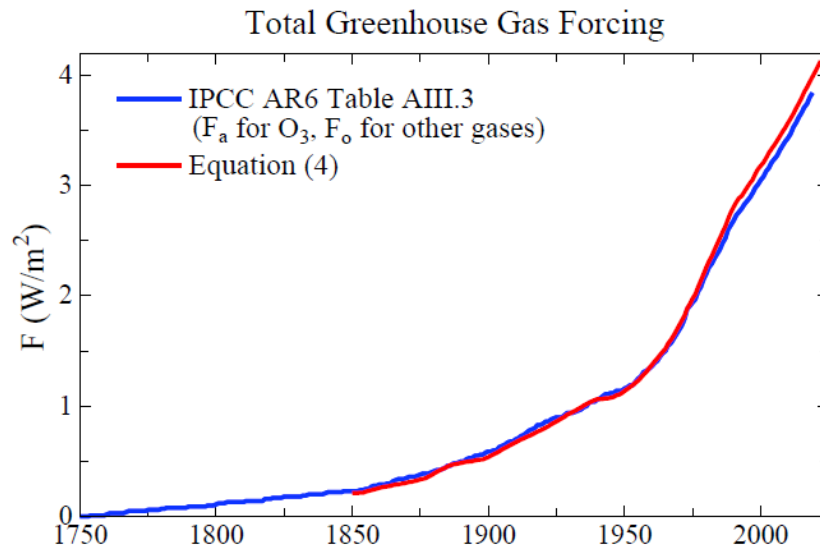
229 AR5 and in a paper<sup>32</sup> hereafter called *Efficacy*. Objectives are to find a definition of F such that  
230 different forcing mechanisms of the same magnitude yield a similar global temperature change,  
231 but also a definition that can be computed easily and reliably. The first four IPCC reports used  
232 adjusted forcing,  $F_a$ , which is Earth’s energy imbalance after stratospheric temperature adjusts to  
233 presence of the forcing agent.  $F_a$  usually yields a consistent response among different forcing  
234 agents, but there are exceptions such as black carbon aerosols;  $F_a$  exaggerates their impact. Also,  
235  $F_a$  is awkward to compute and depends on definition of the tropopause, which varies among  
236 models.  $F_s$ , the fixed SST forcing (including fixed sea ice), is more robust than  $F_a$  as a predictor  
237 of climate response,<sup>32,33</sup> but a GCM is required to compute  $F_s$ . In *Efficacy*,  $F_s$  is defined as

$$238 \quad F_s = F_o + \delta T_o / \lambda \quad (3)$$

239 where  $F_o$  is Earth’s energy imbalance after atmosphere and land surface adjust to the presence of  
240 the forcing agent with SST fixed.  $F_o$  is not a full measure of the strength of a forcing, because a  
241 portion ( $\delta T_o$ ) of the equilibrium warming is already present as  $F_o$  is computed. A GCM run of  
242 about 100 years is needed to accurately define  $F_o$  because of unforced atmospheric variability.  
243 That GCM run also defines  $\delta T_o$ , the global mean surface air temperature change caused by the  
244 forcing with SST fixed.  $\lambda$  is the model’s ECS in °C per W/m<sup>2</sup>.  $\delta T_o / \lambda$  is the portion of the total  
245 forcing ( $F_s$ ) that is “used up” in causing the  $\delta T_o$  warming; radiative flux to space increases by  
246  $\delta T_o / \lambda$  due to warming of the land surface and global air. The term  $\delta T_o / \lambda$  is usually, but not  
247 always, less than 10% of  $F_o$ . Thus, it is better not to neglect  $\delta T_o / \lambda$ . IPCC AR5 and AR6 define  
248 effective radiative forcing as ERF =  $F_o$ . Omission of  $\delta T_o / \lambda$  was intentional<sup>31</sup> and is not an issue if  
249 the practice is followed consistently. However, when the forcing is used to calculate global  
250 surface temperature response, the forcing to use is  $F_s$ , not  $F_o$ . It would be useful if both  $F_o$  and  
251  $\delta T_o$  were reported for all climate models.

252 A further refinement of climate forcing is suggested in *Efficacy*: effective forcing ( $F_e$ ) defined by  
253 a long GCM run with calculated ocean temperature. The resulting global surface temperature  
254 change, relative to that for equal CO<sub>2</sub> forcing, defines the forcing’s efficacy. Effective forcings,  
255  $F_e$ , were found to be within a few percent of  $F_s$  for most forcing agents, i.e., the results confirm  
256 that  $F_s$  is a robust forcing. This support is for  $F_s$ , not for  $F_o = \text{ERF}$ , which is systematically  
257 smaller than  $F_s$ . The Goddard Institute for Space Studies (GISS) GCM<sup>34,35</sup> used for CMIP6<sup>36</sup>  
258 studies, which we label the GISS (2020) model,<sup>37</sup> has higher resolution (2°×2.5° and 40  
259 atmospheric layers) and other changes that yield a moister upper troposphere and lower  
260 stratosphere, relative to the GISS model used in *Efficacy*. GHG forcings reported for the GISS  
261 (2020) model<sup>34,35</sup> are smaller than in prior GISS models, a change attributed<sup>35</sup> to blanketing by  
262 high level water vapor. However, part of the change is from comparison of  $F_o$  in GISS (2020) to  
263  $F_s$  in earlier models. The 2×CO<sub>2</sub> fixed SST simulation with the GISS (2020) model yields  $F_o =$   
264  $3.59 \text{ W/m}^2$ ,  $\delta T_o = 0.27^\circ\text{C}$  and  $\lambda = 0.9 \text{ }^\circ\text{C per W/m}^2$ . Thus  $F_s = 3.59 + 0.30 = 3.89 \text{ W/m}^2$ , which is  
265 only 5.4% smaller than the  $F_s = 4.11 \text{ W/m}^2$  for the GISS model used in *Efficacy*.

266 Our GHG effective forcing,  $F_e$ , was obtained in two steps. Adjusted forcings,  $F_a$ , were calculated  
267 for each gas for a large range of gas amount with a global-mean radiative-convective model that  
268 incorporated the GISS GCM radiation code, which uses the correlated k-distribution method<sup>38</sup>  
269 and high spectral resolution laboratory data.<sup>39</sup> The  $F_a$  are converted to effective forcings ( $F_e$ ) via  
270 efficacy factors ( $E_a$ ; Table 1 of *Efficacy*) based on GCM simulations that include the 3-D  
271 distribution of each gas. The total GHG forcing is



272  
273 Fig. 1. IPCC AR6 Annex III greenhouse gas forcing,<sup>13</sup> which employs  $F_a$  for  $O_3$  and  $F_o$  for other  
274 GHGs, compared with the effective forcing,  $F_e$ , from Eq. (4). See discussion in text.

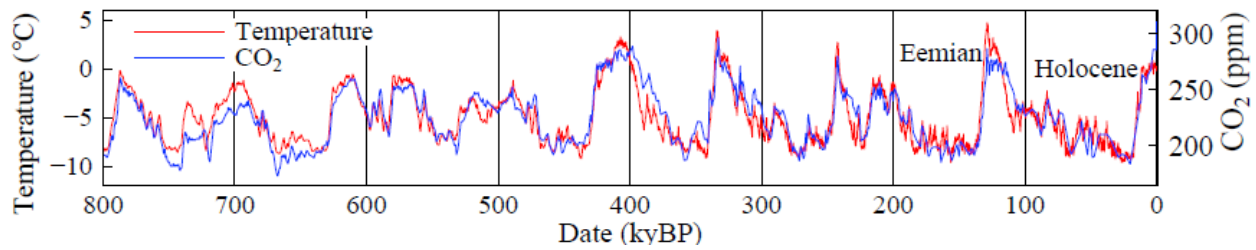
275 
$$F_e = F_a(CO_2) + 1.45 F_a(CH_4) + 1.04 F_a(N_2O) + 1.32 F_a(MPTGs + OTGs) + 0.45 F_a(O_3). \quad (4)$$

276 The  $CH_4$  coefficient (1.45) includes the effect of  $CH_4$  on  $O_3$  and stratospheric  $H_2O$ , as well as the  
277 efficacy (1.10) of  $CH_4$  per se. We assume that  $CH_4$  is responsible for 45% of the  $O_3$  change.<sup>40</sup>  
278 Forcing caused by the remaining 55% of the  $O_3$  change is based on IPCC AR6  $O_3$  forcing ( $F_a =$   
279  $0.47 W/m^2$  in 2019); we multiply this AR6  $O_3$  forcing by  $0.55 \times 0.82 = 0.45$ , where 0.82 is the  
280 efficacy of  $O_3$  forcing from Table 1 of *Efficacy*. Thus, the non- $CH_4$  portion of the  $O_3$  forcing is  
281  $0.21 W/m^2$  in 2019. MPTGs and OTGs are Montreal Protocol Trace Gases and Other Trace  
282 Gases.<sup>41</sup> A list of these gases and a table of annual forcings since 1992 are [available](#) as well as  
283 the [earlier data](#).<sup>42</sup>

284 The climate forcing from our formulae is slightly larger than IPCC AR6 forcings (Fig. 1). In  
285 2019, the final year of AR6 data, our GHG forcing is  $4.00 W/m^2$ ; the AR6 forcing is  $3.84 W/m^2$ .  
286 Our forcing should be larger, because IPCC forcings are  $F_o$  for all gases except  $O_3$ , for which  
287 they provide  $F_a$  (AR6 section 7.3.2.5). Table 1 in *Efficacy* allows accurate comparison:  $\delta T_o$  for  
288  $2 \times CO_2$  for the GISS model used in *Efficacy* is  $0.22^\circ C$ ,  $\lambda$  is  $0.67^\circ C$  per  $W/m^2$ , so  $\delta T_o/\lambda = 0.33$   
289  $W/m^2$ . Thus, the conversion factor from  $F_o$  to  $F_e$  (or  $F_s$ ) is  $4.11/(4.11-0.33)$ . The non- $O_3$  portion  
290 of AR6 2019 forcing ( $3.84 - 0.47 = 3.37$ )  $W/m^2$  increases to  $3.664 W/m^2$ . The  $O_3$  portion of the  
291 AR6 2019 forcing ( $0.47 W/m^2$ ) decreases to  $0.385 W/m^2$  because the efficacy of  $F_a(O_3)$  is 0.82.  
292 The AR6 GHG forcing in 2019 is thus  $\sim 4.05 W/m^2$ , expressed as  $F_e \sim F_s$ , which is  $\sim 1\%$  larger  
293 than follows from our formulae. This precise agreement is not indicative of the true uncertainty  
294 in the GHG forcing, which IPCC AR6 estimates as 10%, thus about  $0.4 W/m^2$ . We concur with  
295 their error estimate and employ it in our ECS uncertainty analysis (Section 6.1).

296 We conclude that the GHG increase since 1750 already produces a climate forcing equivalent to  
297 that of  $2 \times CO_2$  (our formulae yield  $F_e \sim F_s = 4.08 W/m^2$  for 2021 and  $4.13 W/m^2$  for 2022; IPCC  
298 AR6 has  $F_s = 4.14 W/m^2$  for 2021). The human-made  $2 \times CO_2$  climate forcing imagined by  
299 Charney, Tyndall and other greenhouse giants is no longer imaginary. Humanity is now taking  
300 its first steps into the period of consequences. Earth's paleoclimate history helps us assess the  
301 potential outcomes.





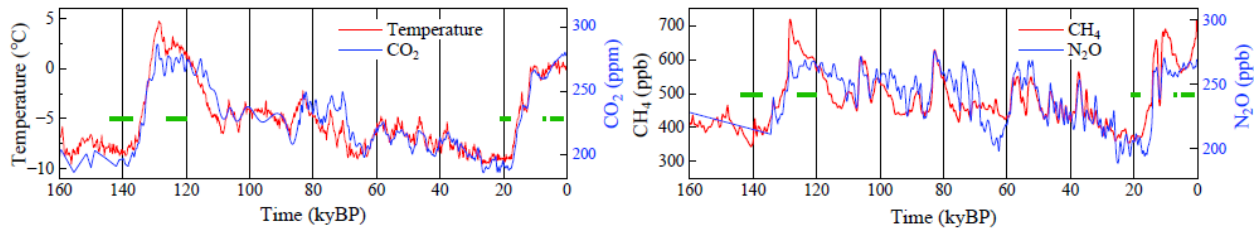
302  
 303 Fig. 2. Antarctic Dome C temperature for past 800 ky from Jouzel *et al.*<sup>43</sup> relative to the mean of  
 304 the last 10 ky and Dome C CO<sub>2</sub> amount from Luthi *et al.*<sup>44</sup> (kyBP is kiloyears before present).

305 **2.4. Glacial-to-interglacial climate oscillations**

306 In this section we describe how ice core data help us assess ECS for climate states from glacial  
 307 conditions to interglacial periods such as the Holocene, the interglacial period of the past 12,000  
 308 years. We discuss climate sensitivity in warmer climates in Section 4 (Cenozoic Era).

309 Air bubbles in Antarctic ice cores – trapped as snow piled up and compressed into ice – preserve  
 310 a record of long-lived GHGs for at least 800,000 years. Isotopic composition of the ice provides  
 311 a measure of temperature in and near Antarctica.<sup>43</sup> Changes of temperature and CO<sub>2</sub> are highly  
 312 correlated (Fig. 2). This does not mean that CO<sub>2</sub> is the primal cause of the climate oscillations.  
 313 Hays *et al.*<sup>45</sup> showed that small changes of Earth’s orbit and the tilt of Earth’s spin axis are  
 314 pacemakers of the ice ages. Orbital changes alter the seasonal and geographical distribution of  
 315 insolation, which affects ice sheet size and GHG amount. Long-term climate is sensitive because  
 316 ice sheets and GHGs act as amplifying feedbacks:<sup>46</sup> as Earth warms, ice sheets shrink, expose a  
 317 darker surface, and absorb more sunlight; also, as Earth warms, the ocean and continents release  
 318 GHGs to the air. These amplifying feedbacks work in the opposite sense as Earth cools. Orbital  
 319 forcings oscillate slowly over tens and hundreds of thousands of years.<sup>47</sup> The picture of how  
 320 Earth orbital changes drive millennial climate change was painted in the 1920s by Milutin  
 321 Milankovitch, who built on 19<sup>th</sup> century hypotheses of James Croll and Joseph Adhémar.  
 322 Paleoclimate changes of ice sheets and GHGs are sometimes described as slow feedbacks,<sup>48</sup> but  
 323 their slow change is paced by the Earth orbital forcing; their slow change does not mean that  
 324 these feedbacks cannot operate more rapidly in response to a rapid climate forcing.

325 We evaluate ECS by comparing stable climate states before and after a glacial-to-interglacial  
 326 climate transition. GHG amounts are known from ice cores and ice sheet sizes are known from  
 327 geologic data. This empirical ECS applies to the range of global temperature covered by ice  
 328 cores, which we will conclude is about  $-7^{\circ}\text{C}$  to  $+1^{\circ}\text{C}$  relative to the Holocene. The Holocene is  
 329 an unusual interglacial. Maximum melt rate was at 13.2 kyBP, as expected,<sup>49</sup> and GHG amounts  
 330 began to decline after peaking early in the Holocene, as in most interglacials. However, several  
 331 ky later, CO<sub>2</sub> and CH<sub>4</sub> increased, raising a question of whether humans were affecting GHGs.  
 332 Ruddiman<sup>50</sup> suggests that deforestation began to affect CO<sub>2</sub> 6500 years ago and rice irrigation  
 333 began to affect CH<sub>4</sub> 5,000 years ago. Those possibilities complicate use of LGM-Holocene  
 334 warming to estimate ECS. However, sea level, and thus the size of the ice sheets, had stabilized  
 335 by 7,000 years ago (Section 5.1). Thus, the millennium centered on 7 kyBP provides a good  
 336 period to compare with the LGM. Comparison of the Eemian interglacial (Fig. 2) with the prior  
 337 glacial maximum (PGM) has potential for independent assessment.



338  
 339 Fig. 3. Dome C temperature (Jouzel *et al.*<sup>43</sup>) and multi-ice core GHG amounts (Schilt *et al.*).<sup>51</sup>  
 340 Green bars (1-5, 6.5-7.5, 18-21, 120-126, 137-144 kyBP) are periods of calculations.

## 341 2.5. LGM-Holocene and PGM-Eemian evaluation of ECS

342 In this section we evaluate ECS by comparing neighboring glacial and interglacial periods when  
 343 Earth was in energy balance within less than  $0.1 \text{ W/m}^2$  averaged over a millennium. Larger  
 344 imbalance would cause temperature or sea level change that did not occur.<sup>52</sup> Thus, we can assess  
 345 ECS from knowledge of atmospheric and surface forcings that maintained these climates.

346 Recent advanced analysis techniques allow improved estimate of paleo temperatures. Tierney *et al.*<sup>53</sup>  
 347 exclude micro biology fossils whose potential to adapt makes them dubious thermometers.  
 348 Instead, they use a large collection of geochemical (isotope) proxies for SST in an analysis  
 349 constrained by climate change patterns defined by GCMs. They find cooling of  $6.1^\circ\text{C}$  (95%  
 350 confidence:  $5.7\text{-}6.5^\circ\text{C}$ ) for the interval 23-19 kyBP. A similarly constrained global analysis by  
 351 Osman *et al.*<sup>54</sup> finds LGM cooling at 21-18 kyBP of  $7.0 \pm 1^\circ\text{C}$  (95% confidence).<sup>55</sup> Tierney  
 352 (priv. comm.) attributes the difference between the two studies to the broader time interval of the  
 353 former study, and suggests that peak LGM cooling was near  $7^\circ\text{C}$ .

354 Seltzer *et al.*<sup>56</sup> use the temperature-dependent solubility of dissolved noble gases in ancient  
 355 groundwater to show that land areas between  $45^\circ\text{S}$  and  $35^\circ\text{N}$  cooled  $5.8 \pm 0.6^\circ\text{C}$  in the LGM.  
 356 This cooling is consistent with 1 km lowering of alpine snowlines found by Rind and Peteet.<sup>26</sup>  
 357 Land response to a forcing exceeds ocean response, but polar amplification makes the global  
 358 response as large as the low latitude land response in GCM simulations with fixed ice sheets (SM  
 359 Fig. S3). When ice sheet growth is added, cooling amplification at mid and high latitudes is  
 360 greater,<sup>7</sup> making  $5.8^\circ\text{C}$  cooling of low latitude land consistent with global cooling of  $\sim 7^\circ\text{C}$ .

361 LGM  $\text{CO}_2$ ,  $\text{CH}_4$  and  $\text{N}_2\text{O}$  amounts are known accurately with the exception of  $\text{N}_2\text{O}$  in the PGM  
 362 when  $\text{N}_2\text{O}$  reactions with dust in the ice core corrupt the data. We take PGM  $\text{N}_2\text{O}$  as the mean of  
 363 the smallest reported PGM amount and the LGM amount; potential error in the  $\text{N}_2\text{O}$  forcing is  
 364  $\sim 0.01 \text{ W/m}^2$ . We calculate  $\text{CO}_2$ ,  $\text{CH}_4$ , and  $\text{N}_2\text{O}$  forcings using Eq. (4) and formulae for each gas  
 365 in Supp. Material for the periods shown by green bars in Fig. 3. The Eemian period avoids early  
 366  $\text{CO}_2$  and temperature spikes, assuring that Earth was in energy balance. Between the LGM (19-  
 367 21 kyBP) and Holocene (6.5-7.5 kyBP), GHG forcing increased  $2.25 \text{ W/m}^2$  with 77% from  $\text{CO}_2$ .  
 368 Between the PGM and Eemian, GHG forcing increased  $2.30 \text{ W/m}^2$  with 79% from  $\text{CO}_2$ .

369 Glacial-interglacial aerosol changes are not included as a forcing. Natural aerosol changes, like  
 370 clouds, are fast feedbacks. Indeed, aerosols and clouds form a continuum and distinction is  
 371 arbitrary as humidity approaches 100 percent. There are many aerosol types, including VOCs  
 372 (volatile organic compounds) produced by trees, sea salt produced by wind and waves, black and  
 373 organic carbon produced by forest and grass fires, dust produced by wind and drought, and

374 marine biologic dimethyl sulfide and its secondary aerosol products, all varying geographically  
375 and in response to climate change. We do not know, or need to know, natural aerosol properties  
376 in prior eras because their changes are feedbacks included in the climate response. However,  
377 human-made aerosols are a climate forcing (an imposed perturbation of Earth's energy balance).  
378 Humans may have begun to affect gases and aerosols by the mid-Holocene (Section 5), but we  
379 minimize that issue by using the 6.5-7.5 kyBP window to evaluate climate sensitivity.

380 Earth's surface change is the other forcing needed to evaluate ECS: (1) change of surface albedo  
381 (reflectivity) and topography by ice sheets, (2) vegetation change, e.g., boreal forests replaced by  
382 brighter tundra, and (3) continental shelves exposed by lower sea level. Forcing by all three can  
383 be evaluated at once with a GCM. Accuracy requires realistic clouds, which shield the surface.  
384 Clouds are the most uncertain feedback.<sup>57</sup> Evaluation is ideal for CMIP<sup>58</sup> (Coupled Model  
385 Intercomparison Project) collaboration with PMIP<sup>59</sup> (Paleoclimate Modelling Intercomparison  
386 Project); a study of LGM surface forcing could aid GCM development and assessment of climate  
387 sensitivity. Sherwood *et al.*<sup>23</sup> review studies of LGM ice sheet forcing and settle on  $3.2 \pm 0.7$   
388  $\text{W/m}^2$ , the same as IPCC AR4.<sup>60</sup> However, some GCMs yield efficacies as low as  $\sim 0.75$ <sup>61</sup> or  
389 even  $\sim 0.5$ ,<sup>62</sup> likely due to cloud shielding. We found<sup>7</sup> a forcing of  $-0.9 \text{ W/m}^2$  for LGM  
390 vegetation by using the Koppen<sup>63</sup> scheme to relate vegetation to local climate, but we thought the  
391 model effect was exaggerated as real-world forests tends to shake off snow albedo effects.  
392 Kohler *et al.*<sup>64</sup> estimate a continental shelf forcing of  $-0.6 \text{ W/m}^2$ . Based on an earlier study<sup>65</sup>  
393 (hereafter *Target CO<sub>2</sub>*), our estimate of LGM-Holocene surface forcing is  $3.5 \pm 1 \text{ W/m}^2$ . Thus,  
394 LGM (18-21 kyBP) cooling of  $7^\circ\text{C}$  relative to mid-Holocene (7 kyBP), GHG forcing of  $2.25$   
395  $\text{W/m}^2$ , and surface forcing of  $3.5 \text{ W/m}^2$  yield an initial ECS estimate  $7/(2.25 + 3.5) = 1.22^\circ\text{C}$  per  
396  $\text{W/m}^2$ . We discuss uncertainties in Section 6.1.

397 PGM-Eemian global warming provides a second assessment of ECS, one that avoids concern  
398 about human influence. PGM-Eemian GHG forcing is  $2.3 \text{ W/m}^2$ . We estimate surface albedo  
399 forcing as  $0.3 \text{ W/m}^2$  less than in the LGM because sea level was about 10 m higher during the  
400 PGM.<sup>66</sup> North American and Eurasian ice sheet sizes differed between the LGM and PGM,<sup>67</sup> but  
401 division of mass between them has little effect on the net forcing (Fig. S4<sup>65</sup>). Thus, our central  
402 estimate of PGM-Eemian forcing is  $5.5 \text{ W/m}^2$ . Eemian temperature reached about  $+1^\circ\text{C}$  warmer  
403 than the Holocene,<sup>68</sup> based on Eemian SSTs of  $+0.5 \pm 0.3^\circ\text{C}$  relative to 1870-1889,<sup>69</sup> or  $+0.65 \pm$   
404  $0.3^\circ\text{C}$  SST and  $+1^\circ\text{C}$  global (land plus ocean) relative to 1880-1920. However, the PGM was  
405 probably warmer than the LGM; it was warmer at Dome C (Fig.2), but cooler at Dronning Maud  
406 Land.<sup>70</sup> Based on deep ocean temperatures (Section 4), we estimate PGM-Eemian warming as  
407  $0.5^\circ\text{C}$  greater than LGM-Holocene warming, i.e.,  $7.5^\circ\text{C}$ . The resulting ECS is  $7.5/5.5 = 1.36^\circ\text{C}$   
408 per  $\text{W/m}^2$ . Although PGM temperature lacks quantification comparable to that of Seltzer *et al.*<sup>56</sup>  
409 and Tierney *et al.*<sup>53</sup> for the LGM, the PGM-Eemian warming provides support for the high ECS  
410 inferred from LGM-Holocene warming.

411 We conclude that ECS for climate in the Holocene-LGM range is  $1.2^\circ\text{C} \pm 0.3^\circ\text{C}$  per  $\text{W/m}^2$ ,  
412 where the uncertainty is the 95% confidence range. The uncertainty estimate is inherently  
413 subjective, as it depends mainly on the ice age surface albedo forcing. The GHG forcing and  
414 glacial-interglacial temperature change are well-defined, but the efficacy of ice age surface  
415 forcing varies among GCMs. This variability is likely related to cloud shielding of surface  
416 albedo, which reaffirms the need for a focus on precise cloud observations and modeling.

## 417 **2.6 State dependence of climate sensitivity**

418 ECS based on glacial-interglacial climate is an average for global temperatures  $-7^{\circ}\text{C}$  to  $+1^{\circ}\text{C}$   
419 relative to the Holocene and in general differs for other climate states because water vapor,  
420 aerosol-cloud and sea ice feedbacks depend on the initial climate. However, ECS is rather flat  
421 between today's climate and warmer climate, based on a study<sup>71</sup> covering a range of 15  $\text{CO}_2$   
422 doublings using an efficient GCM developed by Gary Russell.<sup>72</sup> Toward colder climate, ice-  
423 snow albedo feedback increases nonlinearly, reaching snowball Earth conditions – with snow  
424 and ice on land reaching sea level in the tropics – when  $\text{CO}_2$  declines to a quarter to an eighth of  
425 its 1950 abundance (Fig. 7 of the study).<sup>71</sup> Snowball Earth occurred several times in Earth's  
426 history, most recently about 600 million years ago<sup>73</sup> when the Sun was 6% dimmer<sup>74</sup> than today,  
427 a forcing of about  $-12 \text{ W/m}^2$ . Toward warmer climate, the water vapor feedback increases as the  
428 tropopause rises,<sup>75</sup> the tropopause cold trap disappearing at  $32\times\text{CO}_2$  (Fig. 7).<sup>71</sup> However, for the  
429 range of ECS of practical interest – say from half preindustrial  $\text{CO}_2$  to  $4\times\text{CO}_2$  – state dependence  
430 of ECS is small compared to state dependence of ESS.

431 Earth system sensitivity (ESS) includes amplifying feedbacks of GHGs and ice sheets. When we  
432 consider  $\text{CO}_2$  change as a known forcing, other GHGs provide a feedback that is smaller than the  
433 ice sheet feedback, but not negligible. Ice core data on GHG amounts show that non- $\text{CO}_2$  GHGs  
434 – including  $\text{O}_3$  and stratospheric  $\text{H}_2\text{O}$  produced by changing  $\text{CH}_4$  – provide about 20% of the  
435 total GHG forcing, not only on average for the full glacial-interglacial change, but as a function  
436 of global temperature right up to  $+1^{\circ}\text{C}$  global temperature relative to the Holocene (Fig. S5).  
437 Atmospheric chemistry modeling suggests that non- $\text{CO}_2$  GHG amplification of  $\text{CO}_2$  forcing by  
438 about a quarter continues into warmer climate states.<sup>76</sup> Thus, for climate change in the Cenozoic  
439 era, we approximate non- $\text{CO}_2$  GHG forcing by increasing the  $\text{CO}_2$  forcing by one-quarter.

440 Ice sheet feedback, in contrast to non- $\text{CO}_2$  GHG feedback, is highly nonlinear. Preindustrial  
441 climate was at most a few halvings of  $\text{CO}_2$  from runaway snowball Earth and LGM climate was  
442 even closer to that climate state. The ice sheet feedback is reduced as Earth heads toward warmer  
443 climate today because already two-thirds of LGM ice has been lost. Yet remaining ice on  
444 Antarctica and Greenland constitutes a powerful feedback, which humanity is about to bring into  
445 play. We can illuminate that feedback and the climate path Earth is now on by examining data on  
446 the Cenozoic era – which includes  $\text{CO}_2$  levels comparable to today's amount – but first we must  
447 consider climate response time.

### 448 3. CLIMATE RESPONSE TIME

449 In this section we define response functions for global temperature and Earth’s energy imbalance  
450 that help explain the physics of climate change. Response functions help reveal the role of cloud  
451 feedbacks in amplifying climate sensitivity and the fact that cloud feedbacks buffer the rate at  
452 which the ocean can take up heat.

453 Climate response time was surprisingly long in our climate simulations<sup>7</sup> for the 1982 Ewing  
454 Symposium. The e-folding time – the time for surface temperature to reach 63% of its  
455 equilibrium response – was about a century. The only published atmosphere-ocean GCM – that  
456 of Bryan and Manabe<sup>77</sup> – had a response time of 25 years, while several simplified climate  
457 models referenced in our Ewing paper had even faster responses. The longer response time of  
458 our climate model was largely a result of high climate sensitivity – our model had an ECS of 4°C  
459 for 2×CO<sub>2</sub> while the Bryan and Manabe model had an ECS of 2°C.

460 The physics is straightforward. If the delay were a result of a fixed source of thermal inertia, say  
461 the ocean’s well-mixed upper layer, response time would increase linearly with ECS because  
462 most climate feedbacks come into play in response to temperature change driven by the forcing,  
463 not in direct response to the forcing. Thus, a model with ECS of 4°C takes twice as long to reach  
464 full response as a model with ECS of 2°C, if the mixed layer provides the only heat capacity.  
465 However, while the mixed layer is warming, there is exchange of water with the deeper ocean,  
466 which slows the mixed layer warming. The longer response time with high ECS allows more of  
467 the ocean to come into play. If mixing into the deeper ocean is approximated as diffusive, surface  
468 temperature response time is proportional to the square of climate sensitivity.<sup>78</sup>

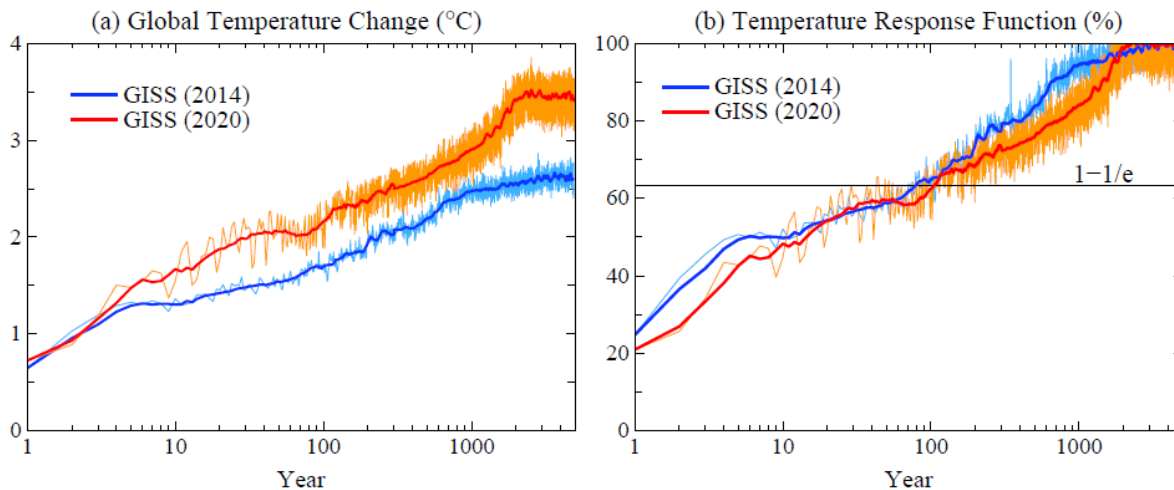
469 Slow climate response accentuates need for the “anticipation” that E.E. David, Jr. spoke about. If  
470 ECS is 4°C (1°C per W/m<sup>2</sup>), more warming is in the pipeline than widely assumed. GHG forcing  
471 today already exceeds 4 W/m<sup>2</sup>. Aerosols reduce the net forcing to about 3 W/m<sup>2</sup>, based on IPCC  
472 estimates (Section 5), but warming still in the pipeline for 3 W/m<sup>2</sup> forcing is 1.8°C, exceeding  
473 warming realized to date (1.2°C). Slow feedbacks increase the equilibrium response even further  
474 (Section 6). Large warmings can be avoided via a reasoned policy response, but definition of  
475 effective policies will be aided by an understanding of climate response time.

#### 476 3.1. Temperature response function

477 In the Bjerknes lecture<sup>79</sup> at the 2008 American Geophysical Union meeting, JEH argued that the  
478 ocean in many<sup>80</sup> GCMs had excessive mixing, and he suggested that GCM groups all report the  
479 response function of their models – the global temperature change versus time in response to  
480 instant CO<sub>2</sub> doubling with the model run long enough to approach equilibrium. The response  
481 function characterizes a climate model and enables a rapid estimate of the global mean surface  
482 temperature change in response to any climate forcing scenario:

$$483 T_G(t) = \int [dT_G(t)/dt] dt = \int \lambda \times R(t) [dF_e/dt] dt. \quad (5)$$

484 T<sub>G</sub> is the Green’s function estimate of global temperature at time t, λ (°C per W/m<sup>2</sup>) the model’s  
485 equilibrium sensitivity, R the dimensionless temperature response function (% of equilibrium



486  
 487 Fig. 4. (a) Global mean surface temperature response to instant CO<sub>2</sub> doubling and (b) normalized  
 488 response function (percent of final change). Thick lines in Figs. 4 and 5 are smoothed<sup>81</sup> results.

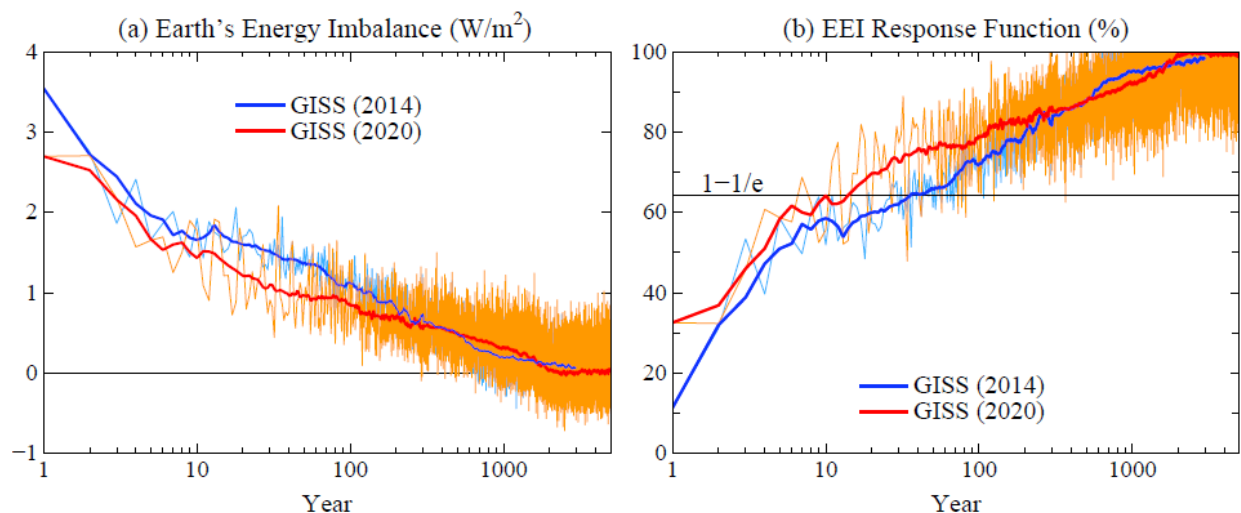
489 response), and  $dF_e$  the forcing change per unit time,  $dt$ . Integration over time begins when Earth  
 490 is in near energy balance, e.g., in preindustrial time. The response function yields an accurate  
 491 estimate of global temperature change for a forcing that does not cause reorganization of ocean  
 492 circulation. Accuracy of this approximation for temperature for one climate model is shown in  
 493 Chart 15 in the Bjerknes presentation and wider applicability has been demonstrated.<sup>82</sup>

494 We study ocean mixing effects by comparing two GCMs: GISS (2014)<sup>83</sup> and GISS (2020),<sup>35</sup>  
 495 both models<sup>84</sup> described by Kelley *et al.* (2020).<sup>34</sup> Ocean mixing is improved in GISS (2020) by  
 496 use of a high-order advection scheme,<sup>85</sup> finer upper-ocean vertical resolution (40 layers), updated  
 497 mesoscale eddy parameterization, and correction of errors in the ocean modeling code.<sup>34</sup> The  
 498 GISS (2020) model has improved variability, including the Madden-Julian Oscillation (MJO), El  
 499 Niño Southern Oscillation (ENSO) and Pacific Decadal Oscillation (PDO), but the spectrum of  
 500 ENSO-like variability is unrealistic and its amplitude is excessive, as shown by the magnitude of  
 501 oscillations in Fig. 4a. Ocean mixing in GISS (2020) may still be excessive in the North Atlantic,  
 502 where the model's simulated penetration of CFCs is greater than observed.<sup>86</sup>

503 Despite reduced ocean mixing, the GISS (2020) model surface temperature response is no faster  
 504 than in the GISS (2014) model (Fig. 4b): it takes 100 years to reach within 1/e of the equilibrium  
 505 response. Slow response is partly explained by the larger ECS of the GISS (2020) model, which  
 506 is 3.5°C versus 2.7°C for the GISS (2014) model, but something more is going on in the newer  
 507 model, as exposed by the response function of Earth's energy imbalance.

### 508 3.2. Earth's energy imbalance (EEI)

509 When a forcing perturbs Earth's energy balance, the imbalance drives warming or cooling to  
 510 restore balance. Observed EEI is now about +1 W/m<sup>2</sup> (more energy coming in than going out)  
 511 averaged over several years.<sup>87</sup> High accuracy of EEI is obtained by tracking ocean warming – the  
 512 primary repository for excess energy – and adding heat stored in warming continents and heat  
 513 used in net melting of ice.<sup>87</sup> Heat storage in air adds an almost negligible amount. Radiation  
 514 balance measured from Earth-orbiting satellites cannot by itself define the absolute imbalance,



515  
516 Fig. 5. (a) Earth's energy imbalance (EEI) for 2×CO<sub>2</sub>, and (b) EEI normalized response function.

517 but, when calibrated with the *in situ* data, satellite Earth radiation budget observations provide  
518 invaluable EEI data on finer temporal and spatial scales than the *in situ* data.<sup>88</sup>

519 After a step-function forcing is imposed, EEI and global surface temperature must each approach  
520 a new equilibrium, but EEI does so more rapidly, especially for the GISS (2020) model (Fig. 5).  
521 EEI in GISS (2020) needs only a decade to reach within 1/e of full response (Fig. 5b), but global  
522 surface temperature requires a century (Fig. 4b). Rapid decline of EEI – to half the forcing in 5  
523 years (Fig. 5a) – has practical implications. First, EEI defines the rate heat is pumped into the  
524 ocean, so if EEI is reduced, ocean warming is slowed. Second, rapid EEI decline implies that it is  
525 wrong to assume that global warming can be stopped by a reduction of climate forcing by the  
526 amount of EEI. Instead, the required reduction of forcing is larger than EEI. The difficulty in  
527 finding additional reduction in climate forcing of even a few tenths of a W/m<sup>2</sup> is substantial.<sup>68</sup>  
528 Calculations that help quantify this matter are discussed in Supp. Material Sec. SM8.

529 What is the physics behind the fast response of EEI? The 2×CO<sub>2</sub> forcing and initial EEI are both  
530 nominally 4 W/m<sup>2</sup>. In the GISS (2014) model, the decline of EEI averaged over the first year is  
531 0.5 W/m<sup>2</sup> (Fig. 5a), a moderate decline that might be largely caused by warming continents and  
532 increased heat radiation to space. In contrast, EEI declines 1.3 W/m<sup>2</sup> in the GISS (2020) model  
533 (Fig. 5a). Such a huge, immediate decline of EEI implies existence of an ultrafast climate  
534 feedback. Climate feedbacks are the heart of climate change and warrant discussion.

### 535 3.3. Slow, fast and ultrafast feedbacks

536 Charney *et al.*<sup>4</sup> described climate feedbacks without discussing time scales. At the 1982 Ewing  
537 Symposium, water vapor, clouds and sea ice were described as “fast” feedbacks<sup>7</sup> presumed to  
538 change promptly in response to global temperature change, as opposed to “slow” feedbacks or  
539 specified boundary conditions such as ice sheet size, vegetation cover, and atmospheric CO<sub>2</sub>  
540 amount, although it was noted that some specified boundary conditions, e.g., vegetation, in  
541 reality may be capable of relatively rapid change.<sup>7</sup>

542 The immediate EEI response (Fig. 5a) implies a third feedback time scale: ultrafast. Ultrafast  
543 feedbacks are not a new concept. When CO<sub>2</sub> is doubled, the added infrared opacity causes the

544 stratosphere to cool. Instant EEI upon CO<sub>2</sub> doubling is only  $F_i = +2.5 \text{ W/m}^2$ , but stratospheric  
545 cooling quickly increases EEI to  $+4 \text{ W/m}^2$ .<sup>89</sup> All models calculate a similar radiative effect, so it  
546 is useful to define an adjusted forcing,  $F_a$ , which is superior to  $F_i$  as a measure of climate forcing.  
547 In contrast, if cloud change – the likely cause of the present ultrafast change – is lumped into the  
548 adjusted forcing, each climate model has its own forcing, losing the merit of a common forcing.

549 Kamae *et al.*<sup>90</sup> review rapid cloud adjustment distinct from surface temperature-mediated  
550 change. Clouds respond to radiative forcing, e.g., via effects on cloud particle phase, cloud  
551 cover, cloud albedo and precipitation.<sup>91</sup> The GISS (2020) model alters glaciation in stratiform  
552 mixed-phase clouds, which increases supercooled water in stratus clouds, especially over the  
553 Southern Ocean [Fig. 1 in the GCM description<sup>34</sup>]. The portion of supercooled cloud water drops  
554 goes from too little in GISS (2014) to too much in GISS (2020). Neither model simulates well  
555 stratocumulus clouds, yet the models help expose real-world physics that affects climate  
556 sensitivity and climate response time. Several models in CMIP6 comparisons find high ECS.<sup>91</sup>  
557 For the sake of revealing the physics, it would be useful if the models defined their temperature  
558 and EEI response functions. Model runs of even a decade can define the important part of Figs.  
559 4a and 5a. Many short (e.g., 2-year) 2×CO<sub>2</sub> climate simulations with each run beginning at a  
560 different point in the model’s control run, could define cloud changes to an arbitrary accuracy. If  
561 the EEI response is faster than the temperature response, it implies that the climate forcing  
562 reduction required to stabilize climate is greater than EEI, as discussed in Supporting Material.  
563 The need for better understanding of ultrafast feedbacks does not alter the high ECS inferred  
564 from paleoclimate data. The main role of GCMs in the paleoclimate analyses that we use to  
565 assess climate sensitivity is to define climate patterns, which allows more accurate assessment of  
566 global temperature change from limited paleo data samples.<sup>53,54,56</sup>

#### 567 **4. CENOZOIC ERA**

568 In this section, we use data from ocean sediment cores to explore causes of climate change in the  
569 past 66 million years. Based on theory and on knowledge of climate change in the past 800,000  
570 years, we anticipate that CO<sub>2</sub> is the principal control knob on global temperature; with that  
571 assumption, we quantify the CO<sub>2</sub> history required to account for Cenozoic temperature change.

572 Cenozoic climate allows us to investigate implications of high climate sensitivity and the danger  
573 that climate models are less sensitive than the real world to a forcing such as CO<sub>2</sub>. We refer to  
574 GCMs, in general, and ice sheet modeling, in particular. Some proxy-based assessments of  
575 Cenozoic CO<sub>2</sub> may be affected by a coupled GCM/ice sheet model finding that transition  
576 between unglaciated and glaciated Antarctica occurs at 700-840 ppm CO<sub>2</sub>.<sup>92</sup> In addition, GCMs  
577 have a long-standing difficulty in producing Pliocene warmth,<sup>93</sup> especially in the Arctic, without  
578 large, probably unrealistic, GHG forcing. Our conclusion in Section 2 that (fast feedback) ECS is  
579 high,  $1.2^\circ\text{C} \pm 0.3^\circ\text{C}$  per  $\text{W/m}^2$ , and our inference in Section 3 that amplifying cloud feedbacks  
580 cause the ECS increase from  $0.6^\circ\text{C}$  to  $1.2^\circ\text{C}$  per  $\text{W/m}^2$ , suggest that GCMs must simulate clouds  
581 well to reproduce Cenozoic climate change. While we cannot develop cloud modeling here, we  
582 can examine the effect of high ECS on interpretation of Cenozoic climate change.

583 Atmospheric CO<sub>2</sub> is a control knob<sup>94</sup> on Earth’s temperature. CO<sub>2</sub> on glacial-interglacial time  
584 scales is largely a feedback spurred by weak astronomical forcing, but Fig. 2 shows the tight



585 control that CO<sub>2</sub> maintains on those time scales. We obtain a more complete picture of CO<sub>2</sub> as a  
586 forcing and feedback with aid of consistent calculations over the entire Cenozoic era.  
587 Specifically, we use our derived ECS and a proxy (oxygen isotope) measure of deep ocean  
588 temperature to infer a history of Earth’s surface temperature and atmospheric CO<sub>2</sub> throughout the  
589 Cenozoic era. Progress has been made in proxy measurement of CO<sub>2</sub> via carbon isotopes in  
590 alkenones and boron isotopes in planktic foraminifera,<sup>95</sup> yet there is still a wide scatter among  
591 the results and fossil plant stomata tend to suggest smaller CO<sub>2</sub> amounts.<sup>96</sup>

592 Proxy measures of CO<sub>2</sub> and indirect constraints on CO<sub>2</sub> based on oxygen isotopes need to work  
593 in concert because of shortcomings in understanding of the physics of both the oxygen isotope  
594 temperature proxy<sup>97</sup> and CO<sub>2</sub> proxies.<sup>95</sup> Merits of the oxygen isotope approach include high  
595 temporal resolution and precision. We aim to show that deep ocean temperature change provides  
596 a useful measure of surface temperature change and that the oxygen isotope proxy provides a  
597 check on CO<sub>2</sub> proxies, as well as better understanding of Cenozoic climate change.

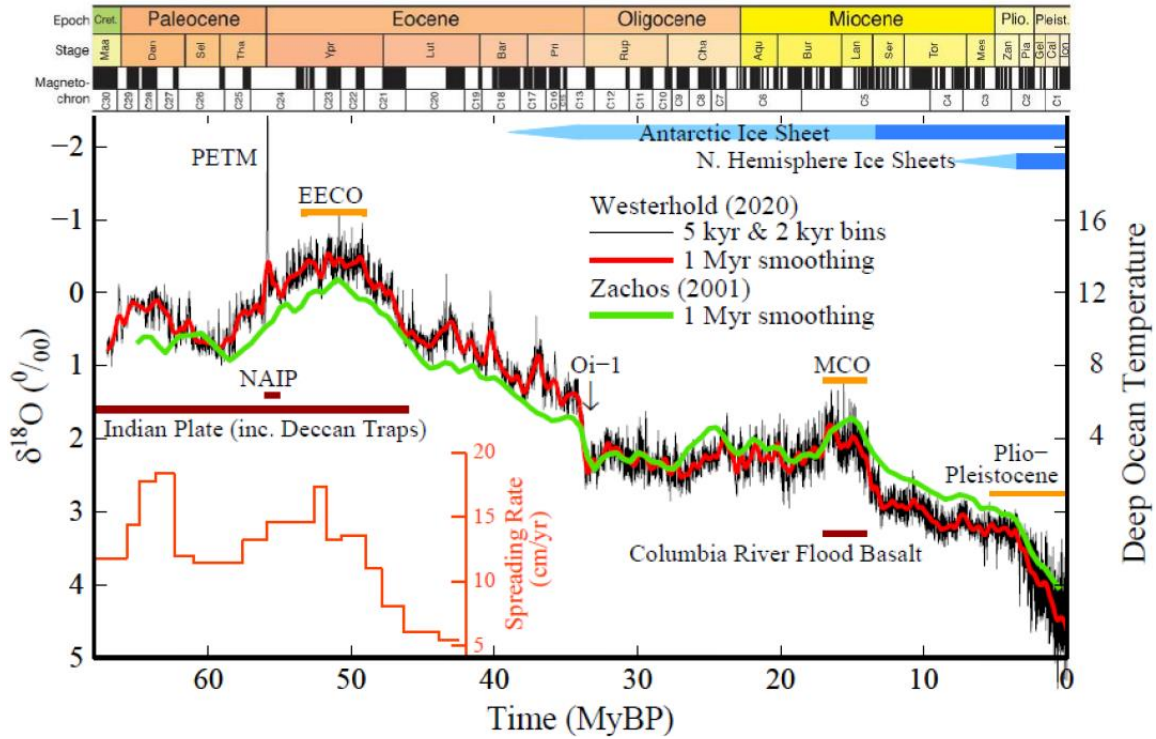
#### 598 **4.1. Deep ocean temperature and sea level from δ<sup>18</sup>O**

599 Glacial-interglacial CO<sub>2</sub> oscillations (Fig. 2) involve exchange of carbon among surface carbon  
600 reservoirs: the ocean, atmosphere, soil and biosphere. Total CO<sub>2</sub> in the reservoirs also can vary,  
601 mainly on longer time scales, as carbon is exchanged with the solid Earth. CO<sub>2</sub> then becomes a  
602 primary agent of long-term climate change, leaving orbital effects as “noise” on larger climate  
603 swings. Oxygen isotopic composition of benthic (deep ocean dwelling) foraminifera shells  
604 provides a starting point for analysis of Cenozoic temperature. Fig. 6 includes the recent high-  
605 resolution record of Westerhold *et al.*<sup>98</sup> and data of Zachos *et al.*<sup>47</sup> that have been used for many  
606 studies in the past quarter century. When Earth has negligible ice sheets, δ<sup>18</sup>O (<sup>18</sup>O amount  
607 relative to a standard), provides an estimate of deep ocean temperature (right scale in Fig. 6)<sup>47</sup>

$$608 \quad T_{do}(^{\circ}\text{C}) = -4 \delta^{18}\text{O} + 12. \quad (5)$$

609 This equation is used for the early Cenozoic, up to the large-scale glaciation of Antarctica at ~34  
610 MyBP (Oi-1 in Fig. 6). At larger δ<sup>18</sup>O (colder climate), lighter <sup>16</sup>O evaporates preferentially from  
611 the ocean and accumulates in ice sheets. In Zachos data, δ<sup>18</sup>O increases by 3 between Oi-1 and  
612 the LGM. Half of this δ<sup>18</sup>O change is due to the 6°C change of deep ocean temperature between  
613 Oi-1 (5°C) and the LGM (−1°C).<sup>99</sup> The other 1.5 of δ<sup>18</sup>O change is presumed to be due to the  
614 ~180 m sea level (SL) change between ice-free Earth and the LGM, with ~60 m from Antarctic  
615 ice and 120 m from Northern Hemisphere ice. Thus, as an approximation to extract both SL and  
616 T<sub>do</sub> from δ<sup>18</sup>O, Hansen *et al.*<sup>71</sup> assumed that SL rose linearly by 60 m as δ<sup>18</sup>O increased from  
617 1.75 to 3.25 and linearly by 120 m as δ<sup>18</sup>O increased from 3.25 to 4.75.

618 As with most climate proxies, δ<sup>18</sup>O is fraught with complexities that affect interpretation.<sup>97,100</sup>  
619 Complications in the Cenozoic record are revealed by differences between the Zachos (Z) and  
620 Westerhold (W) δ<sup>18</sup>O time series (Fig. 6). Despite complications, δ<sup>18</sup>O records carry a great  
621 amount of information on climate change, and a simple linear analysis provides a useful  
622 beginning. We modify prior equations<sup>71</sup> because of differences between the Z and W data. For  
623 example, the mid-Holocene (6-8 kyBP) values of δ<sup>18</sup>O in the Z and W data sets are δ<sup>18</sup>O<sub>H</sub><sup>Z</sup> = 3.32  
624 and δ<sup>18</sup>O<sub>H</sub><sup>W</sup> = 3.88. Thus, sea level (SL) equations, relative to SL = 0 in the mid-Holocene, are:



625  
 626 Fig. 6. Global deep ocean  $\delta^{18}\text{O}$ . Black line: Westerhold *et al.* (2020)<sup>98</sup> data in 5 kyr bins until 34  
 627 MyBP and subsequently 2 kyr bins. Green line: Zachos *et al.* (2001)<sup>47</sup> data at 1 Myr resolution.  
 628 Lower left: velocity<sup>101</sup> of Indian tectonic plate. PETM = Paleocene Eocene Thermal Maximum;  
 629 EECO = Early Eocene Climatic Optimum; Oi-1 marks the transition to glaciated Antarctica;  
 630 MCO = Miocene Climatic Optimum; NAIP = North Atlantic Igneous Province.

631  $SL^Z(\text{m}) = 60 - 38.2 (\delta^{18}\text{O} - 1.75) \quad (\delta^{18}\text{O} < 3.32, \text{ maximum } SL = +60 \text{ m}), \quad (6)$

632  $SL^W(\text{m}) = 60 - 25.2 (\delta^{18}\text{O} - 1.5) \quad (\delta^{18}\text{O} < 3.88, \text{ maximum } SL = +60 \text{ m}), \quad (7)$

633  $SL^Z(\text{m}) = -120 (\delta^{18}\text{O} - 3.32)/1.58 \quad (\delta^{18}\text{O} > 3.32), \quad (8)$

634  $SL^W(\text{m}) = -120 (\delta^{18}\text{O} - 3.88)/1.42 \quad (\delta^{18}\text{O} > 3.88). \quad (9)$

635 The latter two equations are based on LGM  $\delta^{18}\text{O}$  values  $\delta^{18}\text{O}_{\text{LGM}}^Z = 4.9$  and  $\delta^{18}\text{O}_{\text{LGM}}^W = 5.3$ .  
 636 Holocene and LGM deep ocean temperatures are specified as  $1^\circ\text{C}$ <sup>102</sup> and  $-1^\circ\text{C}$ .<sup>99</sup> Coefficients in  
 637 the equations are calculated as shown by the equation (11) example.

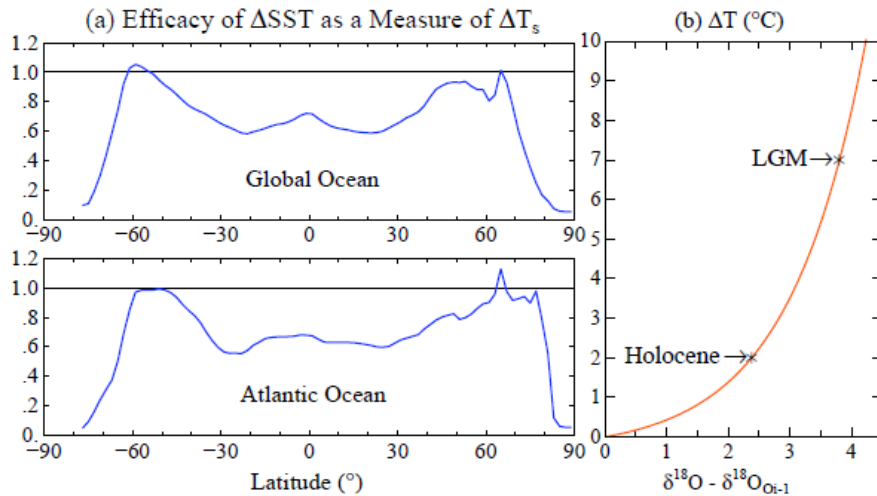
638  $T_{\text{do}}^Z(^\circ\text{C}) = 5 - 2.55 (\delta^{18}\text{O} - 1.75) \quad (1.75 < \delta^{18}\text{O} < 3.32), \quad (10)$

639  $T_{\text{do}}^Z(^\circ\text{C}) = 1 - 2 (\delta^{18}\text{O} - 3.32)/(4.9 - 3.32) = 1 - 1.27 (\delta^{18}\text{O} - 3.32) \quad (3.32 < \delta^{18}\text{O}), \quad (11)$

640  $T_{\text{do}}^W(^\circ\text{C}) = 6 - 2.10 (\delta^{18}\text{O} - 1.5) \quad (1.5 < \delta^{18}\text{O} < 3.88), \quad (12)$

641  $T_{\text{do}}^W(^\circ\text{C}) = 1 - 1.41 (\delta^{18}\text{O} - 3.88) \quad (3.88 < \delta^{18}\text{O}), \quad (13)$

642 Zachos and Westerhold  $\delta^{18}\text{O}$ , SL and  $T_{\text{do}}$  for the full Cenozoic, Pleistocene, and past 800,000  
 643 years are graphed in Supp. Material and sea level is compared to data of Rohling *et al.*<sup>103</sup>. We  
 644 will focus on the W data, which has finer temporal resolution. We discuss differences between  
 645 the W and Z data and interpretations of those differences at the end of Section 4.6.



646  
 647 Fig. 7. (a) Ratio of ΔSST (latitude) to global T<sub>S</sub> change for all ocean and the Atlantic Ocean,  
 648 based on equilibrium response (years 4001-4500) in 2×CO<sub>2</sub> simulations of GISS (2020) model.  
 649 (b) ΔT, the amount by which T<sub>S</sub> change exceeds T<sub>do</sub> change, based on an exponential fit to the  
 650 two data points provided by the Holocene and LGM (see text).

#### 651 4.2. Cenozoic T<sub>S</sub>

652 In this section we combine the rich detail in T<sub>do</sub> provided by benthic δ<sup>18</sup>O with constraints on the  
 653 range of Cenozoic T<sub>S</sub> from surface proxies to produce an estimated history of Cenozoic T<sub>S</sub>.

654 We expect T<sub>do</sub> change, which derives from sea surface temperature (SST) at high latitudes where  
 655 deepwater forms, to approximate T<sub>S</sub> change when T<sub>do</sub> is not near the freezing point. Global SST  
 656 change understates global T<sub>S</sub> (land plus ocean) change because land temperature response to a  
 657 forcing exceeds SST response,<sup>104</sup> e.g., the equilibrium global SST response of the GISS (2020)  
 658 GCM to 2×CO<sub>2</sub> is 70.6% of the global (land plus ocean) response. However, polar amplification  
 659 of the SST response tends to compensate for SST undershoot of global T<sub>S</sub> change. Compensation  
 660 is nearly exact at latitudes of North Atlantic deepwater formation for 2×CO<sub>2</sub> climate change in  
 661 the GISS (2020) climate model (Fig. 7a), but Southern Hemisphere polar amplification does not  
 662 fully cover the 60-75°S latitudes where Antarctic bottom water forms.

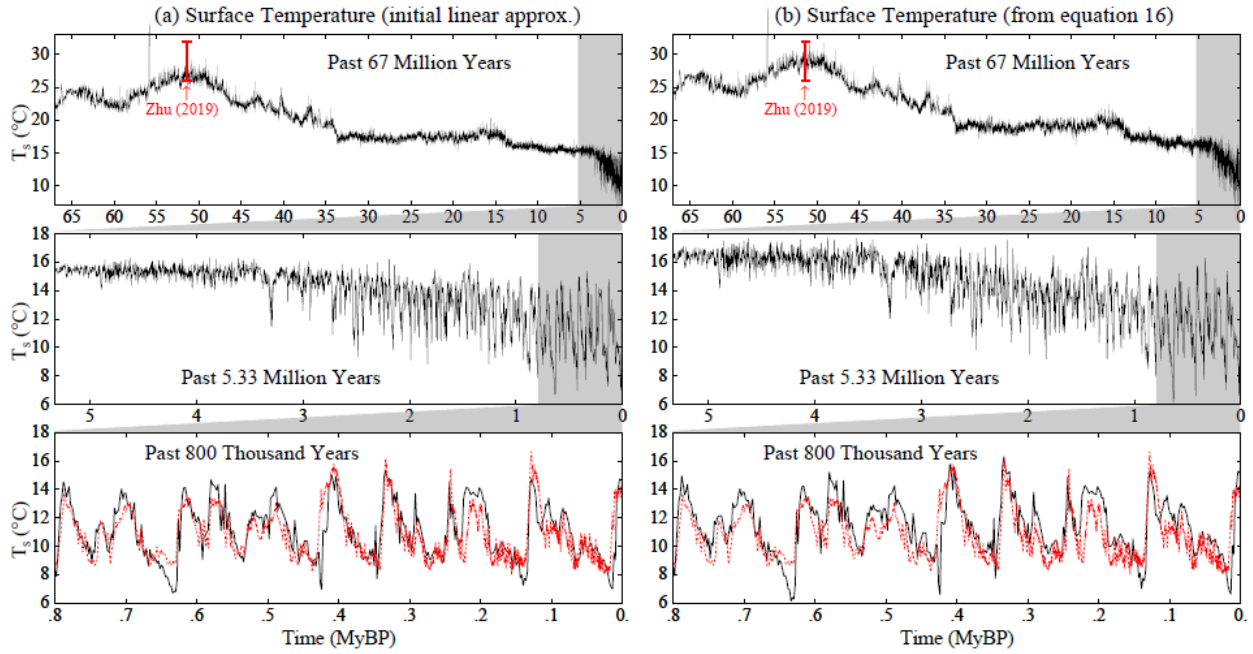
663 As T<sub>do</sub> nears the freezing point, ice forms, adhering to the Antarctic continent, extending today to  
 664 a depth of about 2 km, and also forming floating ice shelves. From the Holocene toward colder  
 665 climate, the effect on temperature change is large: T<sub>S</sub> declines 7°C between the Holocene and  
 666 LGM, but T<sub>do</sub> declines only 2°C (from 1°C to -1°C). From the Holocene toward hotter climate,  
 667 we expect a smaller effect that we can quantify by first neglecting the effect and finding how far  
 668 we underestimate EECO temperature. Thus, as an initial approximation we assume ΔT<sub>S</sub> = ΔT<sub>do</sub>:

$$669 T_S \sim T_{do} - T_{doH} + 14^\circ\text{C} = T_{do} + 13^\circ\text{C}, \quad (\delta^{18}\text{O} < \delta^{18}\text{O}_H) \quad (14)$$

670 where we take Holocene T<sub>S</sub> as 14°C and T<sub>doH</sub> as 1°C. In this initial approximation, we interpolate  
 671 linearly for climate colder than the Holocene, the LGM being ~7°C cooler than the Holocene:

$$672 T_S = 14^\circ\text{C} - 7^\circ\text{C} \times (\delta^{18}\text{O} - \delta^{18}\text{O}_H) / (\delta^{18}\text{O}_{LGM} - \delta^{18}\text{O}_H). \quad (\delta^{18}\text{O} > \delta^{18}\text{O}_H) \quad (15)$$

673 Resulting EECO (Early Eocene Climatic Optimum) T<sub>S</sub> is ~27°C for Westerhold δ<sup>18</sup>O data (Fig.  
 674 8a) and ~25°C for Zachos data (Fig. S9).



675  
 676 Fig. 8. Cenozoic temperature based on linear (equations 14 and 15) and nonlinear (equation 16)  
 677 analyses. Antarctic Dome C data<sup>43</sup> (red) relative to last 1,000 years is multiplied by 0.6 to  
 678 account for polar amplification and 14°C is added for absolute scale.

679 As expected, this initial (linear) approximation undershoots EECO  $T_s$ , which Zhu *et al.*<sup>105</sup> infer  
 680 to be 29°C from a proxy-constrained full-field analysis using a GCM to account for the pattern  
 681 of global temperature change. The moderate undershoot ( $\Delta T = 2^\circ\text{C}$ ) of EECO  $T_s$  based on  
 682 Westerhold data is consistent with the expectation that global warming of a few degrees would  
 683 largely remove Antarctic ice shelves and allow polar amplification to fully cover regions of  
 684 deepwater formation. Moreover,  $\Delta T$  of  $2^\circ\text{C}$  at the Holocene and an additional  $5^\circ\text{C}$  between the  
 685 Holocene and LGM are fit well by an exponential function between Antarctic glaciation and the  
 686 LGM, as needed for  $\Delta T$  to asymptote at the freezing point (Fig. 7b). Thus, we take  $T_s$  as

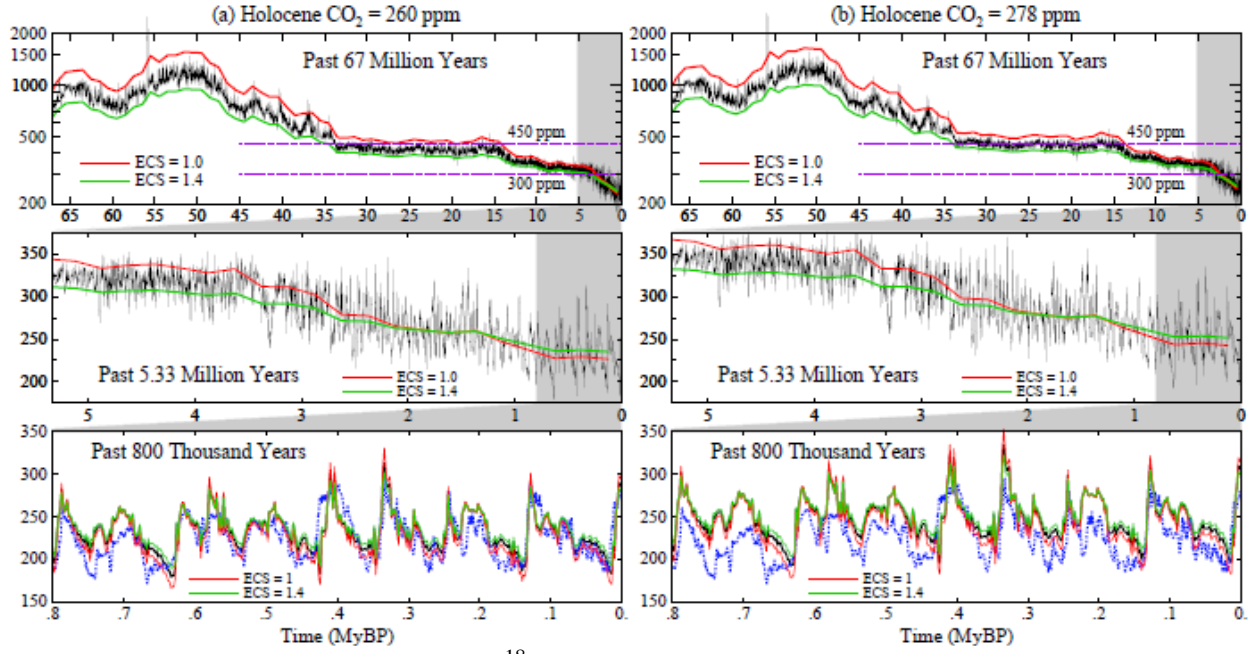
$$687 \quad T_s = T_{\text{do}} - \Delta T + 15^\circ\text{C} = T_{\text{do}} - 0.35(e^{0.8X} - 1) + 15^\circ\text{C}, \quad (16)$$

688 where  $X = \delta^{18}\text{O} - \delta^{18}\text{O}_{\text{O}_i-1}$  and  $T_s$  is normalized to  $14^\circ\text{C}$  in the Holocene.

689 The result is a consistent analysis of global  $T_s$  for the entire Cenozoic (Fig. 8b). Oxygen isotope  
 690  $\delta^{18}\text{O}$  of deep ocean foraminifera reproduces glacial-interglacial temperature change well; more  
 691 detailed agreement is not expected as Antarctic ice core data are for a location that moves,  
 692 especially in its altitude. Our interest is in warmer global climate and its relevance to upcoming  
 693 human-caused climate change. For that purpose, we need to know the forcing that drove  
 694 Cenozoic climate change. With the assumption that non- $\text{CO}_2$  GHG forcings provide 20% of the  
 695 total GHG forcing, it is not difficult to infer the  $\text{CO}_2$  abundance required to cause the Cenozoic  
 696 temperature history in Fig. 8b. Considering the large disagreement among proxy  $\text{CO}_2$  measures,  
 697 this indirect measure of  $\text{CO}_2$  via global  $T_s$  may provide the most accurate Cenozoic  $\text{CO}_2$  history.

### 698 4.3. Cenozoic $\text{CO}_2$

699 We obtain the  $\text{CO}_2$  history required to yield the Cenozoic  $T_s$  history from the relation



700 Fig. 9. Cenozoic CO<sub>2</sub> estimated from δ<sup>18</sup>O of Westerhold *et al.* (see text). Black lines are for  
 701 ECS = 1.2°C per W/m<sup>2</sup>; red and green curves (ECS = 1.0 and 1.4°C per W/m<sup>2</sup>) are 1 My  
 702 smoothed. Blue curves (last 800,000 years) are Antarctica ice core data.<sup>44</sup>  
 703

704 
$$\Delta F(t) = (T_s(t) - 14^\circ\text{C})/\text{ECS}, \quad (17)$$

705 where ΔF(t) (0 at 7 kyBP) includes changing solar irradiance and amplification of CO<sub>2</sub> forcing  
 706 by non-CO<sub>2</sub> GHGs and ice sheets. The GHG amplification factor is taken as 1.25 throughout the  
 707 Cenozoic (Section 2.6). The amplification applies to solar forcing as well as CO<sub>2</sub> forcing because  
 708 it is caused by temperature change, not by CO<sub>2</sub>. Solar irradiance is increasing 10% per billion  
 709 years;<sup>74</sup> thus solar forcing (240 W/m<sup>2</sup> today) increases 2.4 W/m<sup>2</sup> per 100 million years. Thus,

710 
$$\Delta F(t) = 1.25 \times [\Delta F_{\text{CO}_2}(t) + \Delta F_{\text{Sol}}(t)] \times A_s. \quad (\delta^{18}\text{O} > \delta^{18}\text{O}_H) \quad (18)$$

711 A<sub>s</sub>, surface albedo amplification, is smaller in moving from the Holocene to warmer climate –  
 712 when the main effect is shrinking of Antarctic ice – than toward colder climate. For δ<sup>18</sup>O >  
 713 δ<sup>18</sup>O<sub>H</sub>, we take A<sub>s</sub> as its average value over the period from the Holocene to the LGM:

714 
$$A_s = (F_{\text{Ice}} + F_{\text{GHG}})/F_{\text{GHG}} = (3.5 \text{ W/m}^2 + 2.25 \text{ W/m}^2)/(2.25 \text{ W/m}^2) = 2.55. \quad (\delta^{18}\text{O} > \delta^{18}\text{O}_H) \quad (19)$$

715 Thus, for climate colder than the Holocene,

716 
$$\Delta F(t) = 3.19 \times [\Delta F_{\text{CO}_2}(t) + \Delta F_{\text{Sol}}(t)]. \quad (\delta^{18}\text{O} > \delta^{18}\text{O}_H) \quad (20)$$

717 For climate warmer than the Holocene up to O<sub>i-1</sub>, i.e., for δ<sup>18</sup>O<sub>O<sub>i-1</sub></sub> < δ<sup>18</sup>O < δ<sup>18</sup>O<sub>H</sub>,

718 
$$\Delta F(t) = 1.25 \times [\Delta F_{\text{CO}_2}(t) + \Delta F_{\text{Sol}}(t) + F_{\text{IceH}} \times (\delta^{18}\text{O}_H - \delta^{18}\text{O}) / (\delta^{18}\text{O}_H - \delta^{18}\text{O}_{O_{i-1}})]. \quad (21)$$

719 F<sub>IceH</sub>, the (Antarctic plus Greenland) ice sheet forcing between the Holocene and O<sub>i-1</sub>, is  
 720 estimated to be 2 W/m<sup>2</sup> (Fig. S4, *Target CO<sub>2</sub>*). For climate warmer than O<sub>i-1</sub>

721 
$$\Delta F(t) = 1.25 \times [\Delta F_{\text{CO}_2} + \Delta F_{\text{Sol}}(t) + \Delta F_{\text{IceH}}]. \quad (22)$$

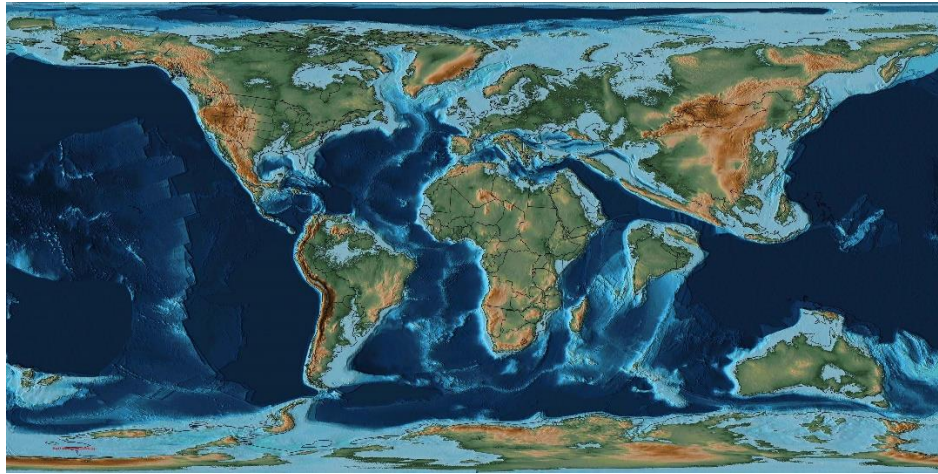
722 All quantities are known except  $\Delta F_{\text{CO}_2}(t)$ , which is thus defined. Cenozoic  $\text{CO}_2$  ( $t$ ) for specified  
723 ECS is obtained from  $T_S(t)$  using the  $\text{CO}_2$  radiative forcing equation (Table 1, Supp. Material).  
724 We use the Westerhold  $T_S$  history, Fig. 8b. Resulting  $\text{CO}_2$  (Fig. 9) is about 1,200 ppm in the  
725 EECO, 450 ppm at Oi-1, and 325 ppm in the Pliocene for the most probable ECS ( $1.2^\circ\text{C}$  per  
726  $\text{W}/\text{m}^2$ ). These values depend on ECS and the assumption that non- $\text{CO}_2$  gases provide 20% of the  
727 GHG forcing, but our lowest value for ECS ( $1^\circ\text{C}$  per  $\text{W}/\text{m}^2$ ) leaves Pliocene  $\text{CO}_2$  near 350 ppm,  
728 rising only to  $\sim 500$  ppm at Oi-1 and  $\sim 1500$  ppm at EECO.

729 Assumed Holocene  $\text{CO}_2$  amount is also a minor factor. We tested two cases: 260 and 278 ppm  
730 (Fig. 9). These were implemented as the  $\text{CO}_2$  values at 7 kyBP, but Holocene-mean values are  
731 similar – a few ppm less than  $\text{CO}_2$  at 7 kyBP. Holocene = 278 ppm increases  $\text{CO}_2$  about 20 ppm  
732 between today and Oi-1, and about 50 ppm at the EECO. However, Holocene  $\text{CO}_2$  278 ppm  
733 causes the amplitude of inferred glacial-interglacial  $\text{CO}_2$  oscillations to be less than reality (Fig.  
734 9b), providing support for the Holocene 260 ppm level and for the interpretation that high late-  
735 Holocene  $\text{CO}_2$  was due to human influence. Proxy measures of Cenozoic  $\text{CO}_2$  yield a notoriously  
736 large range. A recent review<sup>95</sup> constructs a  $\text{CO}_2$  history with Loess-smoothed  $\text{CO}_2 \sim 700$ -1100  
737 ppm at Oi-1. That high Oi-1  $\text{CO}_2$  amount is not plausible without overthrowing the concept that  
738 global temperature is a response to climate forcings. More generally, we conclude that actual  
739  $\text{CO}_2$  during the Cenozoic was near the low end of the range of proxy measurements.

#### 740 **4.4. Interpretation of Cenozoic $T_S$ and $\text{CO}_2$**

741 In this section we consider Cenozoic  $T_S$  and  $\text{CO}_2$  histories, which are rich in insights about  
742 climate change with implications for future climate.

743 In *Target  $\text{CO}_2$* <sup>65</sup> and elsewhere<sup>106</sup> we argue that the broad sweep of Cenozoic temperature is a  
744 result of plate tectonic (popularly “continental drift”) effects on  $\text{CO}_2$ . Solid Earth sources and  
745 sinks of  $\text{CO}_2$  are not balanced at any given time.  $\text{CO}_2$  is removed from surface reservoirs by: (1)  
746 chemical weathering of rocks with deposition of carbonates on the ocean floor, and (2) burial of  
747 organic matter.<sup>107,108</sup>  $\text{CO}_2$  returns via metamorphism and volcanic outgassing at locations where  
748 oceanic crust is subducted beneath moving continental plates. The interpretation in *Target  $\text{CO}_2$*   
749 was that the main Cenozoic source of  $\text{CO}_2$  was associated with the Indian plate (Fig. 10), which  
750 separated from Pangea in the Cretaceous<sup>109,110</sup> and moved through the Tethys (now Indian)  
751 Ocean at a rate exceeding 10 cm/year until collision with the Eurasian plate at circa 50 MyBP.  
752 Associated  $\text{CO}_2$  emissions include those from formation of the Deccan Traps<sup>111</sup> in western India,  
753 a large igneous province (LIP) formed by repeated deposition of large-scale flood basalts, the  
754 smaller Rajahmundry Traps<sup>112</sup> in eastern India, and metamorphism and vulcanism associated  
755 with the moving Indian plate. The Indian plate slowed circa 60 Mya (inset, Fig. 6) before  
756 resuming high speed,<sup>101</sup> leaving an indelible signature in the Cenozoic  $\delta^{18}\text{O}$  history (Fig. 6) that  
757 supports our interpretation of the  $\text{CO}_2$  source. Since the continental collision, subduction and  
758  $\text{CO}_2$  emissions continue at a diminishing rate as the India plate underthrusts the Asian continent  
759 and pushes up the Himalayan mountains.<sup>113</sup> We interpret the decline of  $\text{CO}_2$  over the past 50  
760 million years as, at least in part, a decline of the metamorphic source from continued subduction  
761 of the Indian plate, but burial of organic matter and increased weathering due to exposure of  
762 fresh rock by Himalayan uplift<sup>114</sup> may contribute to  $\text{CO}_2$  drawdown. Quantitative understanding  
763 of these processes is limited,<sup>115</sup> e.g., weathering is both a source and sink of  $\text{CO}_2$ .<sup>116</sup>

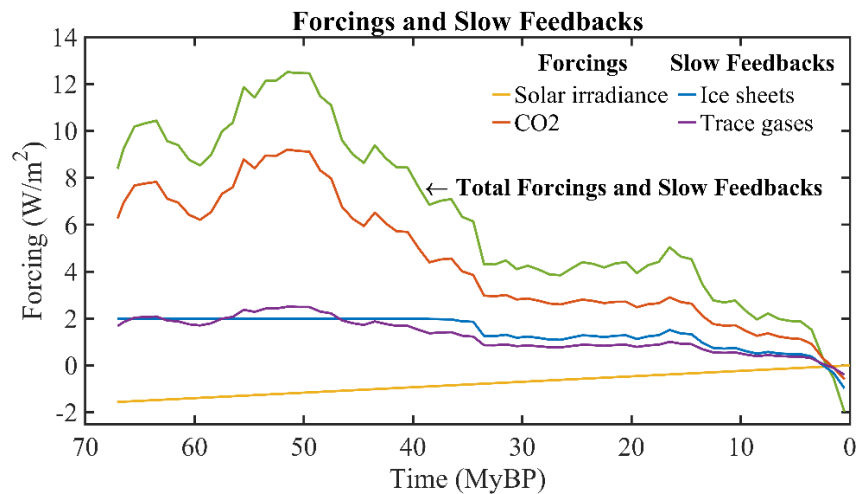


764

765 Fig. 10. Continental configuration 56 MyBP.<sup>117</sup> Continental shelves (light blue) were underwater  
 766 as little water was locked in ice. The Indian plate was moving north at about 15 cm per year.

767 This picture for the broad sweep of Cenozoic CO<sub>2</sub> is consistent with current understanding of the  
 768 long-term carbon cycle,<sup>118</sup> but relative contributions of metamorphism<sup>115</sup> and volcanism<sup>119</sup> are  
 769 uncertain. Also, emissions from rift-induced Large Igneous Provinces (LIPs)<sup>120,121</sup> contribute to  
 770 long-term change of atmospheric CO<sub>2</sub>, with two cases prominent in Fig. 6. The Columbia River  
 771 Flood Basalt at ca. 17-15 MyBP was a principal cause of the Miocene Climatic Optimum,<sup>122</sup> but  
 772 the processes are poorly understood.<sup>123</sup> A more dramatic event occurred as Greenland separated  
 773 from Europe, causing a rift in the sea floor; flood basalt covered more than a million square  
 774 kilometers with magma volume 6-7 million cubic kilometers<sup>121</sup> – the North Atlantic Igneous  
 775 Province (NAIP). Flood basalt volcanism occurred during 60.5-54.5 MyBP, but at 56.1 ± 0.5  
 776 MyBP melt production increased by more than a factor of 10, continued at a high level for about  
 777 a million years, and then subsided (Fig. 5 of Storey *et al.*).<sup>124</sup> The striking Paleocene-Eocene  
 778 Thermal Maximum (PETM) δ<sup>18</sup>O spike (Fig. 6) occurs early in this million-year bump-up of  
 779 δ<sup>18</sup>O. Svensen *et al.*<sup>125</sup> proposed that the PETM was initiated by the massive flood basalt into  
 780 carbon-rich sedimentary strata. Gutjahr *et al.*<sup>126</sup> developed an isotope analysis, concluding that  
 781 most of PETM carbon emissions were volcanic, with climate-driven carbon feedbacks playing a  
 782 lesser role. Yet other evidence,<sup>127</sup> while consistent with volcanism as a trigger for the PETM,  
 783 suggests that climate feedback – perhaps methane hydrate release – may have caused more than  
 784 half of the PETM warming. We discuss PETM warming and CO<sub>2</sub> levels below, but first we must  
 785 quantify the mechanisms that drove Cenozoic climate change and consider where Earth's climate  
 786 was headed before humanity intervened.

787 The sum of climate forcings (CO<sub>2</sub> and solar) and slow feedbacks (ice sheets and non-CO<sub>2</sub> GHGs)  
 788 that maintained EECO warmth was 12.5 W/m<sup>2</sup> (Fig. 11). CO<sub>2</sub> forcing of 9.1 W/m<sup>2</sup> combined  
 789 with solar forcing of – 1.2 W/m<sup>2</sup> to yield a total forcing<sup>128</sup> 8 W/m<sup>2</sup>. Slow feedbacks were 4.5  
 790 W/m<sup>2</sup> forcing (ice albedo = 2 W/m<sup>2</sup> and non-CO<sub>2</sub> GHGs = 2.5 W/m<sup>2</sup>). With today's solar  
 791 irradiance, human-made GHG forcing required for Earth to return to EECO warmth is 8 W/m<sup>2</sup>.  
 792 Present human-made GHG forcing is 4.6 W/m<sup>2</sup> relative to 7 kyBP.<sup>129</sup> Equilibrium response to  
 793 this forcing includes the 2 W/m<sup>2</sup> ice sheet feedback and 25% amplification (of 6.6 W/m<sup>2</sup>) by



794 Fig. 11. Climate forcings and slow feedbacks relative to 7 kyBP from terms in equations (20-22).  
795

796 non-CO<sub>2</sub> GHGs, yielding a total forcing plus slow feedbacks of 8.25 W/m<sup>2</sup>. Thus, equilibrium  
797 global warming for today's GHGs is 10°C.<sup>130</sup> If human-made aerosol forcing is -1.5 W/m<sup>2</sup> and  
798 remains at that level indefinitely, equilibrium warming for today's atmosphere is reduced to 8°C.  
799 Either 10°C or 8°C dwarfs observed global warming of 1.2°C to date. Most of the equilibrium  
800 warming for today's atmosphere has not yet occurred, and need not occur (Section 6.5).

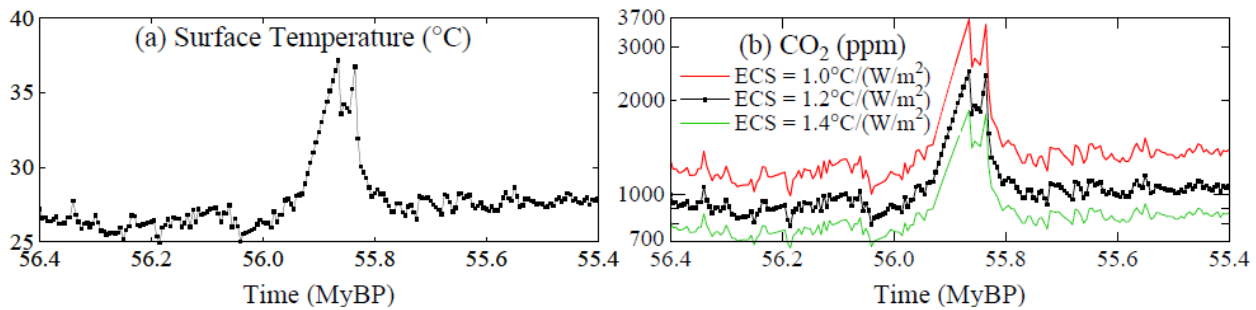
#### 801 4.5 Prospects for another Snowball Earth

802 We would be remiss if we did not comment on the precipitous decline of Earth's temperature  
803 over the last several million years. Was Earth falling off the table into another Snowball Earth?

804 Global temperature plummeted in the past 50 million years, with growing, violent, oscillations  
805 (Figs. 6 and 7). Glacial-interglacial average CO<sub>2</sub> declined from about 325 ppm to 225 ppm in the  
806 past five million years in an accelerating decline (Fig. 9a). As CO<sub>2</sub> fell to 180 ppm in recent  
807 glacial maxima, an ice sheet covered most of Canada and reached midlatitudes in the U.S.  
808 Continents in the current supercontinent cycle<sup>109</sup> are now dispersed, with movement slowing to  
809 2-3 cm/year. Emissions from the last high-speed high-impact tectonic event – collision of the  
810 Indian plate with Eurasia – are fizzling out. The most recent large igneous province (LIP) event –  
811 the Columbia River Flood Basalt about 15 million years ago (Fig. 6) – is no longer a factor, and  
812 there is no evidence of another impending LIP. Snowball conditions are possible, even though  
813 the Sun's brightness is increasing and is now almost 6% greater<sup>74</sup> than it was at the last snowball  
814 Earth, almost 600 million years ago.<sup>73</sup> Runaway snowball likely requires only 1-2 halvings<sup>71</sup> of  
815 CO<sub>2</sub> from the LGM 180 ppm level, i.e., to 45-90 ppm. Although the weathering rate declines in  
816 colder climate,<sup>131</sup> weathering and burial of organic matter continue, so decrease of atmospheric  
817 CO<sub>2</sub> could have continued over millions of years, if the source of CO<sub>2</sub> from metamorphism and  
818 vulcanism continued to decline.

819 Thus, in the absence of human activity, Earth may have been headed for snowball Earth  
820 conditions within the next 10 or 20 million years. However, chance of future snowball Earth is  
821 now academic. Human-made GHG emissions remove that possibility on any time scale of  
822 practical interest. Instead, GHG emissions are now driving Earth toward much warmer climate.





823  
 824 Fig. 12. Temperature and CO<sub>2</sub> implied by δ<sup>18</sup>O, if surface warming equaled deep ocean warming.  
 825 However, PETM surface warming of 5.6°C based on proxy surface temperature data yields peak  
 826 PETM CO<sub>2</sub> = 1630 ppm (see text).

#### 827 4.6. Paleocene Eocene Thermal Maximum (PETM)

828 The PETM event provides an invaluable benchmark for assessing the impact of the human-made  
 829 climate perturbation, as well as the time scale for natural recovery of the climate system.

830 Westerhold data have 10°C deep ocean warming at the PETM, which exceeds warming in proxy  
 831 surface temperature data. Low latitude SST data have 3-4°C PETM warming.<sup>132</sup> GCM-assisted  
 832 data assimilation accounting for patterns of climate change yields PETM global surface warming  
 833 5.6°C (5.4-5.9°C, 95% confidence)<sup>133</sup>. The simplest interpretation is that both results are correct,  
 834 i.e., deep ocean warming at the sampled sites exceeded surface warming during the singular  
 835 PETM event. Nunes and Norris<sup>134</sup> conclude that ocean circulation changed at the start of the  
 836 PETM with a shift in location of deep-water formation that delivered warmer waters to the deep  
 837 sea, a circulation change that persisted at least 40,000 years. The PETM was triggered by a rift in  
 838 the sea floor with massive lave injection into the North Atlantic, so it is not surprising that deep  
 839 ocean temperature was elevated and circulation disrupted during the PETM.

840 We use the 5.6°C global surface warming estimate of Tierney *et al.*<sup>133</sup> and the pre-PETM T<sub>s</sub> and  
 841 CO<sub>2</sub> from our analysis (Fig. 12) to obtain peak PETM CO<sub>2</sub>. With the most likely ECS (1.2°C per  
 842 W/m<sup>2</sup>), pre-PETM (56-56.4 MyBP) CO<sub>2</sub> is 910 ppm and peak PETM CO<sub>2</sub> is 1630 ppm if CO<sub>2</sub>  
 843 provides 80% of the GHG forcing, thus less than a doubling of CO<sub>2</sub>. (In the unlikely case that  
 844 CO<sub>2</sub> caused 100% of the GHG forcing, required CO<sub>2</sub> is 1780, still not quite a doubling.) CO<sub>2</sub>  
 845 amounts for ECS = 1.0 and 1.4°C per W/m<sup>2</sup> are 1165 and 760 ppm in the pre-PETM and 2260  
 846 and 1270 ppm at peak PETM, respectively. In all these ECS cases, the CO<sub>2</sub> forcing of the PETM  
 847 is less than or approximately a CO<sub>2</sub> doubling. Our assumed 20% contribution by non-CO<sub>2</sub> GHGs  
 848 (amplification factor 1.25, Section 2), is nominal; indeed, Hopcroft *et al.*, e.g., estimate a 30%  
 849 contribution from non-CO<sub>2</sub> GHGs,<sup>135</sup> thus an amplification factor 1.43.

850 GHG forcing that drove PETM warming, therefore, was less than or about that for CO<sub>2</sub> doubling  
 851 (~4 W/m<sup>2</sup>), less than today's estimated GHG climate forcing (4.6 W/m<sup>2</sup>) that is still growing 0.5  
 852 W/m<sup>2</sup> per decade. The PETM is relevant to policy considerations, but we must bear in mind two  
 853 differences between the PETM and human-made climate change. First, there were no large ice  
 854 sheets on Earth in the PETM era. Ice sheets on Antarctica and Greenland today make Earth  
 855 system sensitivity (ESS) greater than it was during the PETM. Equilibrium response to today's  
 856 human-made climate forcing would include deglaciation of Antarctica and Greenland, sea level

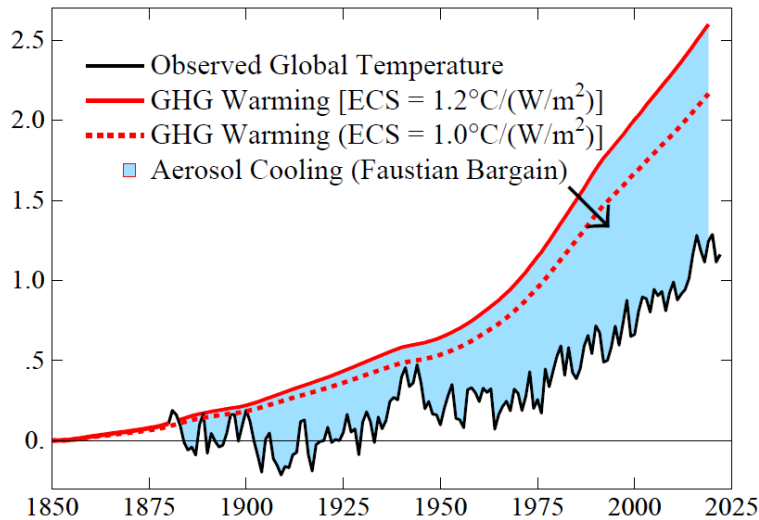
857 rise of 60 m (about 200 feet), and surface albedo forcing of 2 W/m<sup>2</sup>. The second difference  
858 between the PETM and today is the rate of change of the climate forcing. Most of today's  
859 climate forcing was introduced in a century, which is 10 times or more faster than the PETM  
860 forcing growth. Although a bolide impact<sup>136</sup> has been proposed as a trigger for the PETM, the  
861 issue is the time scale on which the climate forcing – increased GHGs – occurred. Despite  
862 uncertainty in the carbon source(s), data and modeling point to duration of a millennium or more  
863 for PETM emissions.<sup>132,137</sup>

864 Better understanding of the PETM could inform us on climate feedbacks. Gutjahr *et al.*<sup>126</sup> argue  
865 persuasively that PETM emissions were mostly volcanic, yet we know of no other large igneous  
866 province that produced such great, temporally-isolated emissions. Further, numerous Cenozoic  
867 hyperthermal events<sup>138</sup> testify to important contributions of feedbacks to CO<sub>2</sub> amount. Northern  
868 peatlands today contain more than 1000 Gt carbon,<sup>139</sup> much of which could be mobilized at  
869 PETM warming levels.<sup>140</sup> The double peak in deep ocean δ<sup>18</sup>O (thus in inferred temperatures, cf.  
870 Fig. 12, where each square is a binning interval of 5,000 years) is also found in terrestrial data.<sup>141</sup>  
871 Perhaps the sea floor rift occurred in two bursts, or the rift was followed tens of thousands of  
872 years later by methane hydrate release as a feedback to the ocean warming; much of today's  
873 methane hydrate is in stratigraphic deposits hundreds of meters below the sea floor, where  
874 millennia may pass before a thermal wave from the surface reaches the deposits.<sup>142</sup> Emissions  
875 from such feedbacks, including permafrost, seem to be more chronic than catastrophic on the  
876 short-term, but if policies are not designed to terminate growth of these feedbacks (Section 6), it  
877 may become impossible to avoid climate catastrophe.

878 The PETM draws attention to differences between the Westerhold and Zachos δ<sup>18</sup>O data. The  
879 PETM warming of 10°C in W data is twice as large as that in Z data. Zachos attributes the larger  
880 PETM response in W data to the shallow (less than 1 km) depth of the Walvis Ridge core that  
881 covers the PETM period in the W data, while Westerhold points out the affect of modern  
882 analytical techniques that affect the amplitude of Cenozoic temperature change (see Supp.  
883 Material SM9). Differences between the W and Z data sets have limited effect on conclusions of  
884 our paper, as we reduce differences via scaling (equations 6-13) for agreement at the LGM, mid-  
885 Holocene, and Oi-1 points. This approach addresses, e.g., the cumulative effect in combining  
886 data splices noted by Zachos in SM9. Further, we set the EECO global temperature relative to the  
887 Holocene and the PETM temperature relative to pre-PETM based on proxy-constrained, full-  
888 field, GCM analyses of Tierney *et al.*<sup>133</sup> and Zhu *et al.*<sup>105</sup> Nevertheless, improved understanding  
889 of the differences between the W and Z data is needed. Potential insights from the PETM are  
890 especially important, given the comparable magnitude of human-made and PETM climate  
891 forcings. The PETM provides perhaps the best empirical check on understanding of the  
892 atmospheric lifetime of fossil fuel CO<sub>2</sub>,<sup>143</sup> but for that purpose we must untangle as well as  
893 possible the time dependence of the PETM CO<sub>2</sub> source and feedbacks. If a continuing magma  
894 flow is a substantial portion of PETM CO<sub>2</sub>, it may lead to exaggeration of CO<sub>2</sub> lifetime.

895 Policy discussion requires also an understanding of the role of aerosols in climate change.

896



897  
 898 Fig. 13. Observed global surface temperature (black line) and expected GHG warming with two  
 899 choices for ECS. The blue area is the estimated aerosol cooling effect. The temperature peak in  
 900 the World War II era is in part an artifact of inhomogeneous ocean data in that period.<sup>68</sup>

## 901 5. AEROSOLS

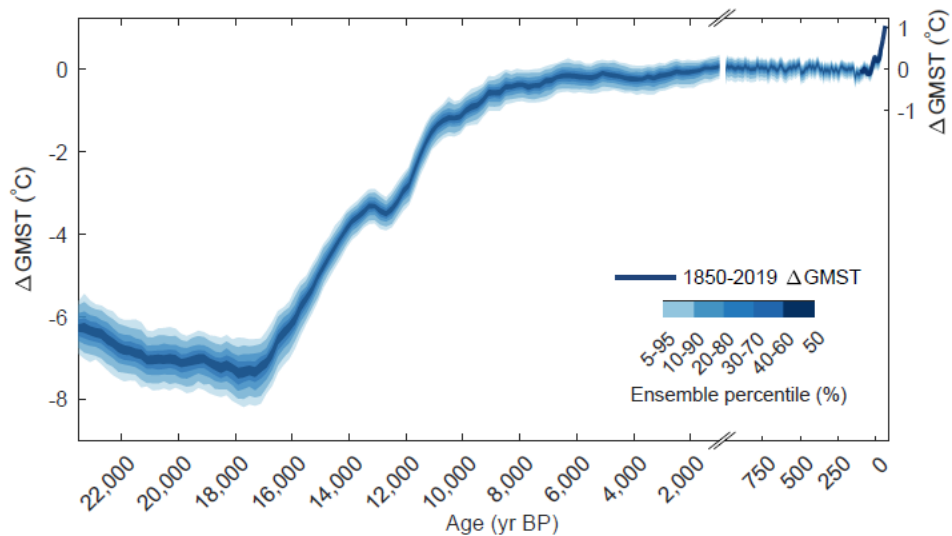
902 The role of aerosols in climate change is uncertain because aerosol properties are not measured  
 903 well enough to define their climate forcing. In this section we find ways to estimate the climate  
 904 forcing via aerosol effects on Earth’s temperature and Earth’s energy imbalance.

905 Aerosol impact is suggested by the gap between observed global warming and expected warming  
 906 due to GHGs based on ECS inferred from paleoclimate (Fig. 13). Expected warming is from Eq.  
 907 4 with the normalized response function of the GISS (2020) model. Our best estimate for ECS,  
 908 1.2°C per W/m<sup>2</sup>, yields a gap of 1.5°C between expected and actual warming in 2022. Aerosols  
 909 are the likely cooling source. The other negative forcing discussed by IPCC – surface albedo  
 910 change – is estimated by IPCC (Chapter 7, Table 7.8) to be  $-0.12 \pm 0.1$  W/m<sup>2</sup>, an order of  
 911 magnitude smaller than aerosol forcing.<sup>13</sup> Thus, for clarity, we focus on GHGs and aerosols.

912 Absence of global warming over the 70-year period 1850-1920 (Fig. SPM.1 of IPCC AR6 WG1  
 913 report<sup>13</sup>) is a clue about aerosol forcing. GHG forcing increased 0.54 W/m<sup>2</sup> in 1850-1920, which  
 914 causes an expected warming  $\sim 0.4^\circ\text{C}$  by 1920 for ECS = 1°C per W/m<sup>2</sup>. Natural forcings – solar  
 915 irradiance and volcanic aerosols – might contribute to lack of warming, but no persuasive case  
 916 has been made for the required downward trends of those forcings. Human-made aerosols are the  
 917 likely offset of GHG warming. Such aerosol cooling is a Faustian bargain<sup>106</sup> because payment in  
 918 enhanced global warming will come due once we can no longer tolerate the air pollution.  
 919 Ambient air pollution causes millions of deaths per year, with particulates most responsible.<sup>144</sup>

### 920 5.1. Evidence of aerosol forcing in the Holocene

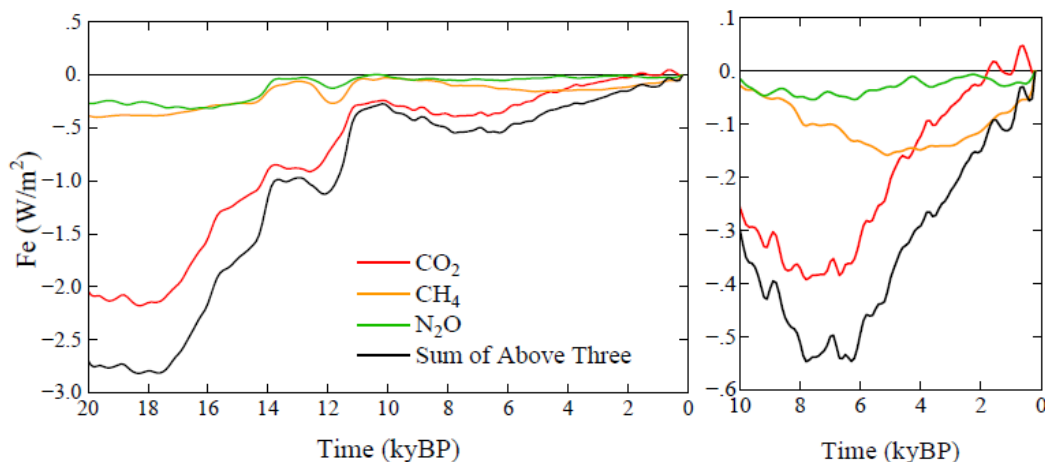
921 In this section we infer evidence of human-made aerosols in the last half of the Holocene from  
 922 the absence of global warming. Some proxy-based analyses<sup>145</sup> report cooling in the last half of  
 923 the Holocene, but a recent analysis<sup>54</sup> that uses GCMs to overcome spatial and temporal biases in  
 924 proxy data finds rising global temperature in the first half of the Holocene followed by nearly



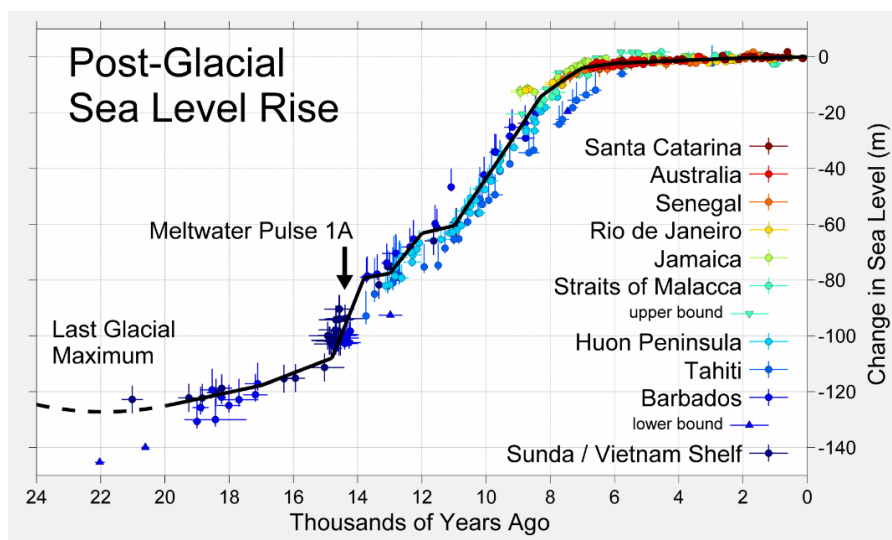
925  
926 Fig. 14. Global mean surface temperature change over the past 24 ky, reproduced from Fig. 2 of  
927 Osman et al.<sup>54</sup> including Last Millennium reanalysis of Tardif *et al.*<sup>146</sup>

928 constant temperature in the last 6,000 years until the last few centuries (Fig. 14). Antarctic, deep  
929 ocean, and tropical sea surface data all show stable temperature in the last 6,000 years (Fig. S6 of  
930 reference<sup>65</sup>). GHG forcing increased  $0.5 \text{ W/m}^2$  during those 6,000 years (Fig. 15), yet Earth did  
931 not warm. Fast feedbacks alone should yield at least  $+0.5^\circ\text{C}$  warming and 6,000 years is long  
932 enough for slow feedbacks to also contribute. How can we interpret the absence of warming?

933 Humanity's growing footprint deserves scrutiny. Ruddiman's suggestion that deforestation and  
934 agriculture began to affect  $\text{CO}_2$  6500 year ago and rice agriculture began to affect  $\text{CH}_4$  5,000  
935 years ago has been criticized<sup>50</sup> mainly because of the size of proposed sources. Ruddiman sought  
936 sources sufficient to offset declines of  $\text{CO}_2$  and  $\text{CH}_4$  in prior interglacial periods, but such large  
937 sources are not needed to account for Holocene GHG levels. Paleoclimate GHG decreases are  
938 slow feedbacks that occur in concert with global cooling. However, if global cooling did not  
939 occur in the past 6,000 years, feedbacks did not occur. Earth orbital parameters 6,000 years ago  
940 kept the Southern Ocean warm, as needed to maintain strong overturning ocean circulation<sup>147</sup>  
941 and minimize carbon sequestration in the deep ocean. Maximum insolation at  $60^\circ\text{S}$  was in late-



942  
943 Fig. 15. GHG climate forcing in past 20 ky with vertical scale expanded for the past 10 ky on the  
944 right. GHG amounts are from Schilt *et al.*<sup>51</sup> and formulae for forcing are in Supporting Material.



945

946 Fig. 16. Sea level since the last glacial period relative to present. Credit: Robert Rohde<sup>148</sup>

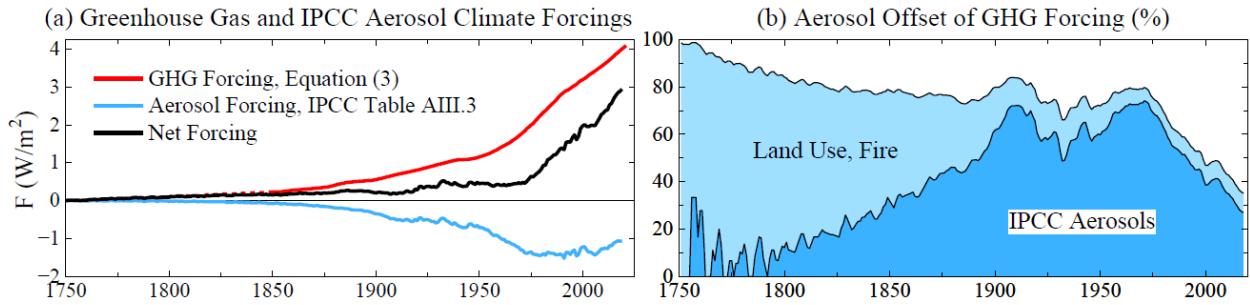
947 spring (mid-November); since then, maximum insolation at 60°S slowly advanced through the  
 948 year, recently reaching mid-summer (mid-January, Fig. 26b of *Ice Melt*<sup>14</sup>). Maximum insolation  
 949 from late-spring through mid-summer is optimum to warm the Southern Ocean and promote  
 950 early warm-season ice melt, which reduces surface albedo and magnifies regional warming.<sup>48</sup>

951 GHG forcing of  $-0.2 \text{ W/m}^2$  in 10-6 kyBP (Fig. 15) was exceeded by forcing of  $+1 \text{ W/m}^2$  due to  
 952 ice sheet shrinkage (Supp. Material in *Target CO<sub>2</sub>*<sup>65</sup>) for a 40 m sea level rise (Fig. 16). Net  $0.8$   
 953  $\text{W/m}^2$  forcing produced expected  $1^\circ\text{C}$  global warming (Fig. 14). The mystery is the absence of  
 954 warming in the past 6,000 years. Hansen *et al.*<sup>48</sup> suggested that aerosol cooling offset GHG  
 955 warming. Growing population, agriculture and land clearance produced aerosols and  $\text{CO}_2$ ; wood  
 956 was the main fuel for cooking and heating. Nonlinear aerosol forcing is largest in a pristine  
 957 atmosphere, so it is unsurprising that aerosols tended to offset  $\text{CO}_2$  warming as civilization  
 958 developed. Hemispheric differences could provide a check. GHG forcing is global, while aerosol  
 959 forcing is mainly in the Northern Hemisphere. Global offset implies a net negative Northern  
 960 Hemisphere forcing and positive Southern Hemisphere forcing. Thus, data and modeling studies  
 961 (including orbital effects) of regional response are warranted but beyond the scope of this paper.

## 962 5.2. Industrial era aerosols

963 Scientific advances often face early resistance from other scientists.<sup>149</sup> Examples are the  
 964 snowball Earth hypothesis<sup>150</sup> and the role of an asteroid impact in extinction of non-avian  
 965 dinosaurs,<sup>151</sup> which initially were highly controversial but are now more widely accepted.  
 966 Ruddiman's hypothesis, right or wrong, is still controversial. Thus, we minimize this issue by  
 967 showing aerosol effects with and without preindustrial human-made aerosols.

968 Global aerosols are not monitored with detail needed to define aerosol climate forcing.<sup>152,153</sup>  
 969 IPCC<sup>13</sup> estimates forcing (Fig. 17a) from assumed precursor emissions, a herculean task due to  
 970 many aerosol types and complex cloud effects. Aerosol forcing uncertainty is comparable to its  
 971 estimated value (Fig. 17a), which is constrained more by observed global temperature change  
 972 than by aerosol measurements.<sup>154</sup> IPCC's best estimate of aerosol forcing (Fig. 107) and GHG



973  
 974 Fig. 17. (a) Estimated greenhouse gas and aerosol forcings relative to 1750 values. (b) Aerosol forcing as  
 975 percent of GHG forcing. Forcings for dark blue area are relative to 1750. Light blue area adds 0.5 W/m<sup>2</sup>  
 976 forcing estimated for human-caused aerosols from fires, biofuels and land use.

977 history define the percent of GHG forcing offset by aerosol cooling – the dark blue area in Fig.  
 978 17b. However, if human-made aerosol forcing was  $-0.5 \text{ W/m}^2$  by 1750, offsetting  $+0.5 \text{ W/m}^2$   
 979 GHG forcing, this forcing should be included. Such aerosol forcing – largely via effects of land  
 980 use and biomass fuels on clouds – continues today. Thirty million people in the United States use  
 981 wood for heating.<sup>155</sup> Such fuels are also common in Europe<sup>156,157</sup> and much of the world.

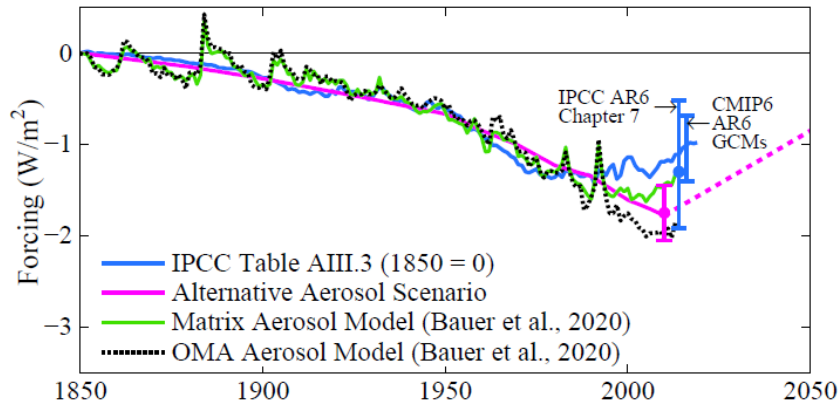
982 Fig. 17b encapsulates two alternative views of aerosol history. IPCC aerosol forcing slowly  
 983 becomes important relative to GHG forcing. In our view, civilization always produced aerosols  
 984 as well as GHGs. As sea level stabilized, organized societies and population grew as coastal  
 985 biologic productivity increased<sup>158</sup> and agriculture developed. Wood was the main fuel. Aerosols  
 986 travel great distances, as shown by Asian aerosols in North America.<sup>159</sup> Humans contributed to  
 987 both rising GHG and aerosol climate forcings in the past 6,000 years. One result is that human-  
 988 caused aerosol climate forcing is at least  $0.5 \text{ W/m}^2$  more than usually assumed. Thus, the  
 989 Faustian payment that will eventually come due is also larger, as discussed in Section 6.

### 990 5.3. Ambiguity in aerosol climate forcing

991 In this section we discuss uncertainty in the aerosol forcing. We discuss why global warming in  
 992 the past century – often used to infer climate sensitivity – is ill-suited for that purpose.

993 Recent global warming does not yield a unique ECS because warming depends on three major  
 994 unknowns with only two basic constraints. Unknowns are ECS, net climate forcing (aerosol  
 995 forcing is unmeasured), and ocean mixing (many ocean models are too diffusive). Constraints  
 996 are observed global temperature change and Earth's energy imbalance (EEI).<sup>87</sup> Knutti<sup>160</sup> and  
 997 Hansen<sup>79</sup> suggest that many climate models compensate for excessive ocean mixing (which  
 998 reduces surface warming) by using aerosol forcing less negative than the real world, thus  
 999 achieving realistic surface warming. This issue is unresolved and complicated by the finding that  
 1000 cloud feedbacks can buffer ocean heat uptake (Section 3), affecting interpretation of EEI.

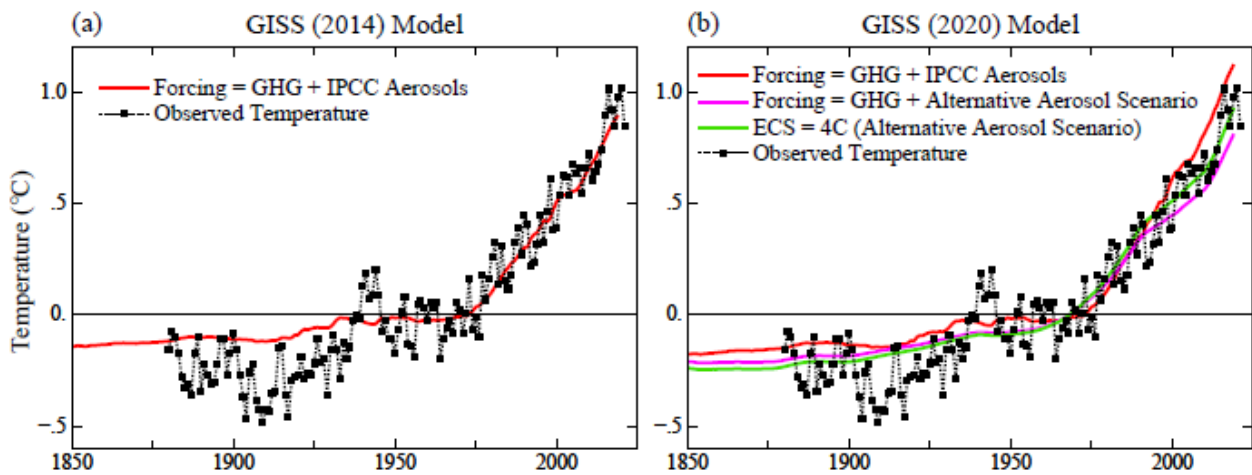
1001 IPCC AR6 WG1 best estimate of aerosol forcing (Table AIII.3)<sup>13</sup> is near maximum (negative)  
 1002 value by 1975, then nearly constant until rising in the 21<sup>st</sup> century to  $-1.09 \text{ W/m}^2$  in 2019 (Fig.  
 1003 18). We use this IPCC aerosol forcing in climate simulations here. We also use an alternative  
 1004 aerosol scenario<sup>161</sup> that reaches  $-1.63 \text{ W/m}^2$  in 2010 relative to 1880 and  $-1.8 \text{ W/m}^2$  relative to  
 1005 1850 (Fig. 18) based on modeling of Koch<sup>162</sup> that included changing technology factors defined  
 1006 by Novakov.<sup>163</sup> This alternative scenario<sup>164</sup> is comparable to the forcing in some current aerosol



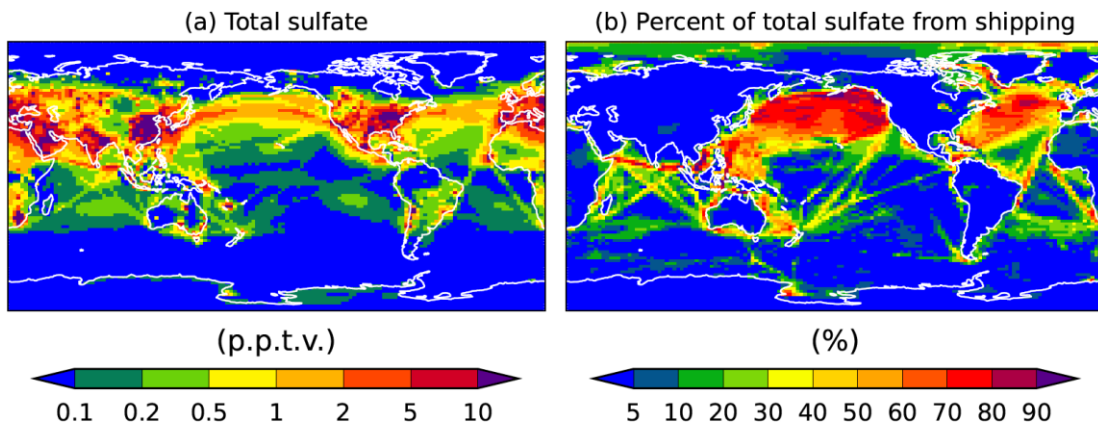
1007  
 1008 Fig. 18. Aerosol forcing relative to 1850 from IPCC AR6, an alternative aerosol scenario<sup>161</sup> and  
 1009 two aerosol model scenarios of Bauer et al. (2020).<sup>165</sup>

1010 models (Fig. 18). Human-made aerosol forcing relative to several millennia ago may be even  
 1011 more negative, by about  $-0.5 \text{ W/m}^2$  as discussed above, but the additional forcing was offset by  
 1012 increasing GHGs and thus those additional forcings are neglected, with climate assumed to be in  
 1013 approximate equilibrium in 1850.

1014 Many combinations of climate sensitivity and aerosol forcing can fit observed global warming.  
 1015 The GISS (2014) model ( $\text{ECS} = 2.6^\circ\text{C}$ ) with IPCC AR6 aerosol forcing can match observed  
 1016 warming (Fig. 19) in the last half century (when human-made climate forcing overwhelmed  
 1017 natural forcings, unforced climate variability, and flaws in observations). However, agreement  
 1018 also can be achieved by climate models with high ECS. The GISS (2020) model (with  $\text{ECS} =$   
 1019  $3.5^\circ\text{C}$ ) yields greater warming than observed if IPCC aerosol forcing is used, but less than  
 1020 observed for the alternative aerosol scenario (Fig. 19). This latter aerosol scenario achieves  
 1021 agreement with observed warming if  $\text{ECS} \sim 4^\circ\text{C}$  (green curve in Fig. 19).<sup>166</sup> Agreement can be  
 1022 achieved with even higher ECS by use of a still more negative aerosol forcing.



1023  
 1024 Fig. 19. Global temperature change  $T_G$  due to aerosols + GHGs calculated with Green's function  
 1025 Eq (5) using GISS (2014) and GISS (2020) response functions (Fig. 4). Observed temperature is  
 1026 the NASA GISS analysis.<sup>167,168</sup> Base period: 1951-1980 for observations and model.



1027  
1028 Fig. 20. Total sulfate (parts per trillion by volume) and percentage of total sulfate provided by  
1029 shipping in simulations of Jin *et al.*<sup>169</sup> prior to IMO regulations on sulfur content of fuels.

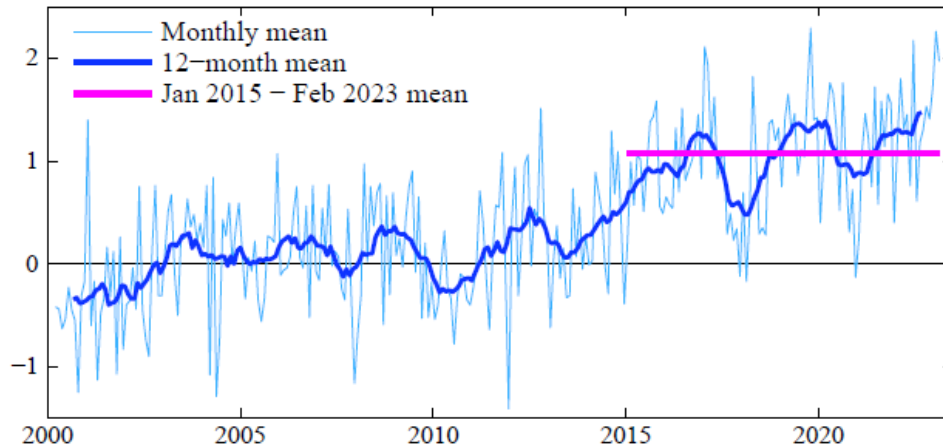
1030 The issue we raise is the magnitude of the aerosol forcing, with implications for future warming  
1031 when particulate air pollution is likely to be reduced. We suggest that IPCC reports may have  
1032 gravitated toward climate sensitivity near 3°C for 2×CO<sub>2</sub> in part because of difficulty that  
1033 models have in realistically simulating amplifying cloud feedbacks and a climate model tendency  
1034 for excessive mixing of heat into the deep ocean. Our finding from paleoclimate analysis that  
1035 ECS is 1.2°C ± 0.3°C per W/m<sup>2</sup> (4.8°C ± 1.2°C for 2×CO<sub>2</sub>) implies that the (unmeasured)  
1036 aerosol forcing must be more negative than IPCC’s best estimate. In turn – because aerosol-  
1037 cloud interactions are the main source of uncertainty in aerosol forcing – this finding emphasizes  
1038 the need to measure both global aerosol and cloud particle properties.

1039 The case for monitoring global aerosol climate forcing will grow as recognition of the need to  
1040 slow and reverse climate change emerges. Aerosol and cloud particle microphysics must be  
1041 measured with precision adequate to define the forcing.<sup>170,152</sup> In the absence of such Keeling-like  
1042 global monitoring, progress can be made via more limited satellite measurements of aerosol and  
1043 cloud properties, field studies, and aerosol and cloud modeling. As described next, a great  
1044 opportunity to study aerosol and cloud physics is provided by a recent change in the IMO  
1045 (International Maritime Organization) regulations on ship emissions.

#### 1046 5.4. The great inadvertent aerosol experiment

1047 Sulfate aerosols are cloud condensation nuclei (CCN), so sulfate emissions by ships result in a  
1048 larger number of smaller cloud particles, thus affecting cloud albedo and cloud lifetime.<sup>171</sup> Ships  
1049 provide a large percentage of sulfates in the North Pacific and North Atlantic regions (Fig. 20). It  
1050 has been suggested that cooling by these clouds is overestimated because of cloud liquid water  
1051 adjustments,<sup>172</sup> but Manshausen *et al.*<sup>173</sup> present evidence that liquid water path (LWP) effects  
1052 are substantial even in regions without visible ship-tracks; they estimate a LWP forcing  $-0.76 \pm$   
1053  $0.27$  W/m<sup>2</sup>, in stark contrast with the IPCC estimate of  $+0.2 \pm 0.2$  W/m<sup>2</sup>. Wall *et al.*<sup>174</sup> use  
1054 satellite observations to quantify relationships between sulfates and low-level clouds; they  
1055 estimate a sulfate indirect aerosol forcing of  $-1.11 \pm 0.43$  W/m<sup>2</sup> over the global ocean. The  
1056 range of aerosol forcings used in CMIP6 and AR6 GCMs (small blue bar in Fig. 18) is not a  
1057 measure of aerosol forcing uncertainty. The larger bar, from Chapter 7<sup>175</sup> of AR6, has negative  
1058 forcing as great as  $-2$  W/m<sup>2</sup>, but even that does not measure the full uncertainty.



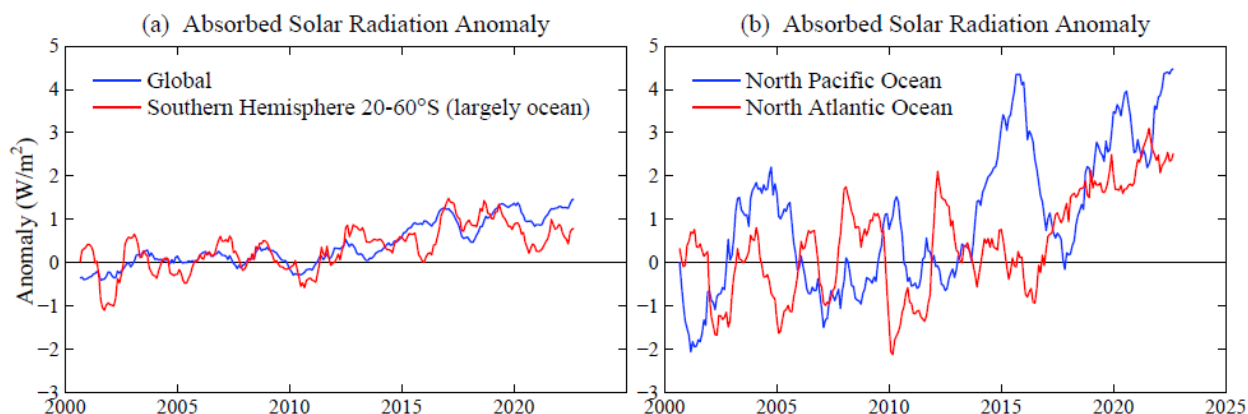


1059  
 1060 Fig. 21. Global absorbed solar radiation ( $\text{W}/\text{m}^2$ ) relative to mean of the first 120 months of  
 1061 CERES data. CERES data are available at [http://ceres.larc.nasa.gov/order\\_data.php](http://ceres.larc.nasa.gov/order_data.php)

1062 Changes of IMO emission regulations provide a great opportunity for insight into aerosol climate  
 1063 forcing. Sulfur content of fuels was limited to 1% in 2010 near the coasts of North America and  
 1064 in the North Sea, Baltic Sea and English Channel, and further restricted there to 0.1% in 2015.<sup>176</sup>  
 1065 In 2020 a limit of 0.5% was imposed worldwide. The 1% limit did not have a noticeable effect  
 1066 on ship-tracks, but a striking reduction of ship-tracks was found after the 2015 IMO regulations,  
 1067 especially in the regions near land where emissions were specifically limited.<sup>177</sup> Following the  
 1068 additional 2020 regulations,<sup>178</sup> global ship-tracks were reduced more than 50%.<sup>179</sup>

1069 Earth's albedo (reflectivity) measured by CERES (Clouds and Earth's Radiant Energy System)  
 1070 satellite-borne instruments<sup>88</sup> over the 22-years March 2000 to March 2022 reveal a decrease of  
 1071 albedo and thus an increase of absorbed solar energy coinciding with the 2015 change of IMO  
 1072 emission regulations. Global absorbed solar energy is  $+1.05 \text{ W}/\text{m}^2$  in the period January 2015  
 1073 through December 2022 relative to the mean for the first 10 years of data (Fig. 21). This increase  
 1074 is 5 times greater than the standard deviation ( $0.21 \text{ W}/\text{m}^2$ ) of annual absorbed solar energy in the  
 1075 first 10 years of data and 4.5 times greater than the standard deviation ( $0.23 \text{ W}/\text{m}^2$ ) of CERES  
 1076 data through December 2014. The increase of absorbed solar energy is notably larger than  
 1077 estimated potential CERES instrument drift, which is  $<0.085 \text{ W}/\text{m}^2$  per decade.<sup>88</sup> Increased solar  
 1078 energy absorption occurred despite 2015-2020 being the declining phase of the  $\sim 11$ -year solar  
 1079 irradiance cycle.<sup>180</sup> Nor can increased absorption be attributed to correlation of Earth's albedo  
 1080 (and absorbed solar energy) with the Pacific Decadal Oscillation (PDO): the PDO did shift to the  
 1081 positive phase in 2014-2017, but it returned to the negative phase in 2017-2022.<sup>181</sup>

1082 Given the large increase of absorbed solar energy, cloud changes are likely the main cause.  
 1083 Quantitative analysis<sup>181</sup> of contributions to the 20-year trend of absorbed solar energy show that  
 1084 clouds provide most of the change. Surface albedo decrease due to sea ice decline contributes to  
 1085 the 20-year trend in the Northern Hemisphere, but that sea ice decline occurred especially in  
 1086 2007, with minimum sea ice cover reached in 2012; over the past decade as global and  
 1087 hemispheric albedos declined, sea ice had little trend.<sup>182</sup> Potential causes of the cloud changes  
 1088 include: 1) reduced aerosol forcing, 2) cloud feedbacks to global warming, 3) natural  
 1089 variability.<sup>183</sup> Absorbed solar energy was  $0.80 \text{ W}/\text{m}^2$  greater in Jan2015-Feb2023 than in the first



1090  
 1091 Fig. 22. Absorbed solar radiation for indicated regions relative to first 120 months of CERES  
 1092 data. Southern Hemisphere 20-60°S is 89% ocean. North Atlantic is (20-60°N, 0-60°W) and  
 1093 North Pacific is (20-60°N, 120-220°W). Data source: [http://ceres.larc.nasa.gov/order\\_data.php](http://ceres.larc.nasa.gov/order_data.php)

1094 decade of CERES data at latitudes 20-60°S (Fig. 22), a region of relatively little ship traffic. This  
 1095 change is an order of magnitude larger than the estimate of potential detector degradation.<sup>88</sup>  
 1096 Climate models predict a reduction of cloud albedo in this region as a feedback effect driven by  
 1097 global warming.<sup>184</sup> Continued monitoring of absorbed energy can confirm the reality of the  
 1098 change, but without global monitoring of detailed physical properties of aerosols and clouds,<sup>152</sup> it  
 1099 will be difficult to apportion observed change among the candidate causes.

1100 The North Pacific and North Atlantic regions of heavy ship traffic are ripe for more detailed  
 1101 study of cloud changes and their causes, although unforced cloud variability is large in such sub-  
 1102 global regions. North Pacific and North Atlantic regions both have increased absorption of solar  
 1103 radiation after 2015 (Fig. 22). The 2014-2017 maximum absorption in the North Pacific is likely  
 1104 enhanced by reduced cloud cover during the positive PDO, but the more recent high absorption  
 1105 is during the negative PDO phase. In the North Atlantic, the persistence of increased absorption  
 1106 for the past several years exceeds prior variability, but longer records plus aerosol and cloud  
 1107 microphysical data are needed for full interpretation.

## 1108 6. SUMMARY

1109 Earth's climate is characterized – ominously – by amplifying feedbacks and delayed response.  
 1110 Feedbacks and delayed response have been recognized for at least 40 years, but they are difficult  
 1111 to quantify. Feedbacks determine climate sensitivity to applied forcing. Delayed response makes  
 1112 human-made climate forcing a threat to today's public and future generations because of the  
 1113 practical difficulty of reversing the forcing once consequences become apparent to the public.  
 1114 Thus, there is a premium on knowledge of climate sensitivity and response time, and the  
 1115 implications must be delivered to the public as soon as possible. This objective confronts the  
 1116 barrier of scientific reticence, which is illustrated by the following example: Richard Feynman  
 1117 needed fellow physicists about their reticence to challenge authority,<sup>185</sup> using the famous oil  
 1118 drop experiment in which Millikan derived the electron charge. Millikan's result was a bit off.  
 1119 Later researchers only moved his result in small increments – uncertainties and choices in  
 1120 experiments require judgment – and it thus required years for the community to achieve an  
 1121 accurate value. Their reticence to contradict Millikan was an embarrassment to the physics

1122 community, but it caused no harm to society. Scientific reticence,<sup>186</sup> in part, may be a  
1123 consequence of the scientific method, which is fueled by objective skepticism. Another factor  
1124 that contributes to irrational reticence among rational scientists is “delay discounting,” a  
1125 preference for immediate over delayed rewards.<sup>187</sup> The penalty for “crying wolf” is immediate,  
1126 while the danger of being blamed for having “fiddled while Rome was burning” is distant. Also,  
1127 one of us has noted<sup>188</sup> evidence that larding of papers and research proposals with caveats and  
1128 uncertainties notably increases chances of obtaining research support. “Gradualism” that results  
1129 from reticence seems to be comfortable and well-suited for maintaining long-term support.

1130 Reticence and gradualism reach a new level with the Intergovernmental Panel on Climate  
1131 Change (IPCC). The prime example is IPCC’s history in evaluating climate sensitivity, the most  
1132 basic measure of climate change, as summarized in our present paper. IPCC reports must be  
1133 approved by UN-assembled governments, but that constraint should not dictate reticence and  
1134 gradualism. Climate science clearly reveals the threat of being too late. “Being too late” refers  
1135 not only to assessment of the climate threat, but also to technical advice on the implications of  
1136 climate science for policy. Are not we as scientists complicit if we allow reticence and comfort  
1137 to obfuscate our description of the climate situation and its implications? Does our training –  
1138 years of graduate study and decades of experience – not make us the best-equipped to advise the  
1139 public on the climate situation and its implications for policy? As professionals with the deepest  
1140 understanding of planetary change and as guardians of young people and their future, do we not  
1141 have an obligation, analogous to the code of ethics of medical professionals, to render to the  
1142 public our full and unencumbered diagnosis and its implications? That is our aim here.

### 1143 **6.1. Equilibrium climate sensitivity (ECS)**

1144 The 1979 Charney study<sup>4</sup> considered an idealized climate sensitivity in which ice sheets and non-  
1145 CO<sub>2</sub> GHGs are fixed. The Charney group estimated that the equilibrium response to 2×CO<sub>2</sub>, a  
1146 forcing of 4 W/m<sup>2</sup>, was 3°C, thus an ECS of 0.75°C per W/m<sup>2</sup>, with one standard deviation  
1147 uncertainty  $\sigma = 0.375^\circ\text{C}$ . Charney’s estimate stood as the canonical ECS for more than 40 years.  
1148 The current IPCC report<sup>13</sup> concludes that 3°C for 2×CO<sub>2</sub> is their best estimate for ECS.

1149 We compare recent glacial and interglacial climates to infer ECS with a precision not possible  
1150 with climate models alone. Uncertainty about Last Glacial Maximum (LGM) temperature has  
1151 been resolved independently with consistent results by Tierney *et al.*<sup>53</sup> and Seltzer *et al.*<sup>56</sup> The  
1152 Tierney approach, using a collection of geochemical temperature indicators in a global analysis  
1153 constrained by climate change patterns defined by a global climate model, is used by Osman *et*  
1154 *al.*<sup>54</sup> to find peak LGM cooling  $7.0 \pm 1^\circ\text{C}$  ( $2\sigma$ , 95% confidence) at 21-18 kyBP. We show that,  
1155 accounting for polar amplification, these analyses are consistent with the  $5.8 \pm 0.6^\circ\text{C}$  LGM  
1156 cooling of land areas between 45°S and 35°N found by Seltzer *et al.* using the temperature-  
1157 dependent solubility of dissolved noble gases in ancient groundwater. The forcing that  
1158 maintained the 7°C LGM cooling was the sum of  $2.25 \pm 0.45 \text{ W/m}^2$  ( $2\sigma$ ) from GHGs and  $3.5 \pm$   
1159  $1.0 \text{ W/m}^2$  ( $2\sigma$ ) from the LGM surface albedo, thus  $5.75 \pm 1.1 \text{ W/m}^2$  ( $2\sigma$ ). ECS implied by the  
1160 LGM is thus  $1.22 \pm 0.29^\circ\text{C}$  ( $2\sigma$ ) per W/m<sup>2</sup>, which, at this final step, we round to  $1.2 \pm 0.3^\circ\text{C}$  per  
1161 W/m<sup>2</sup>. For transparency, we have combined uncertainties via simple RMS (root-mean-square).  
1162 ECS as low as 3°C for 2×CO<sub>2</sub> is excluded at the 3 $\sigma$  level, i.e., with 99.7% confidence.

1163 More sophisticated mathematical analysis, which has merits but introduces opportunity for prior  
1164 bias and obfuscation, is not essential; error assessment ultimately involves expert judgement.  
1165 Instead, focus is needed on the largest source of error: LGM surface albedo change, which is  
1166 uncertain because of the effect of cloud shielding on the efficacy of the forcing. As cloud  
1167 modeling is advancing rapidly, the topic is ripe for collaboration of CMIP<sup>58</sup> (Coupled Model  
1168 Intercomparison Project) with PMIP<sup>59</sup> (Paleoclimate Modelling Intercomparison Project).  
1169 Simulations should include at the same time change of surface albedo and topography of ice  
1170 sheets, vegetation change, and exposure of continental shelves due to lower sea level.

1171 Knowledge of climate sensitivity can be advanced further via analysis of the wide climate range  
1172 in the Cenozoic era (Section 6.3). However, interpretation of data and models, and especially  
1173 projections of climate change, depend on understanding of climate response time.

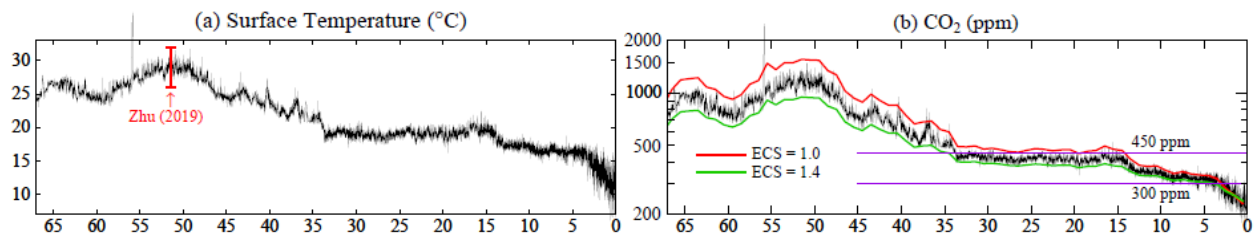
## 1174 **6.2. Climate response time**

1175 We expected climate response time – the time for climate to approach a new equilibrium after  
1176 imposition of a forcing – to become faster as mixing of heat in ocean models improved.<sup>79</sup> That  
1177 expectation was not met when we compared two generations of the GISS GCM. The GISS  
1178 (2020) GCM is demonstrably improved<sup>34,35</sup> in its ocean simulation over the GISS (2014) GCM  
1179 as a result of higher vertical and horizontal resolution, more realistic parameterization of sub-grid  
1180 scale motions, and correction of errors in the ocean computer program.<sup>34</sup> Yet the time required  
1181 for the model to achieve 63% of its equilibrium response remains about 100 years. There are two  
1182 reasons for this, one that is obvious and one that is more interesting and informative.

1183 The surface in the newer model warms as fast as in the older model, but it must achieve greater  
1184 warming to reach 63% of equilibrium because its ECS is higher, which is the first reason that the  
1185 response time remains long. The other reason is that Earth's energy imbalance (EEI) in the newer  
1186 model decreases rapidly. EEI defines the rate that heat is pumped into the ocean, so a smaller  
1187 EEI implies a longer time for the ocean to reach its new equilibrium temperature. Quick drop of  
1188 EEI – in the first year after introduction of the forcing – implies existence of ultrafast feedback in  
1189 the GISS (2020) model. For want of an alternative with such a large effect on Earth's energy  
1190 budget, we infer a rapid cloud feedback and we suggest (Section 3.3) a set of brief GCM runs  
1191 that could define cloud changes and other diagnostic quantities to an arbitrary accuracy.

1192 The Charney report<sup>4</sup> recognized that clouds were a main cause of a wide range in ECS estimates.  
1193 Today, clouds still cast uncertainty on climate predictions. Several CMIP6<sup>36</sup> GCMs have ECS of  
1194 ~ 4-6°C for 2×CO<sub>2</sub><sup>189,190</sup> with the high sensitivity caused by cloud feedbacks.<sup>91</sup> As cloud  
1195 modeling progresses, it will aid understanding if climate models report their 2×CO<sub>2</sub> response  
1196 functions for both temperature and EEI (Earth's energy imbalance).

1197 Fast EEI response – faster than global temperature response – has a practical effect: observed  
1198 EEI understates the reduction of climate forcing required to stabilize climate. Although the  
1199 magnitude of this effect is uncertain (see Supporting Material SM6), it makes the task of  
1200 restoring a hospitable climate and saving coastal cities more challenging. On the other hand, long  
1201 climate response time implies the potential for educated policies to affect the climate outcome  
1202 before the most undesirable consequences occur.



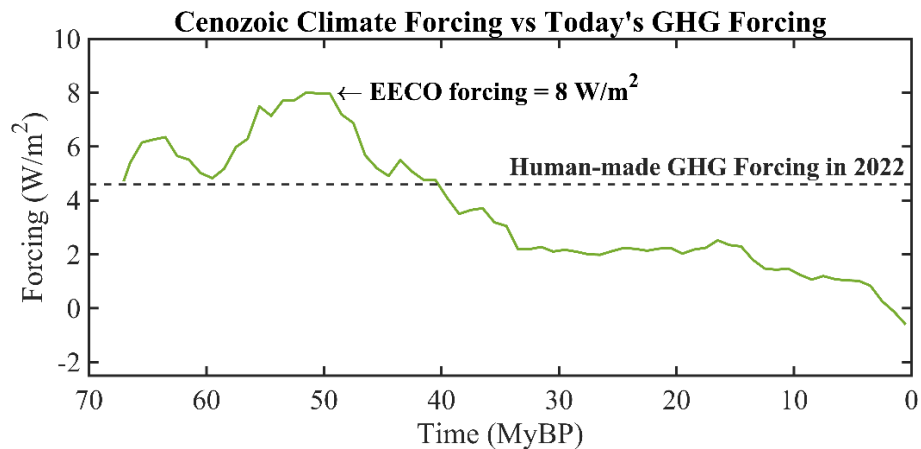
1203  
 1204 Fig. 23. (a) Cenozoic surface temperature estimated from deep ocean oxygen isotope data of  
 1205 Westerhold *et al.*<sup>98</sup> and (b) implied CO<sub>2</sub> history for ECS = 1.2°C per W/m<sup>2</sup> (black curve); red and  
 1206 green curves for ECS = 1.0 and 1.4°C per W/m<sup>2</sup> are 1 My smoothed.

1207 The time required for climate to reach a new equilibrium is relevant to policy (Section 6.6), but  
 1208 there is another response time of practical importance. With climate in a state of disequilibrium,  
 1209 how much time do we have before we pass the point of no return, the point where major climate  
 1210 impacts are locked in, beyond our ability to control? That’s a complex matter; it requires  
 1211 understanding of “slow” feedbacks, especially ice sheets. It also depends on how far climate is  
 1212 out of equilibrium. Thus, we first consider the full Earth system sensitivity.

### 1213 6.3. Earth system sensitivity (ESS)

1214 The Cenozoic era – the past 66 million years – provides an opportunity to study Earth system  
 1215 sensitivity via a consistent analysis for climate ranging from hothouse conditions with Earth  
 1216 15°C warmer and sea level 60 m higher than preindustrial climate to glacial conditions with  
 1217 Earth 7°C cooler and sea level 120 m lower than preindustrial. Atmospheric CO<sub>2</sub> amount in the  
 1218 past 800,000 years, known from bubbles of air trapped in the Antarctic ice sheet, confirms  
 1219 expectation that CO<sub>2</sub> is the main control knob<sup>94</sup> on global temperature (Fig. 2). We can assume  
 1220 this control existed at earlier times when CO<sub>2</sub> amount was larger as a result of CO<sub>2</sub> emissions  
 1221 caused by plate tectonics (continental drift). The two-step<sup>101</sup> that the Indian plate executed as it  
 1222 moved through the Tethys (now Indian) ocean left an indelible signature in atmospheric CO<sub>2</sub> and  
 1223 global temperature. CO<sub>2</sub> emissions from subduction of ocean crust were greatest when the Indian  
 1224 plate was moving fastest (inset, Fig. 6) and peaked at its hard collision with the Eurasian plate at  
 1225 50 MyBP. Diminishing metamorphic CO<sub>2</sub> emissions continue as the Indian plate is subducted  
 1226 beneath the Eurasian plate, pushing up the Himalayan Mountains, but carbon drawdown from  
 1227 weathering and burial of organic carbon exceeds emissions. Motion of the Indian Plate thus  
 1228 dominates the broad sweep of Cenozoic CO<sub>2</sub>, but igneous provinces play a role. The North  
 1229 Atlantic Igneous Province (caused by a rift in the sea floor as Greenland pulled away from  
 1230 Europe) that triggered the Paleocene-Eocene Thermal Maximum (PETM) event about 56 MyBP  
 1231 and the Columbia River Flood Basalt about 15 MyBP (Fig. 6) are most notable.

1232 We infer the Cenozoic history of sea surface temperature (SST) at sites of deepwater formation  
 1233 from the oxygen isotope  $\delta^{18}\text{O}$  in shells of deep-ocean-dwelling foraminifera preserved in ocean  
 1234 sediments.<sup>47,98</sup> The high latitude SST change – including a correction term as SST approaches  
 1235 the freezing point – provides an accurate estimate of global surface temperature change. This  
 1236 Cenozoic temperature history and climate sensitivity inferred from the LGM cooling define the  
 1237 Cenozoic CO<sub>2</sub> history. We suggest that this whole-Cenozoic approach defines the CO<sub>2</sub> history  
 1238 (Fig. 23b) more accurately than CO<sub>2</sub> proxy measurements. We find CO<sub>2</sub> about 325 ppm in the  
 1239 early Pliocene and 450 ppm at transition to glaciated Antarctica. Global climate models (GCMs)



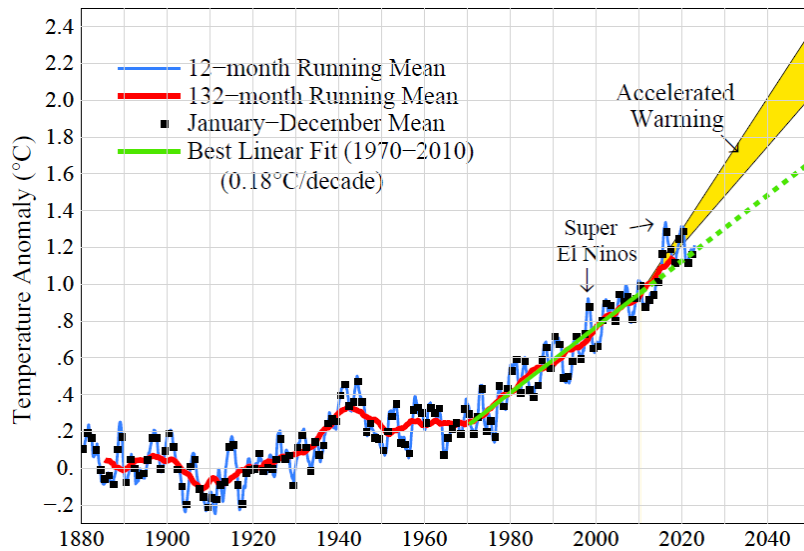
1240 Fig. 24. Forcing required to yield Cenozoic temperature for today’s solar irradiance, compared  
 1241 with human-made GHG forcing in 2022.  
 1242

1243 that isolate on the Pliocene tend to use CO<sub>2</sub> levels of order 400 ppm in attempts to match actual  
 1244 Pliocene warmth and ice sheet models use CO<sub>2</sub> of order 700 ppm or greater to achieve ice sheet  
 1245 disintegration on Antarctica, which suggests that the models are not realistically capturing  
 1246 amplifying feedback processes (see Section 4.3).

1247 The Cenozoic provides a perspective on present greenhouse gas (GHG) levels. The dashed line  
 1248 in Fig. 24 marks the “we are here” level of GHG climate forcing, which is more than half of the  
 1249 forcing that maintained EECO global temperature of +15°C relative to the Holocene. Today’s  
 1250 GHG forcing of 4.6 W/m<sup>2</sup> is relative to mid-Holocene CO<sub>2</sub> of 260 ppm; we present evidence in  
 1251 Section 4.3 that 260 ppm is the natural Holocene CO<sub>2</sub> level. GHG forcing today already is well  
 1252 above the level needed to deglaciate Antarctica, if the forcing is left in place long enough. We  
 1253 are not predicting deglaciation of Antarctica on a time scale that today’s people would care about  
 1254 – rather we are drawing attention to how far today’s climate is out of equilibrium with today’s  
 1255 GHG level. The extent that the climate is out of equilibrium with atmospheric composition is one  
 1256 measure of how strongly humanity is pushing the climate system. Hope of approximately  
 1257 stabilizing climate requires removing the disequilibrium by reducing human-made climate  
 1258 forcing. The danger is that – if deglaciation is allowed to get well underway – it will become  
 1259 difficult if not impossible to prevent large sea level rise.

1260 GHGs are not the only large human-made climate forcing. Understanding of ongoing climate  
 1261 change requires that we also include the effect of aerosols (fine airborne particles).

1262



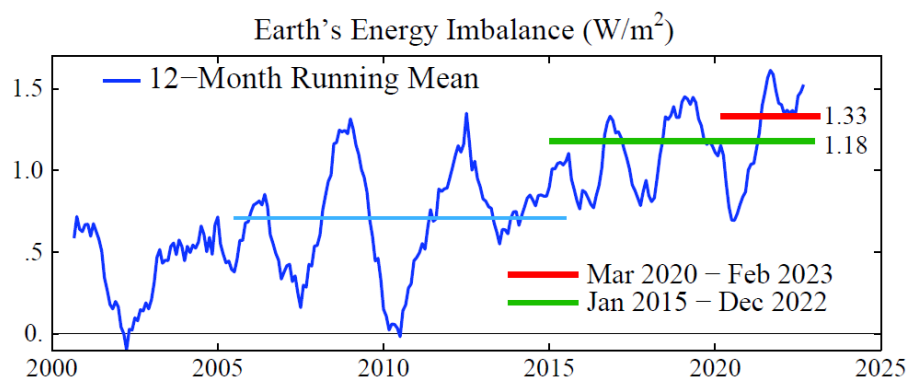
1263  
 1264 Fig. 25. Global temperature relative to 1880-1920. Edges of the predicted post-2010 accelerated  
 1265 warming rate (see text) are 0.36 and 0.27°C per decade.

1266 **6.4. Aerosols**

1267 Aerosol climate forcing is larger than the IPCC AR6 estimate and has probably been significant  
 1268 for millennia. We know of no other persuasive explanation for the absence of global warming in  
 1269 the last half of the Holocene (Fig. 14) as GHG forcing increased 0.5 W/m<sup>2</sup> (Fig. 15). Climate  
 1270 models that do not incorporate a growing negative aerosol forcing yield significant warming in  
 1271 that period,<sup>191</sup> a warming that, in fact, did not occur. Negative aerosol forcing, increasing as  
 1272 civilization developed and population grew, is expected. As humans burned fuels at a growing  
 1273 rate – wood and other biomass for millennia and fossil fuels in the industrial era – aerosols as  
 1274 well as GHGs were an abundant, growing, biproduct. The aerosol source from wood-burning has  
 1275 continued in modern times.<sup>192</sup> GHGs are long-lived and accumulate, so their forcing dominates  
 1276 eventually, unless aerosol emissions grow higher and higher – the Faustian bargain.<sup>106</sup>

1277 We estimate peak (negative) aerosol forcing – in the first decade of this century – of at least 1.5-  
 1278 2 W/m<sup>2</sup>, but aerosol amount now seems to be in decline. We estimate that GHG plus aerosol  
 1279 forcing during 1970-2010 grew +0.3 W/m<sup>2</sup> per decade (+0.45 from GHG, – 0.15 from aerosols),  
 1280 which produced warming of 0.18°C per decade. With current policies, we expect climate forcing  
 1281 for a few decades post-2010 to increase 0.5-0.6 W/m<sup>2</sup> per decade and produce global warming of  
 1282 at least +0.27°C per decade. In that case, global warming will reach 1.5°C by the end of the  
 1283 2020s and 2°C before 2050 (Fig. 25). Such acceleration is highly dangerous in a climate system  
 1284 that is already far out of equilibrium and dominated by multiple amplifying feedbacks.

1285 In the absence of global monitoring of aerosol microphysics, the sharp change of ship emissions  
 1286 in 2015 and especially in 2020 (Section 5.4) may provide an indirect measure of aerosol effects.  
 1287 Diamond<sup>193</sup> finds evidence of a cloud brightness decrease amounting to a forcing of order 1  
 1288 W/m<sup>2</sup> in a shipping corridor. Satellite measurement of absorbed solar radiation (Fig. 22) that  
 1289 include the effect of cloud cover change suggest a somewhat larger effect. However, the single  
 1290 best sentinel for climate, our best measure of where global temperature is headed in the next  
 1291 decade, is Earth’s energy imbalance.



1292 Fig. 26. 12-month running-mean of Earth's energy imbalance from CERES satellite data<sup>88</sup>  
 1293 normalized to 0.71 W/m<sup>2</sup> mean for July 2005 – June 2015 (light blue bar) from in situ data.<sup>87</sup>  
 1294

1295 **6.5. Earth's energy imbalance**

1296 Earth's energy imbalance (EEI) is the net gain (or loss) of energy by the planet, the difference  
 1297 between absorbed solar energy and emitted thermal (heat) radiation. As long as EEI is positive,  
 1298 Earth will continue to get hotter. EEI is hard to measure, a small difference between two large  
 1299 quantities (Earth absorbs and emits about 240 W/m<sup>2</sup> averaged over the entire planetary surface),  
 1300 but change of EEI can be well-measured from space.<sup>88</sup> Absolute calibration is from the change of  
 1301 heat in the heat reservoirs, mainly the global ocean, over a period of at least a decade, as required  
 1302 to reduce error due to the finite number of places that the ocean is sampled.<sup>87</sup> EEI varies year-to-  
 1303 year (Fig. 26), largely because global cloud amount varies with weather and ocean dynamics, but  
 1304 averaged over several years EEI helps inform us about what is needed to stabilize climate.

1305 The data suggest that EEI has doubled since the first decade of this century (Fig. 26). This  
 1306 increase is one basis for our prediction of post-2010 acceleration of the global warming rate. The  
 1307 EEI increase may be partly due to restrictions on maritime aerosol precursor emissions imposed  
 1308 in 2015 and 2020 (Section 5.4), but the growth rate of GHG climate forcing also increased in  
 1309 2015 and since has remained at the higher level (Section 6.6).

1310 The reduction of climate forcing required to reduce EEI to zero is greater than EEI. The added  
 1311 burden is a result of ultrafast cloud feedback (Section 3.3). Cloud feedbacks are only beginning  
 1312 to be simulated well, but climate sensitivity near 1.2°C per W/m<sup>2</sup> implies that the net cloud  
 1313 feedback is large, with clouds accounting for as much as half of equilibrium climate sensitivity.

1314 Continuation of precise monitoring of EEI is essential as a sentinel for future climate change and  
 1315 for the purpose of assessing efforts to stabilize climate and avoid undesirable consequences.  
 1316 Global satellite monitoring of geographical and temporal changes of the imbalance and ocean in  
 1317 situ monitoring (especially in polar regions of rapid change) are both needed for the sake of  
 1318 understanding ongoing climate change.

1319 **6.6. Global warming and sea level rise in the pipeline**

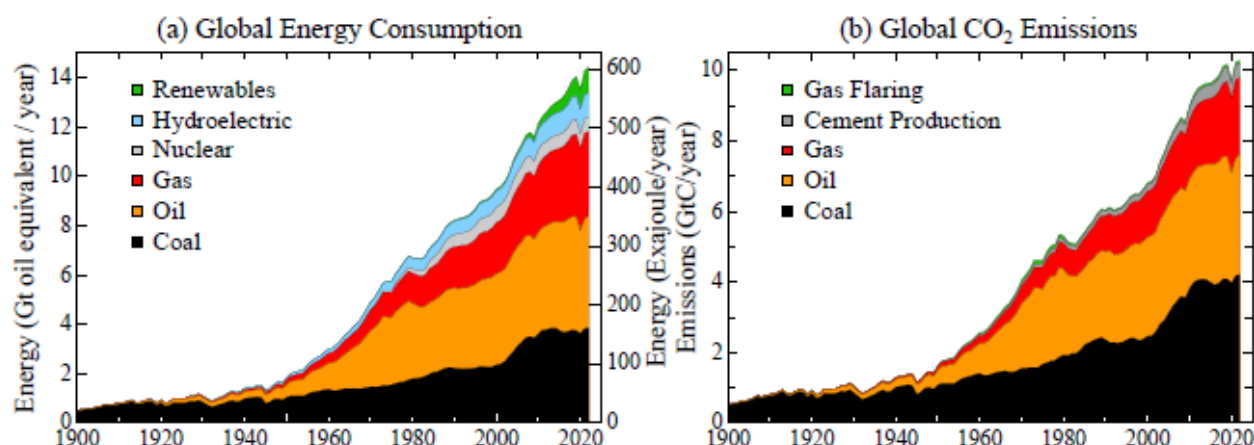
1320 Cenozoic CO<sub>2</sub> and climate histories reveal where climate is headed, if present human-made  
 1321 climate forcings remain in place. GHG climate forcing is now 4.6 W/m<sup>2</sup> relative to the mid-  
 1322 Holocene (7kyBP) or 4.1 W/m<sup>2</sup> relative to 1750. We argue that 4.6 W/m<sup>2</sup> is the human-made



1323 forcing, but there is little point to debate whether it should be  $4.6 \text{ W/m}^2$  or  $4.1 \text{ W/m}^2$  because the  
1324 GHG forcing is increasing  $0.5 \text{ W/m}^2$  per decade (Section 6.7). One merit of consistent analysis  
1325 for the full Cenozoic era is revelation that the human-made climate forcing exceeds the forcing at  
1326 transition from a largely ice-free planet to glaciated Antarctica, even with inclusion of a large,  
1327 negative, aerosol climate forcing. Equilibrium global warming for today's GHG level is  $10^\circ\text{C}$  for  
1328 our central estimate  $\text{ECS} = 1.2^\circ\text{C} \pm 0.3^\circ\text{C}$  per  $\text{W/m}^2$ , including amplifications from disappearing  
1329 ice sheets and non- $\text{CO}_2$  GHGs (Sec. 4.4). Aerosols reduce equilibrium warming to about  $8^\circ\text{C}$ .  
1330 Equilibrium sea level change is  $+60 \text{ m}$  (about 200 feet).

1331 Discussions<sup>194</sup> between the first author (JEH) and field glaciologists<sup>195</sup> 20 years ago revealed a  
1332 frustration of the glaciologists with the conservative tone of IPCC's assessment of ice sheets and  
1333 sea level rise. One of the glaciologists said – regarding a photo<sup>196</sup> of a moulin (a vertical shaft  
1334 that carries meltwater to the base of the ice sheet) on Greenland – “the whole ice sheet is going  
1335 down that damned hole!” Their concern was based on observed ice sheet changes and  
1336 paleoclimate evidence of sea level rise by several meters in a century, which suggest that ice  
1337 sheet collapse is an exponential process. Thus, as an alternative to the IPCC approach that relies  
1338 on ice sheet models coupled to atmosphere-ocean GCMs (global climate models), a study was  
1339 made that avoided use of an ice sheet model, as described in the paper *Ice Melt*.<sup>14</sup> In the GCM  
1340 simulation, a growing amount of freshwater was added to the ocean surface mixed layer around  
1341 Greenland and Antarctica, with the flux in the early 21<sup>st</sup> century based on estimates from *in situ*  
1342 glaciological studies<sup>197</sup> and satellite observations of sea level trends near Antarctica.<sup>198</sup> Doubling  
1343 times of 10 and 20 years were used for the growth of freshwater flux. One merit of the GCM  
1344 used in *Ice Melt* was its reduced, more realistic, small-scale ocean mixing, with a result that  
1345 Antarctic Bottom Water in the model was formed close to the Antarctic coast<sup>14</sup> as it is in the real  
1346 world. Continued growth of GHG emissions and meltwater led to shutdown of the North Atlantic  
1347 and Southern Ocean overturning circulations, amplified warming at the foot of the ice shelves  
1348 that buttress the ice sheets, and other feedbacks consistent with “nonlinearly growing sea level  
1349 rise, reaching several meters over a time scale of 50-150 years.”<sup>14</sup> This paper exposed urgency to  
1350 understand the dynamical change and the climate chaos that would occur with ice sheet collapse,  
1351 a situation that may have occurred during the Eemian period when it was about as warm as  
1352 today, as discussed in the *Ice Melt* paper. That period has potential to help us understand how  
1353 close we are to a point of no return and sea level rise of several meters.

1354 *Ice Melt* was blackballed from IPCC's AR6 report, which is a form of censorship,<sup>15</sup> as alternative  
1355 views normally are acknowledged in science. Science grants ultimate authority to nature. In the  
1356 opinion of JEH, IPCC is comfortable with gradualism and does not want its authority challenged.  
1357 Caution has merits, but with a climate system characterized by a delayed response and  
1358 amplifying feedbacks, excessive reticence is a danger, especially for young people. Concern  
1359 about locking in nonlinearly growing sea level rise is amplified in our present paper by the  
1360 revelation that the equilibrium response to current atmospheric composition is a nearly ice-free  
1361 Antarctica. Portions of the ice sheets well above sea level may be recalcitrant to rapid change,  
1362 but enough ice is in contact with the ocean to provide of the order of  $25 \text{ m}$  (80 feet) of sea level  
1363 rise. The implication is that if we allow a few meters of sea level rise, that may lock in a much  
1364 larger sea level rise. Happily, we will suggest that it is still feasible to stabilize sea level.



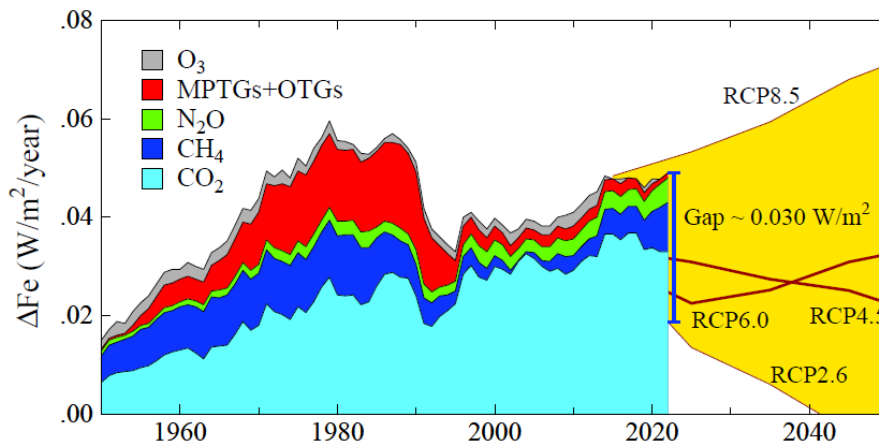
1365  
1366 Fig. 27. Global energy consumption and CO<sub>2</sub> emissions (Hefner et al.<sup>199</sup> and BP<sup>200</sup>).

1367 **6.7. Policy implications**

1368 This section is the first author’s perspective based on more than 20 years of experience on policy  
1369 issues beginning with workshops that he organized at the East-West Center in Hawaii, meetings  
1370 and workshops with energy experts, and trips to more than a dozen nations for consultations with  
1371 government officials, energy experts, and environmentalists.

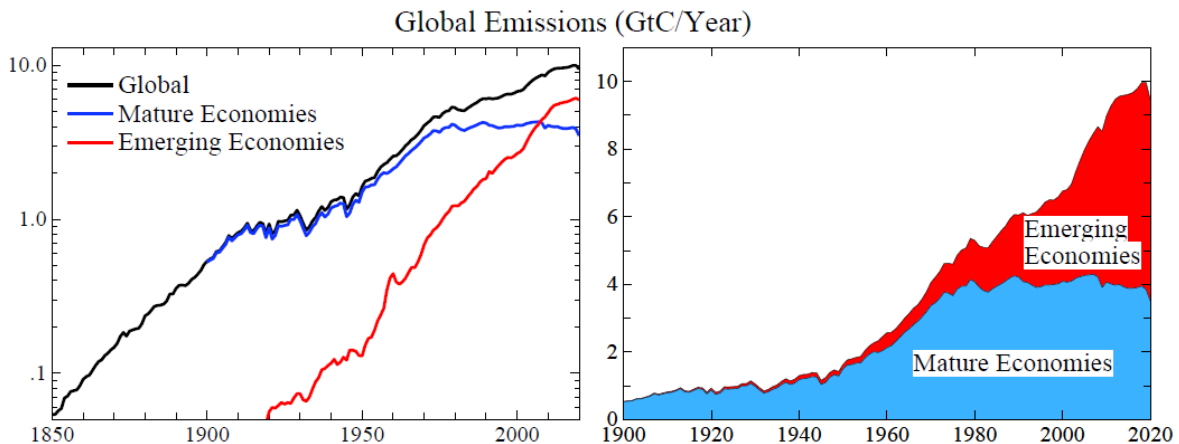
1372 Global warming “in the pipeline” is not “committed warming” that necessarily will occur.  
1373 Warming in the pipeline<sup>78</sup> is the difference between equilibrium temperature for current  
1374 atmospheric composition and the current temperature, consistent with Charney’s study;<sup>4</sup> it thus  
1375 depends on whether “slow” feedbacks are fixed (ECS) or allowed to vary (ESS). Committed  
1376 warming is complex; it depends on assumed future emissions and other potential actions to affect  
1377 Earth’s energy balance. Committed warming depends on aerosol change as well as GHG change.  
1378 Scenarios confined to plausible GHG emission reductions alone are unlikely to keep global  
1379 warming below 2°C, as shown below. The next several years are a crucial time to quantify the  
1380 threat of passing the point of no return that locks in sea level rise of many meters and to assess  
1381 potential ways to avoid that outcome. Assessment should develop the full scientific toolbox  
1382 including better understanding of climate change during the Eemian period that was moderately  
1383 warmer than the Holocene, the effects of natural “experiments” such as the Pinatubo volcanic  
1384 eruption, and analysis of the effects of ongoing changes of atmospheric gases and aerosols.

1385 The world’s present energy and climate path has good reason. Fossil fuels powered the industrial  
1386 revolution and raised living standards in much of the world. Fossil fuels still provide most of the  
1387 world’s energy (Fig. 27a) and produce most CO<sub>2</sub> emissions (Fig. 27b). Fossil fuel reserves and  
1388 recoverable resources could provide most of the world’s energy for the rest of this century.<sup>201</sup>  
1389 Much of the world is still in early or middle stages of economic development. Energy is needed  
1390 and fossil fuels are a convenient, affordable source of energy. One gallon (3.6 liters) of gasoline  
1391 (petrol) provides the work equivalent of more than 400 hours labor by a healthy adult. These  
1392 benefits are the basic reason for continued emissions.

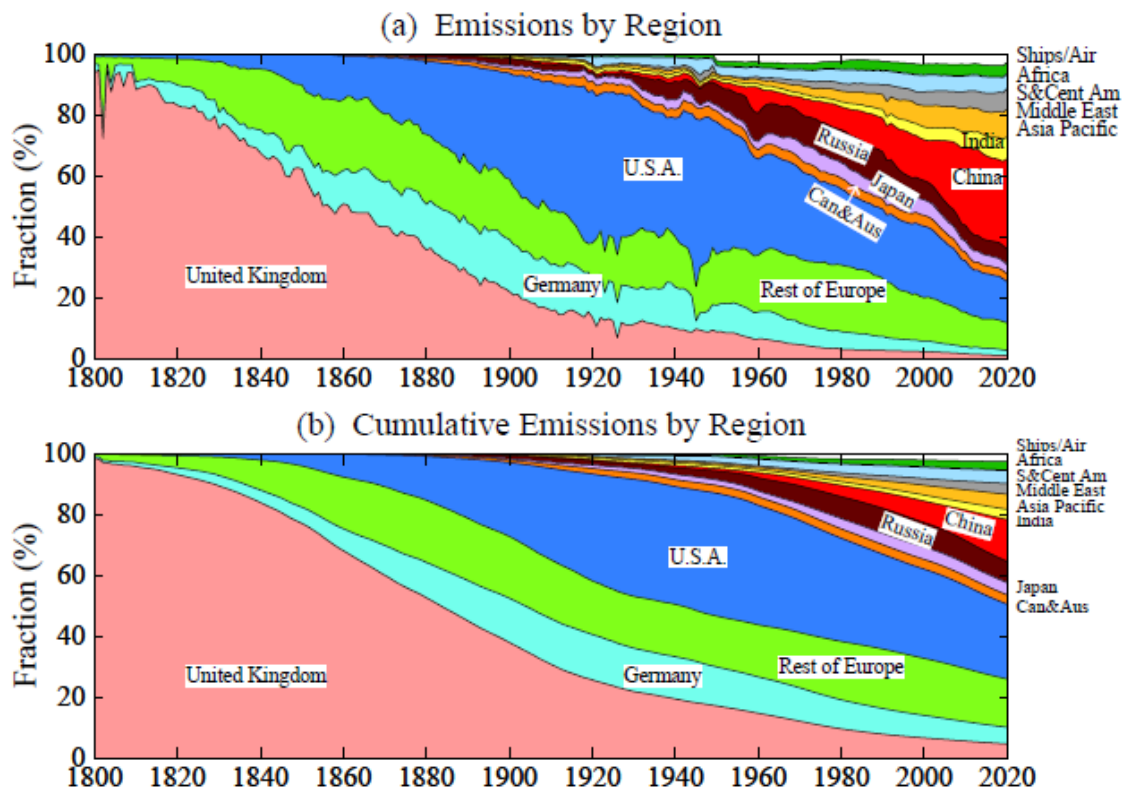


1393  
 1394 Fig. 28. Annual growth of climate forcing by GHGs<sup>41</sup> including part of O<sub>3</sub> forcing not included  
 1395 in CH<sub>4</sub> forcing (Supp. Material). MPTG and OTG are Montreal Protocol and Other Trace Gases.

1396 The United Nations employs targets for a global warming limit and for emission reductions as a  
 1397 tool to cajole progress in limiting climate change. IPCC has defined scenarios that help us judge  
 1398 progress toward meeting such targets. Among the RCP scenarios (Fig. 28) in the IPCC AR5  
 1399 report, the RCP2.6 scenario defines rapid downward trend of greenhouse gas climate forcings  
 1400 needed to prevent global warming from exceeding 2°C relative to preindustrial climate. The gap  
 1401 between that scenario and reality continues to grow. In principle, the 0.03 W/m<sup>2</sup> gap in 2022  
 1402 could be closed by extraction of CO<sub>2</sub> from the air. However, the required negative emissions  
 1403 (CO<sub>2</sub> extracted from the air and placed in permanent storage) must be larger than the desired  
 1404 atmospheric CO<sub>2</sub> reduction by a factor of about 1.7.<sup>68</sup> Thus, the required CO<sub>2</sub> extraction is 2.1  
 1405 ppm, which is 7.6 GtC. Based on a pilot carbon capture plant built in Canada, Keith<sup>202</sup> estimates  
 1406 an extraction cost of \$450-920 per tC, as clarified elsewhere.<sup>203</sup> Keith's cost range yields an  
 1407 extraction cost of \$3.4-7.0 trillion. This is for excess emissions in 2022 only; it is an annual cost.  
 1408 Given the difficulty the UN faced in raising \$0.1 trillion for climate purposes and the growing  
 1409 annual emissions gap (Fig. 28), this example shows both the need to reduce emissions as rapidly  
 1410 as practical and the fact that carbon capture cannot be viewed as the solution, although it may  
 1411 play a role in a portfolio of policies, if its cost is driven down.



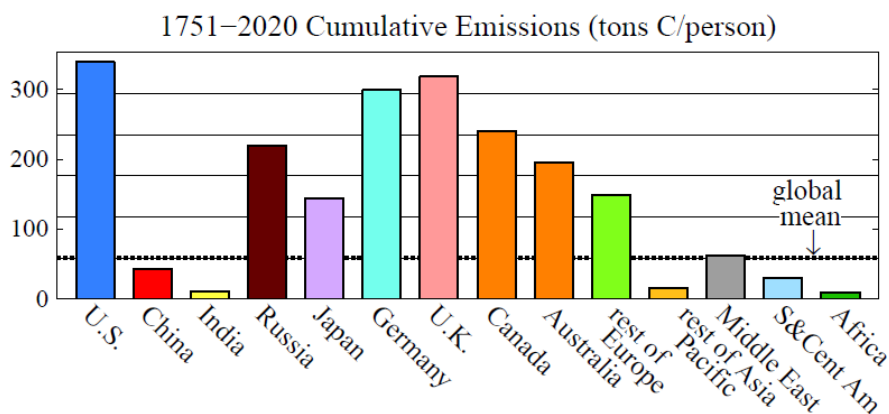
1412  
 1413 Fig. 29. Fossil fuel CO<sub>2</sub> emissions from mature and emerging economies. China is counted as an  
 1414 emerging economy. Data sources: Heffner *et al.*<sup>199</sup> for 1751-2017 and BP<sup>200</sup> for 2018-2020.



1415  
 1416 Fig. 30. Fossil fuel CO<sub>2</sub> emissions by nation or region as a fraction of global emissions. Data  
 1417 sources: Heffner *et al.*<sup>199</sup> for 1751-2017 and BP<sup>200</sup> for 2018-2020.

1418 Climate policy under the Framework Convention demonstrably fails to curb and reverse growth  
 1419 of GHGs (Figs. 27-29). [The Covid pandemic dented emissions, but 2022 global emissions are at  
 1420 a record high level.] This is the “tragedy of the commons”: as long as fossil fuel pollution can be  
 1421 dumped in the air free of charge, agreements such as the 1997 Kyoto Protocol<sup>204</sup> and 2015 Paris  
 1422 Agreement have little effect on global emissions. Energy is needed to raise living standards and  
 1423 fossil fuels are still the most convenient, affordable source of that energy. Thus, growth of  
 1424 emissions is occurring in emerging economies (Figs. 29 and 30a), while mature economies are  
 1425 still the larger source of the cumulative emissions (Fig. 30b) that drive climate change.<sup>205,206</sup>  
 1426 Thus, exhortations at UN meetings, imploring reduced emissions, have limited global effect.

1427 Meanwhile, climate science has exposed a crisis that the world is loath to appreciate. IPCC, the  
 1428 scientific body advising the world on climate, does not bluntly inform the world that the present  
 1429 “wishful thinking” geopolitical approach will be disastrous for today’s young people and their  
 1430 children. Political leaders profess ambitions for dubious net-zero emissions while fossil fuel  
 1431 extraction expands. The only IPCC scenarios that phase down human-made climate change  
 1432 amount to “a miracle will occur.” The one IPCC scenario that moves rapidly to negative global  
 1433 emissions has biomass-burning powerplants that capture and sequester CO<sub>2</sub>, a nature-ravaging  
 1434 proposition without scientific and engineering credibility and without a realistic chance of being  
 1435 deployed at scale and on time to address the climate threat.



1436  
1437 Fig. 31. Cumulative per capita national fossil fuel emissions.<sup>207</sup>

1438 A new plan is essential. The plan must cool the planet to preserve our coastlines. Even today’s  
1439 temperature would cause eventual multimeter sea level rise, and a majority of the world’s large  
1440 and historic cities are on coastlines. Cooling will also address other major problems caused by  
1441 global warming. We should aim to return to a climate close to that in which civilization  
1442 developed, in which the nature that we know and love thrived. As far as is known, it is still  
1443 feasible to do that without passing through an irreversible disaster such as many-meter sea level  
1444 rise. Given the situation that we have allowed to develop, three actions are now essential.

1445 First, a rising global price on GHG emissions must underly energy and climate policies, with  
1446 enforcement by border duties on products from countries that do not have an internal carbon fee  
1447 or tax. Public buy-in and maximum effectiveness require that the collected funds be distributed  
1448 to the public, an approach that helps address global wealth disparities. Economists in the U.S.  
1449 overwhelmingly support carbon fee-and-dividend<sup>208</sup>; college and high school students, who have  
1450 much at stake, join in advocacy.<sup>209</sup> Science rationale for a rising carbon price with a level playing  
1451 field for energy efficiency, renewable energies, nuclear power, and all innovations has long been  
1452 understood, but not achieved. Instead, fossil fuels and renewable energy are heavily subsidized,  
1453 including use of “renewable portfolio standards” that let utilities pass added costs to consumers.  
1454 Thus, nuclear energy has been disadvantaged and excluded as a “clean development mechanism”  
1455 under the Kyoto Protocol, based in part on myths about damage caused by nuclear energy that  
1456 are not supported by scientific facts.<sup>210</sup> A rising carbon price is not a panacea – many other  
1457 actions are needed – but it is the *sine qua non*. Without it, fossil fuels will continue to be used  
1458 extensively and global warming and climate impacts will continue to grow.

1459 Second, effective global cooperation is needed to achieve reduction of GHG climate forcing.  
1460 High income countries, mainly in the West, are responsible for most of the cumulative fossil fuel  
1461 CO<sub>2</sub> emissions (Fig. 30b and Fig. 31), which are the main drive for global warming,<sup>205,206</sup> even  
1462 though the West is a small fraction of global population. De facto cooperation between the West  
1463 and China drove down the price of renewable energy, but more cooperation is needed to develop  
1464 emission-free technologies for the rest of the world, which will be the source of most future  
1465 GHG emissions (Fig. 29a). A crucial need is carbon-free electricity, the essential, growing,  
1466 clean-energy carrier. In the West, except for limited locations with large hydropower, the main  
1467 source of clean electricity has been nuclear power, and nations with emerging economies are  
1468 eager to have modern nuclear power because of its small environmental footprint. Thus, China-  
1469 U.S. cooperation in development of modern nuclear power was proposed, but then stymied by

1470 U.S. prohibition of technology transfer.<sup>211</sup> Competition is normal, but it can be managed if there  
1471 is a will, reaping benefits of cooperation over confrontation.<sup>212</sup> Of late, priority has been given  
1472 instead to economic and military hegemony, despite recognition of the climate threat, and  
1473 without consultation with young people or seeming consideration of their aspirations. We must  
1474 not foreclose the possibility of return to a more ecumenical perspective of our shared future.  
1475 Scientists can improve global prospects by maintaining and expanding international cooperation.  
1476 Awareness of the gathering climate storm will grow this decade, so we must increase scientific  
1477 understanding worldwide as needed for climate restoration.

1478 Third, we must take actions to reduce and reverse Earth's energy imbalance to keep global  
1479 climate within a habitable range. Highest priority must be on phasing down emissions, but, due  
1480 to past failure to reduce GHG emissions, it is now implausible to achieve the needed timely  
1481 change of Earth's energy balance solely via GHG emission reductions. Phasedown of emissions  
1482 cannot restore Earth's energy balance within less than several decades, which is too slow to  
1483 prevent grievous escalation of climate impacts and probably too slow to avoid locking in loss of  
1484 the West Antarctic ice sheet and sea level rise of several meters. Given that several years are  
1485 needed to forge a political approach for climate restoration, as discussed below, intense  
1486 investigation of potential actions should proceed now. This will not deter action on mitigation of  
1487 emissions; on the contrary, it will spur such action and allow search for "a miracle." A promising  
1488 – and probably necessary – approach to overcome humanity's harmful geo-transformation of  
1489 Earth is temporary solar radiation management (SRM). Risks of such intervention must be  
1490 defined, as well as risks of no intervention; thus, the U.S. National Academy of Sciences  
1491 recommends research on SRM.<sup>213</sup> An example of SRM is injection of atmospheric aerosols at  
1492 high southern latitudes, which global simulations suggest would cool the Southern Ocean at  
1493 depth and limit melting of Antarctic ice shelves.<sup>15,214</sup> The most innocuous aerosols may be fine  
1494 salty droplets extracted from the ocean and sprayed into the air by autonomous sailboats.<sup>215</sup> This  
1495 approach has been discussed for potential use on a global scale,<sup>216</sup> but even use limited to  
1496 Southern Hemisphere high latitudes requires research and forethought to avoid unintended  
1497 adverse effects.<sup>217</sup> The present decade is probably our last chance to develop the knowledge,  
1498 technical capability, and political will for the actions needed to save global coastal regions from  
1499 long-term inundation.

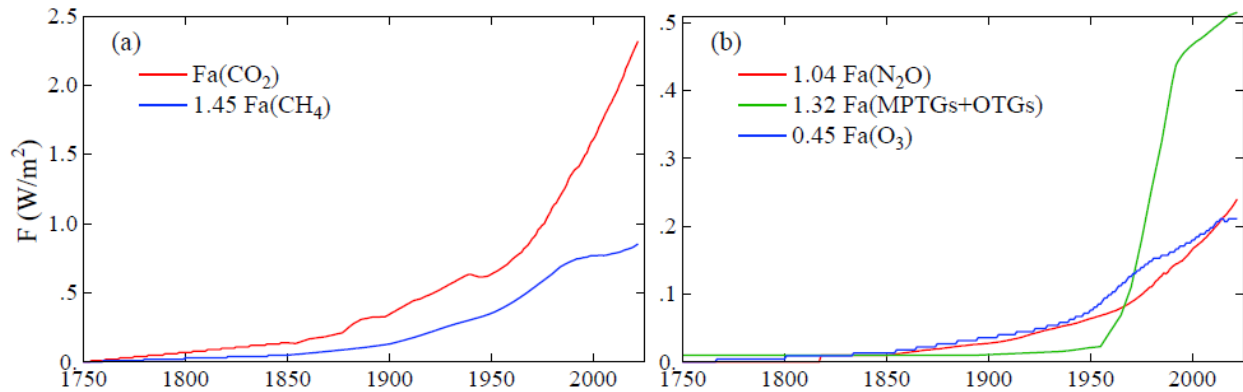
1500 These three basic actions are feasible, but they are not happening. Did we scientists inform the  
1501 public and policymakers well? Opportunities for progress often occur in conjunction with crises.  
1502 Before describing today's crisis and opportunity, we should review prior cases. In 1992, it was  
1503 the climate crisis per se, with the Framework Convention on Climate Change. William Clinton  
1504 was elected President of the United States with his party in control of both houses of Congress.  
1505 Clinton's most climate-consequential action was in his first State-of-the-Union address as he  
1506 declared "We are eliminating programs that are no longer needed, such as nuclear power  
1507 research and development." For 30 years since, renewable energy received unlimited subsidy via  
1508 renewable portfolio standards, and renewable energies are now ready for prime time. However,  
1509 nuclear power, the potential carbon-free complement to renewables for baseload electricity, was  
1510 denied such support, so today most electricity worldwide is from fossil fuels. At the next global  
1511 crisis, the financial crisis of 2008, Barack Obama was elected President of the United States,  
1512 with his party in control of both houses of Congress. Obama had pledged to address "a planet in  
1513 peril" in his campaign, but with Congress poised – indeed, forced – to pass economic legislation,  
1514 Obama did not attempt to include the most fundamental needed action: a price on carbon.

1515 Today, the world faces a crisis – extreme political polarization, especially in the United States –  
1516 that threatens effective governance. Yet it is a great time to be a young person, because the crisis  
1517 offers the opportunity to help shape the future – of the nation and the planet. The problem and  
1518 solution are not hard to understand. Following World War II, the United States exercised  
1519 leadership in the formation of the United Nations, the World Bank, the Marshall Plan, and the  
1520 Universal Declaration of Human Rights. Centuries-long progress toward equal rights continued,  
1521 albeit slowly. The “American dream” of economic opportunity was real, as most people willing  
1522 to work hard could afford college. Immigration policy welcomed the brightest; NASA in the  
1523 1960s invited scientists from European countries, Japan, China, India, Canada – those wanting to  
1524 stay found immigration to be straightforward. But the power of special interests in Washington  
1525 grew, government became insular and inefficient, and Congress refused to police itself as their  
1526 first priority became reelection and maintenance of elite status, supported by special interests.  
1527 Thousands of pages of giveaways to special interests lard every funding bill, including the  
1528 climate bill titled “Inflation Reduction Act” – Orwellian double-speak – as every dollar is  
1529 borrowed from young people via deficit spending. The public is fed up with the Washington  
1530 swamp but hamstrung by rigid two-party elections focused on a polarized cultural war, while the  
1531 elite is satisfied with a system that allows them to accumulate wealth without paying taxes.

1532 A political party that takes no money from special interests is needed to address political  
1533 polarization, which is essential if the West is to be capable of helping preserve the planet and a  
1534 bright future for coming generations. Young people showed their ability to drive an election –  
1535 via their support of Obama and later Bernie Sanders – without any funding from special interests.  
1536 Groundwork is being laid to allow third party candidates in 2026 and 2028 elections in the U.S.  
1537 Ranked voting is being advocated in every state – to avoid the “spoiler” effect of a third party. It  
1538 is asking a lot to expect young people to grasp the situation that they have been handed – but a  
1539 lot is at stake for them. As they realize that they are being handed a planet in decline, the first  
1540 reaction may be to stamp their feet and demand that governments do better, but the effect of that  
1541 is limited. Nor is it sufficient to parrot the big environmental organizations, which have become  
1542 part of the problem, as they are largely supported by the fossil fuel industry and wealthy donors  
1543 who are comfortable with the status quo. Instead, young people have the opportunity to provide  
1544 the drive for a revolution that restores the ideals of democracy while developing the technical  
1545 knowledge that is needed to navigate the stormy sea that their world is setting out upon.

1546 Required political and scientific timings are consistent. Several years are needed to alter the  
1547 political system such that the will of the majority has an opportunity to be realized. Several years  
1548 of continued climate change will elevate the priority of climate change and confirm the  
1549 inadequacy of the present policy approach. Several years will permit improved understanding of  
1550 the climate science and thus help to assess risks and benefits of alternative actions.

1551 **SUPPORTING MATERIAL**



1552  
 1553 Fig. S1. Greenhouse gas (GHG) climate forcings for the five terms in Equation (4). The forcings  
 1554 incorporate efficacies, including effects of a 3-dimensional atmosphere and seasonal change,  
 1555 which alter the adjusted forcings calculated with a 1-dimensional radiative-convective model.

1556 **SM1. GHG forcing formulae and comparison with IPCC forcings**

1557 Formulae<sup>218</sup> (Table 1) for adjusted forcing,  $F_a$ , were numerical fits to 1-D calculations with the  
 1558 GISS GCM radiation code using the correlated k-distribution method.<sup>38</sup> Gas absorption data  
 1559 were from high spectral resolution laboratory data.<sup>39</sup> These  $F_a$  were converted to  $F_e$  via GCM  
 1560 calculations that include 3-D effects, as summarized in Eq. (4), where the coefficients are from  
 1561 Table 1 of *Efficacy*.<sup>32</sup> The factor 1.45 for  $CH_4$  includes the effect of  $CH_4$  change on stratospheric  
 1562  $H_2O$  and tropospheric  $O_3$ . We assume that  $CH_4$  is responsible for 45% of the  $O_3$  change.<sup>40</sup> The  
 1563 remaining 55% of the  $O_3$  forcing is obtained by multiplying the IPCC AR6  $O_3$  forcing (0.47  
 1564  $W/m^2$  in 2019) by 0.55 and by 0.82, where the latter factor is the efficacy that converts  $F_a$  to  $F_e$ .  
 1565 The non- $CH_4$  portion of the  $O_3$  forcing is thus 0.21  $W/m^2$  in 2019. The time-dependence of this  
 1566 portion of the  $O_3$  forcing is from Table AIII.3 in IPCC AR6. MPTGs and OTGs are Montreal  
 1567 Protocol Trace Gases and Other Trace Gases.<sup>41</sup> An updated list of these gases and a table of  
 1568 their annual forcings since 1992 are [available](#) as are [earlier data](#).<sup>42</sup>

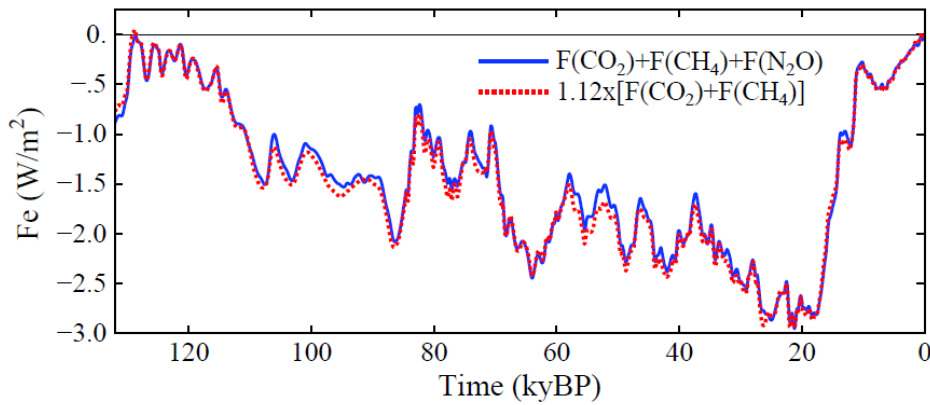
**Table 1. Greenhouse gas radiative forcings**

Gas	Radiative forcing
$CO_2$	$F = f(c) - f(c_o)$ , where $f(c) = 4.996 \ln(c + 0.0005c^2)$
$CH_4$	$F = 0.0406(\sqrt{m} - \sqrt{m_o}) - [g(m, n_o) - g(m_o, n_o)]$
$N_2O$	$F = 0.136(\sqrt{n} - \sqrt{n_o}) - [g(m_o, n) - g(m_o, n_o)]$ , where $g(m, n) = 0.5 \ln[1 + 2 \times 10^{-5}(mn)^{0.75}]$
CFC-11	$F = 0.264(x - x_o)$
CFC-12	$F = 0.323(y - y_o)$

$c$ ,  $CO_2$  (ppm);  $m$ ,  $CH_4$  (ppb);  $n$ ,  $N_2O$  (ppb);  $x/y$ , CFC-11/12 (ppb).

1569

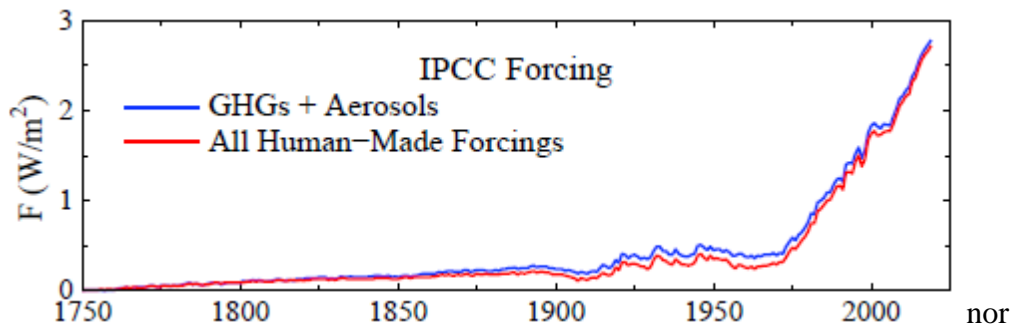




1570  
1571 Fig. S2. Test of accuracy of 2-term approximation for forcing by the three gases.

1572 **SM2. Approximation for N<sub>2</sub>O forcing**

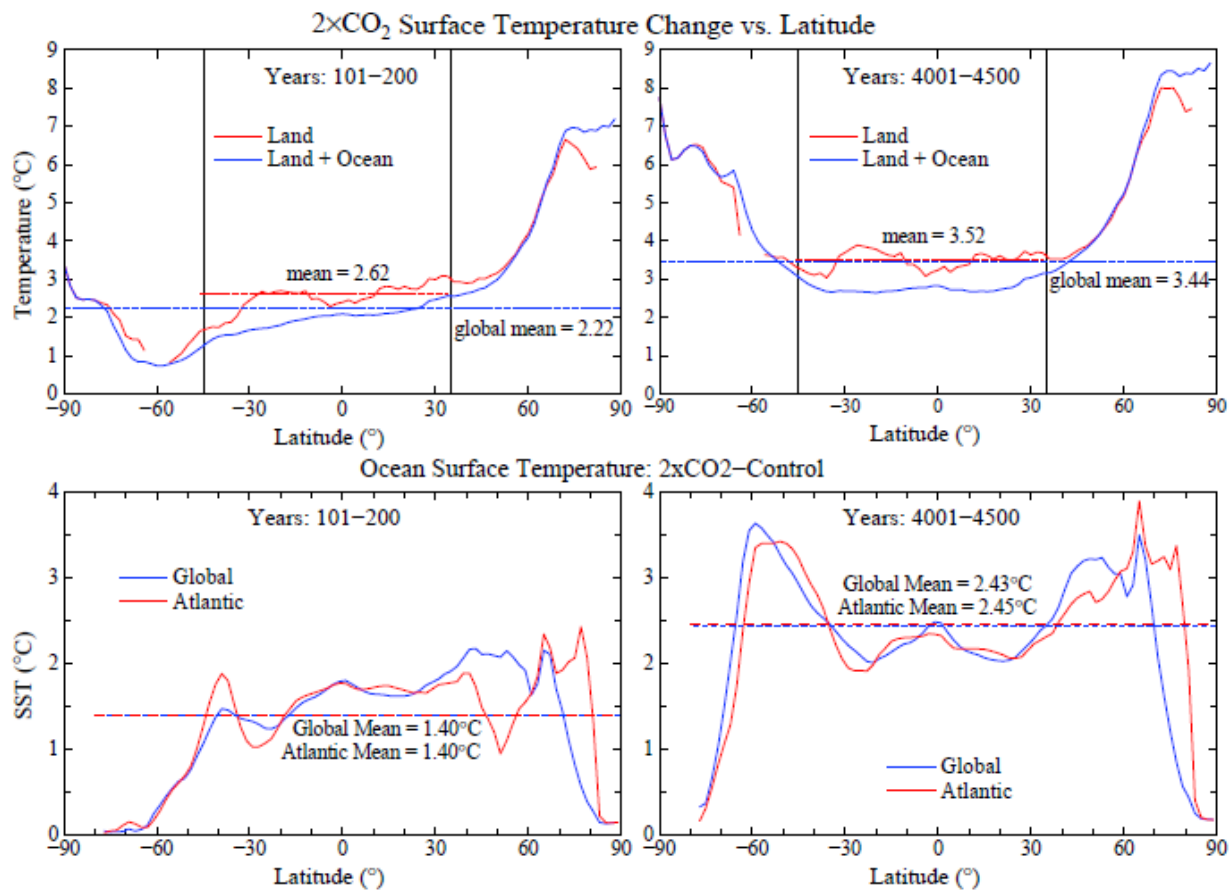
1573 CO<sub>2</sub> and CH<sub>4</sub> are well-preserved in ice cores. However, the N<sub>2</sub>O record is corrupted in some time  
1574 intervals by chemical reactions with dust particles in the ice core. For such intervals we  
1575 approximate the N<sub>2</sub>O forcing by increasing the sum of CO<sub>2</sub> and CH<sub>4</sub> forcings by 12%, i.e., we  
1576 approximate the forcing for all three gases as  $1.12 \times [F(\text{CO}_2) + F(\text{CH}_4)]$ . The accuracy of this  
1577 approximation is checked in Fig. S2 via computations for the past 132 ky, when data are  
1578 available for all three gases from the multi-core composite of Schilt et al.<sup>51</sup>



1579  
1580 Fig. S3. Climate forcings provided in current IPCC report<sup>13</sup> for GHGs plus aerosols and for all  
1581 human-made forcings, i.e., excluding only volcano and solar forcings.

1582 **SM3. Comparison of GHG + Aerosol forcing with All Human-Made forcing**

1583 IPCC all human-made forcings include land-use effects and contrails, which have large relative  
1584 uncertainties. The forcings in Fig. S3 are those provided by IPCC (cf. Annex III of the current  
1585 IPCC physical sciences report).<sup>13</sup>



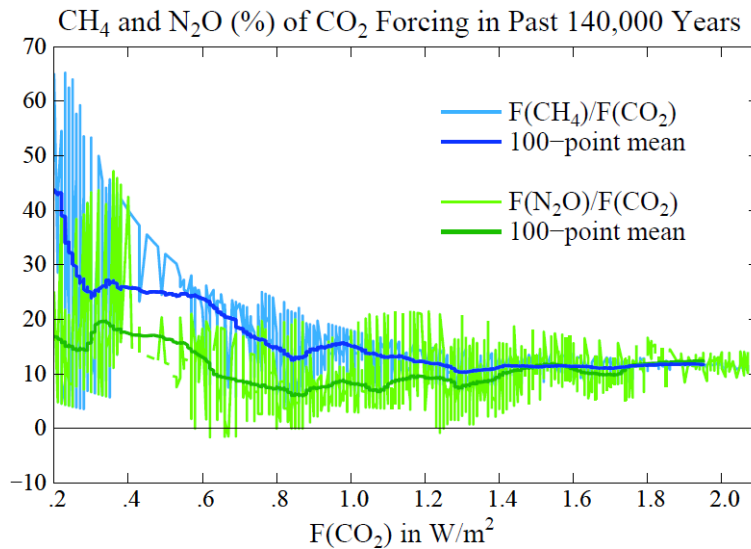
1586  
1587 Fig. S4. Surface temperature response to 2×CO<sub>2</sub> of GISS (2020) GCM (Sections 3).

1588 **SM4. Land warming vs. global warming: effect of polar amplification**

1589 Land areas usually have a larger response to a forcing as shown by the response in Fig. S4 of the  
 1590 GISS (2020) GCM to 2×CO<sub>2</sub> forcing. The warming over land at latitudes 45°S to 35°N (2.62°C)  
 1591 after 150 years (mean for years 101-200 is 18% larger than the global mean warming. However,  
 1592 the equilibrium warming (3.52°C) of this low-latitude land is only 2% larger than global  
 1593 warming (3.44°C), as a result of the polar amplification of global warming. This result indicates  
 1594 that – for a case in which ice sheets are held fixed – the measurement of Seltzer *et al.*<sup>56</sup> of LGM  
 1595 cooling of 5.8°C for land area 45°S-35°N is representative of the equilibrium temperature change  
 1596 for a planet in which the ice sheets are held fixed, as polar amplification of temperature change  
 1597 offsets the fact that land response to a forcing exceeds ocean response. Moreover, in the LGM  
 1598 the real world, ice sheets were not fixed. Polar amplification of temperature change in the LGM,  
 1599 compared to the Holocene, was substantially increased by the growth of ice sheets, as shown in  
 1600 Fig. 9 of Hansen *et al.* (1984).<sup>7</sup> Thus, the LGM global cooling would be substantially greater  
 1601 than the 5.8°C cooling of land area 45°S-35°N.

1602 **SM5. CH<sub>4</sub> and N<sub>2</sub>O forcings as percent of CO<sub>2</sub> forcing in Antarctic ice cores.**

1603 Based on the CO<sub>2</sub>, CH<sub>4</sub> and N<sub>2</sub>O amounts in the multi-ice core GHG tabulation of Schilt *et al.*<sup>51</sup>  
 1604 for the past 140 ky, we calculated the ratio of CH<sub>4</sub> and N<sub>2</sub>O forcings to the CO<sub>2</sub> forcing (Fig. S5).  
 1605 The data cover a range of global temperature from the LGM minimum to the Eemian maximum.



1606  
1607 Fig. S5. CH<sub>4</sub> and N<sub>2</sub>O radiative forcings as a percent of the CO<sub>2</sub> forcing in past 140 ky.

1608 **SM6. Global warming in the pipeline: Green’s function calculations**

1609 Global warming in the pipeline ( $\Delta T_{pl}$ ) after a CO<sub>2</sub> doubling is the portion of the equilibrium  
1610 response ( $T_{eq}$ ) that remains to occur at time  $t$ , i.e.,  $\Delta T_{pl} = T_{eq} - T(t)$ . If EEI were equivalent to a  
1611 climate forcing, warming in the pipeline would be the product of EEI and climate sensitivity ( $^{\circ}\text{C}$   
1612 per  $\text{W}/\text{m}^2$ ), i.e., warming in the pipeline would be  $\text{EEI} \times \text{ECS}/4$ , where we have approximated the  
1613  $2 \times \text{CO}_2$  forcing as  $4 \text{ W}/\text{m}^2$ .

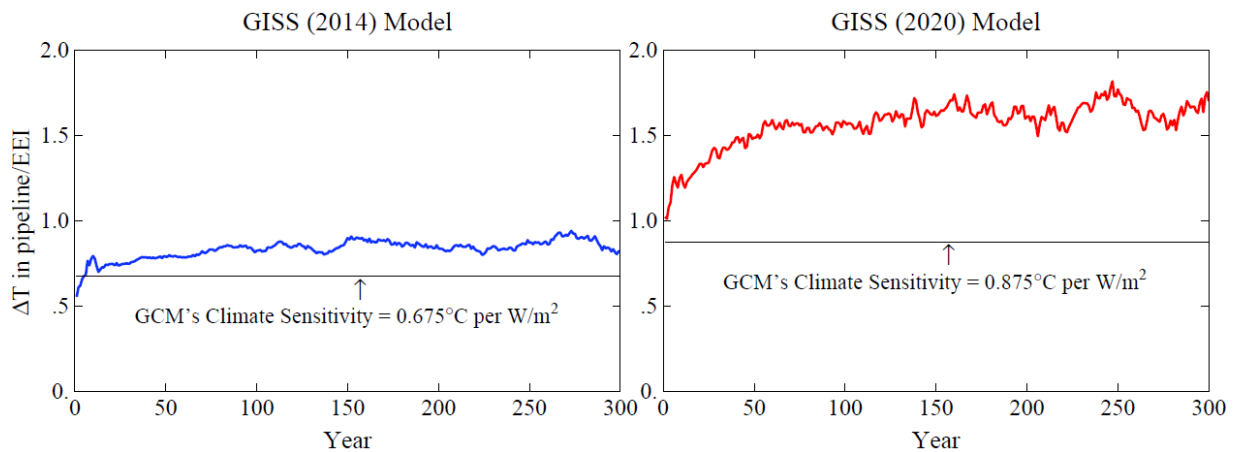
1614 Fig. S6 shows the  $2 \times \text{CO}_2$  results for the GISS (2014) and GISS (2020) GCMs. EEI is not a good  
1615 measure of the warming in the pipeline, especially for the newer GISS model. The warming in  
1616 the pipeline for the GISS (2014) model is typically  $\sim 30\%$  larger than implied by EEI and  $\sim 90\%$   
1617 larger in the GISS (2020) model. If these results are realistic, they suggest that reduction of the  
1618 human-made climate forcing by an amount equal to EEI will leave a planet that is still pumping  
1619 heat into the ocean at a substantial rate.

1620 Real-world climate forcing is added year-by-year with much of the GHG growth in recent years,  
1621 which Fig. 4 suggests will limit the discrepancy between actual warming in the pipeline and that  
1622 inferred from EEI. Thus, we also make Green’s function calculations of global temperature and  
1623 EEI for 1750-2019 for GHG plus IPCC aerosol forcings. Green’s function calculations are  
1624 useful, with a caveat noted below, for quantities for which the response is proportional to the  
1625 forcing. We calculate  $T_G(t)$  using Eq. (4) and  $\text{EEI}_G(t)$  using

1626 
$$\text{EEI}_G(t) = \int [1 - R_{\text{EEI}}(t)] \times [dF(t)/dt] dt, \tag{S1}$$

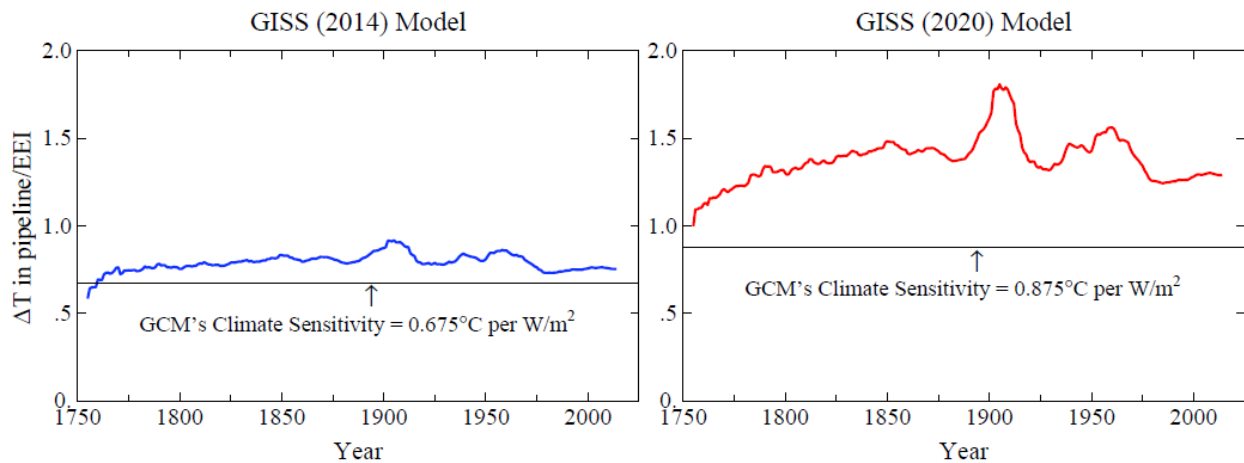
1627 where  $R_{\text{EEI}}$  (Fig. 5b) is the EEI response function (% of equilibrium response) and  $dF$  is forcing  
1628 change per unit time. Integrations begin in 1750, when we assume Earth was in energy balance.

1629 The results (Fig. S7) show that the excess warming in the pipeline (excess over expectations  
1630 based on EEI) is reduced to 15-20% for the GISS (2014) model, but it is still 70-80% for the  
1631 GISS (2020) model. This topic thus seems to warrant further examination, but it is beyond the  
1632 scope of our present paper.



1633  
 1634 Fig. S6. Ratio of warming in the pipeline to EEI,  $(T_{eq} - T)/EEI$ , for the first 300 years after  
 1635 instant doubling of  $CO_2$  for (a) GISS(2014) model and (b) GISS 2020 model.

1636 The first matter to investigate is the cause of the ultrafast response of EEI (Fig. 5 of the main  
 1637 paper), which could be done via the model diagnostics discussed in that section of our paper. If  
 1638 the large difference between the EEI response functions of the two GISS models is related to  
 1639 supercooled cloud water, Fig. 1 of Kelley *et al.* (2020)<sup>34</sup> suggests that the real-world effect may  
 1640 fall between that of the two models. If the higher climate sensitivity of the GISS (2020) model is  
 1641 related to this cloud water phase problem, more realistic treatment of the latter may yield a  
 1642 climate sensitivity between that of the 2014 and 2020 models.



1643  
 1644 Fig. S7. Ratio of warming in the pipeline to EEI,  $(T_{eq} - T_G)/EEI_G$ , in response to GHG and  
 1645 IPCC aerosol forcing for the period 1750-2019 using the response functions for the GISS (2014)  
 1646 model (left) and (b) GISS (2020) model (right).

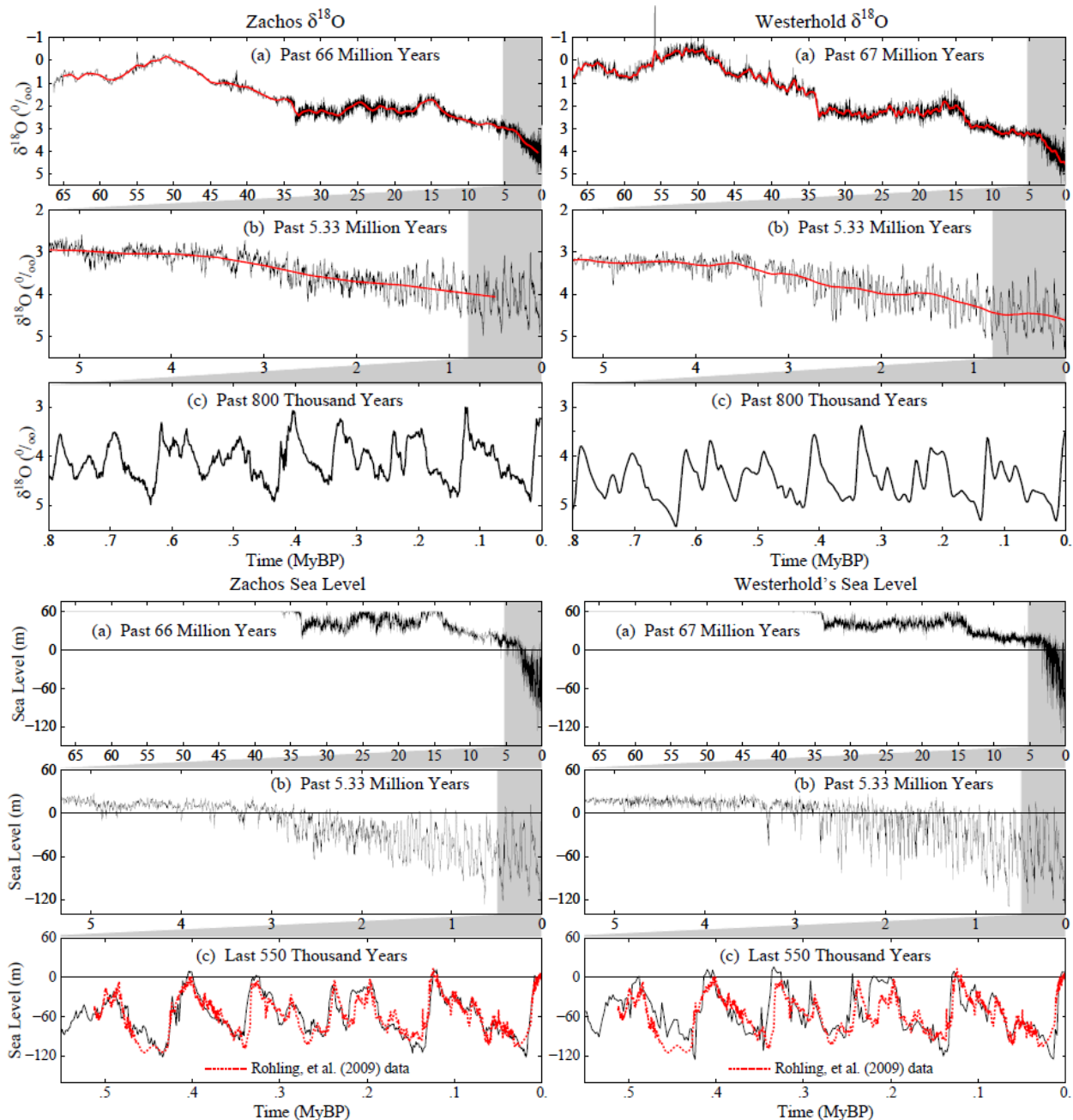
1647 If real world climate sensitivity for  $2 \times CO_2$  is near  $4^\circ C$  or higher, as we have concluded, the total  
 1648 cloud feedback is likely to be even higher than that of the GISS (2020) model. We suggest that it  
 1649 would be useful to calculate response functions for other models, especially models with high  
 1650 climate sensitivity, to help analyze feedbacks and to allow inexpensive climate simulations for  
 1651 arbitrary forcing scenarios. One major caveat: we have used a single response function calculated  
 1652 for  $2 \times CO_2$ . Especially in view of cloud feedbacks, it seems likely that the response function for

1653 aerosol forcing is different from that for CO<sub>2</sub> forcing, because most tropospheric aerosols exist  
1654 well below the clouds. Much might be learned from calculating response functions for GHGs,  
1655 tropospheric aerosols, stratospheric aerosols, and solar irradiance, for example.

1656 The response functions for global temperature and EEI, for both the 2014 and 2020 models,  
1657 smoothed and unsmoothed, are available at <http://www.columbia.edu/~mhs119/ResponseFunctionTables/>

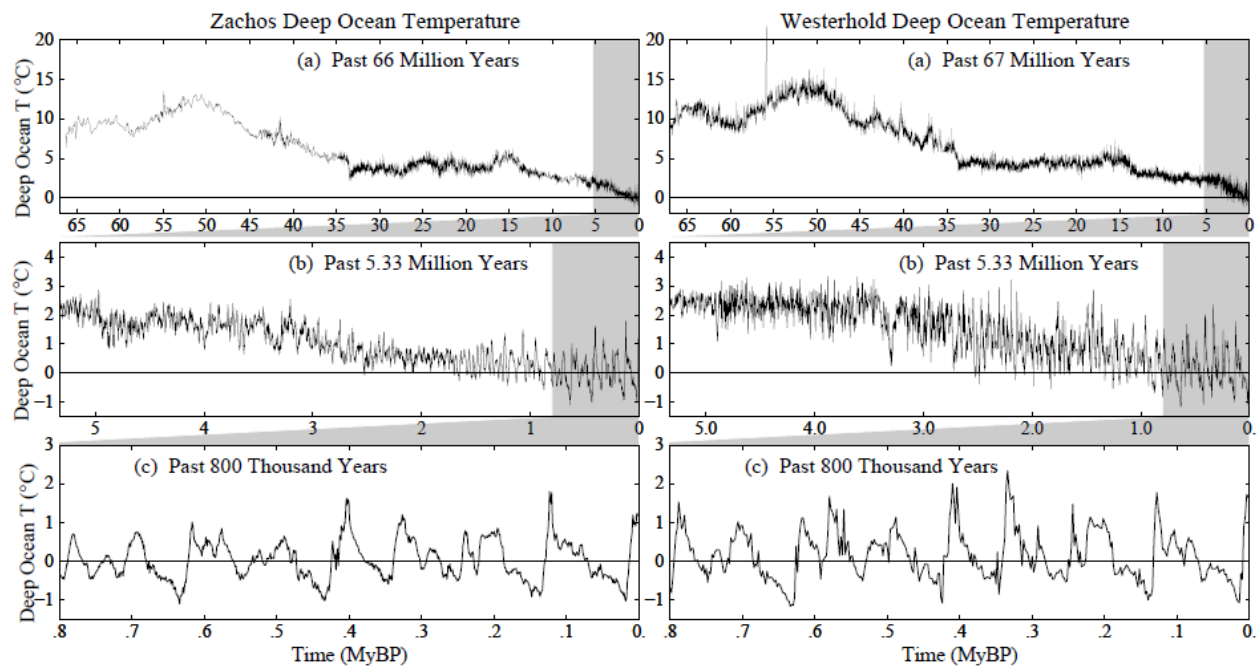
1658 **SM7.  $\delta^{18}\text{O}$  data of Zachos and Westerhold and inferred sea level and  $T_{\text{do}}$**

1659 Zachos and Westerhold  $\delta^{18}\text{O}$  for the full Cenozoic, the Pleistocene, and past 800 thousand years  
1660 are shown in Fig. S8, as well as the inferred sea level and  $T_{\text{do}}$  (sea level is compared to data of  
1661 Rohling *et al.*<sup>103</sup>).

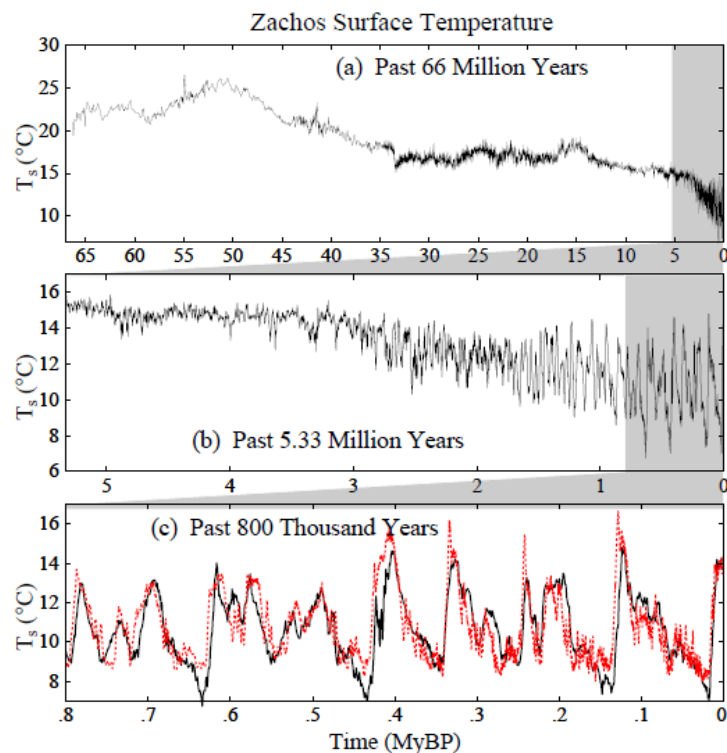


1662

1663



1664  
 1665 Fig. S8. Zachos and Westerhold  $\delta^{18}\text{O}$  and inferred sea level and  $T_{\text{do}}$  for the full Cenozoic, the  
 1666 Pleistocene, and the past 800 thousand years. Sea level data are from Rohling *et al.*<sup>103</sup>



1667  
 1668 Fig. S9. Surface temperature inferred from Zachos  $\delta^{18}\text{O}$ .

1669 **SM8. Global warming in the pipeline: Green's function calculations**

1670 Surface temperature (Fig. S9) from equations (14) and (15) using Zachos  $\delta^{18}\text{O}$ . Antarctic Dome  
 1671 C temperatures<sup>43</sup> (red) relative to last 1,000 years are multiplied by 0.6 to account for polar  
 1672 amplification and 14°C is added for absolute scale.

1673 **SM9. Communications from James Zachos and Thomas Westerhold**

1674 Following is the 3 February 2023 response by Jim Zachos to a query by the first author (JEH) re  
1675 Zachos' interpretation of the differences between the Westerhold and Zachos  $\delta^{18}\text{O}$  data sets:

1676 There are two contributing factors that I am aware of. Because I was just stacking/averaging  
1677 data across sites/basins, the only adjustment applied was for species vital effects (typically  
1678  $<0.5\%$ ), in order to adjust to the "equilibrium" calcite values.

1679 The Westerhold curve/splice required adjusting each splice to the one above based on the overlap  
1680 offset (+/-) between records (from different basins). Because this would be repeated with each  
1681 splice, the effect is cumulative further back in time (see the [Westerhold] paper for the overlap  
1682 adjustments). In the end, the thought was that the overlap adjustments would balance out.

1683 The PETM signal is large because the splice used for that interval was that of Site 1263, Walvis  
1684 Ridge, which has an unusually large  $d18\text{O}$  anomaly, almost double that of other pelagic sites.  
1685 Why? Because it was relatively shallow ( $<1$  km) and thus is capturing a shallow intermediate  
1686 water signal which could be locally amplified with the introduction of warmer more saline  
1687 waters (from a lower latitude source).

1688 The long-term T patterns and even with the orbital cycles are generally similar throughout the  
1689 deep sea, but there are T gradients and thus regional differences in absolute T. This is the  
1690 limitation of the mega splice for estimating mean ocean T.

1691 Following are relevant excerpts (lightly edited for clarity) of a 2 June 2023 response of Thomas  
1692 Westerhold to questions by the first author (JEH). First question: whether the Zachos data are  
1693 more globally distributed and thus reflect more Antarctic Bottom Water conditions, while  
1694 Westerhold data put more weight on North Atlantic Deep Water:

1695 Please look at Sampling Biases in the supplement:<sup>98</sup> For the 66 to 45 Ma part, it is interesting to  
1696 note that  $\delta^{18}\text{O}$  records from the Pacific Shatsky Rise Site 12209 and the Atlantic Walvis Ridge  
1697 Sites 1262/1263 show a consistent pattern. The benthic record is a good monitor for the higher  
1698 latitude temperature development, assuming that most deep water is formed in the high latitudes.  
1699 Thus, it will be biased towards "polar" changes.

1700 Figure S13<sup>98</sup> gives a good idea how the "raw" data look before adjusting. For stitching the curve  
1701 together, we had to correct for the isotopic offsets from different ocean basins. The Pacific  
1702 Ocean is the largest ocean and probably best resembles a global mean, therefore all data were  
1703 offset with respect to the equatorial Pacific values (Sites 1218, U1337, U1338; Fig. S14). One  
1704 has to realize that single, continuous, individual high-resolution records for each of the different  
1705 ocean basins and spanning the entire Cenozoic are unrealistic due to local sedimentation effects  
1706 (gaps and condensed intervals) in available deep-sea sections.

1707 We took the Ceara Rise benthic stack of Wilkens et al. (2017) that stacks available data and is on  
1708 an age model independent from isotope tuning. To compensate, the Ceara record as given in  
1709 Table S33 was corrected  $\delta^{18}\text{O} +0.45$  per mil;  $\delta^{13}\text{C} -1.00$  per mil, Fig. S15, to make it consistent  
1710 with U1337 from the equatorial Pacific.

1711 The Zachos data from EECO are a mix of high latitude data (Kerguelen Plateau, Maude Rise),  
1712 mid latitude South Atlantic Walvis Ridge data and equatorial Pacific data (865 and 577), and  
1713 Indian Ocean. The EECO data for CENOGRID come from Walvis Ridge Southeast Atlantic and  
1714 Equatorial Atlantic Demerara Rise. Compared to Equatorial Pacific, those  $\delta^{18}\text{O}$  are very similar  
1715 (graph provided). Thus, I think the CENOGRID is a good general deep sea temperature indicator  
1716 for the EECO.

1717 Zachos data are generally isotopically heavier, which could be because it is “old” data. We know  
1718 for example that using a common acid bath is not so good to have reliable data for  $\delta^{18}\text{O}$ ; those  
1719 data are from Shackleton, for example. Since the use of Kiel devices, this issue is solved.

1720 Second question: whether a greater weight on North Atlantic Deep Water (which, more reliably  
1721 than Antarctic Bottom Water, includes polar amplification of temperature change) may make the  
1722 Westerhold data yield a more realistic estimate of Cenozoic temperature change?

1723 It is more realistic because the data are of much better quality using modern analytical  
1724 techniques, however we do not know how much is ice volume and salinity effect, and pH change  
1725 in the deep sea. Nele Meckler *et al.* (2022) just published a paper<sup>219</sup> suggesting that temperature  
1726 could be even higher in the deep ocean than given by  $\delta^{18}\text{O}$ .

## 1727 **DATA AVAILABILITY**

1728 "The data used to create the figures in this paper are available in the Zenodo repository,  
1729 at [https://dx.doi.org/\[doi\]](https://dx.doi.org/[doi])."

## 1730 **ACKNOWLEDGMENTS**

1731 We thank Eelco Rohling for inviting JEH to describe our perspective on global climate response  
1732 to human-made forcing. JEH began to write a review of past work, but a paper on the LGM by  
1733 Jessica Tierney *et al.*<sup>53</sup> and data on changing ship emissions provided by Leon Simons led to the  
1734 need for new analyses and division of the paper into two parts. We thank Jessica also for helpful  
1735 advice on other related research papers and Ed Dlugokencky of the NOAA Earth System  
1736 Research Laboratory for continually updated GHG data. JEH designed the study and carried out  
1737 the research with help of Makiko Sato and Isabelle Sangha; Larissa Nazarenko provided data  
1738 from GISS models and helped with analysis; Leon Simons provided ship emission information  
1739 and aided interpretations; Norman Loeb and Karina von Schuckmann provided EEI data and  
1740 insight about implications; Matthew Osman provided paleoclimate data and an insightful review  
1741 of the entire paper; Qinjian Jin provided simulations of atmospheric sulfate and interpretations;  
1742 Eunbi Jeong reviewed multiple drafts and advised on presentation; all authors contributed to our  
1743 research summarized in the paper and reviewed and commented on the manuscript.

1744 All authors declare that they have no conflicts of interest. Climate Science, Awareness and  
1745 Solutions, which is directed by JEH and supports MS and PK is a 501(C3) non-profit supported  
1746 100% by public donations. Principal supporters in the past few years have been the Grantham  
1747 Foundation, Frank Batten, Carl Page, Eric Lemelson, James and Krisann Miller, Ian Cumming,  
1748 Peter Joseph, Gary and Claire Russell, Donald and Jeanne Keith Ferris, Aleksandar Totic, Chris  
1749 Arndt, Jeffrey Miller, Morris Bradley and about 150 more contributors to annual appeals.



- 
- <sup>1</sup> Tyndall J. [On the absorption and radiation of heat by gases and vapours](#). *Phil Mag* 1861;**22**:169-194, 273-285
- <sup>2</sup> Hansen J. [Greenhouse giants](#), Chapter 15 in *Sophie's Planet*. New York: Bloomsbury, 1-8, 2023. Tyndall and Svante Arrhenius in the 1890s made the greatest early contributions to understanding of the greenhouse effect. Eunice Foote earlier did experiments to investigate the effect of individual gases on absorption of solar radiation and speculated on the role of CO<sub>2</sub> in altering Earth's temperature; Tyndall showed that the greenhouse effect is due to absorption of infrared radiation. Draft Chapters 10 (Runaway Greenhouse), 15, 16 (Farmers' Forecast vs End-of-Century) and 17 (Charney's Puzzle: How Sensitive is Earth?) are available [here](#); criticisms are welcome.
- <sup>3</sup> Revelle R, Broecker W, Craig H *et al.* [Appendix Y4 Atmospheric Carbon Dioxide](#). In: President's Science Advisory Committee. *Restoring the Quality of Our Environment*. Washington: The White House, 1965,111-33
- <sup>4</sup> Charney J, Arakawa A, Baker D *et al.* *Carbon Dioxide and Climate: A Scientific Assessment*. Washington: National Academy of Sciences Press, 1979
- <sup>5</sup> Nierenberg WA. [Changing Climate: Report of the Carbon Dioxide Assessment Committee](#). Washington: National Academies Press, 1983
- <sup>6</sup> Hansen JE, Takahashi T (eds). [AGU Geophysical Monograph 29 Climate Processes and Climate Sensitivity](#). Washington: American Geophysical Union, 1984
- <sup>7</sup> Hansen J, Lacis A, Rind D *et al.* [Climate sensitivity: analysis of feedback mechanisms](#). In: Hansen JE, Takahashi T (eds). [AGU Geophysical Monograph 29 Climate Processes and Climate Sensitivity](#). Washington: American Geophysical Union, 1984,130-63
- <sup>8</sup> David EE Jr. [Inventing the Future: Energy and the CO<sub>2</sub> "Greenhouse" Effect](#). In: Hansen JE, Takahashi T (eds). [AGU Geophysical Monograph 29 Climate Processes and Climate Sensitivity](#). Washington: American Geophysical Union, 1984,David1-5
- <sup>9</sup> David EE, Jr later became a global warming denier
- <sup>10</sup> Oreskes N, Conway E. *Merchants of Doubt: How a Handful of Scientists Obscured the Truth on Issues from Tobacco Smoke to Global Warming*. London: Bloomsbury, 2010.
- <sup>11</sup> Intergovernmental Panel on Climate Change. *History of the IPCC*. <https://www.ipcc.ch/about/history> (last accessed 7 March 2023)
- <sup>12</sup> United Nations Framework Convention on Climate Change. *What is the United Nations Framework Convention on Climate Change?* <https://unfccc.int/process-and-meetings/what-is-the-united-nations-framework-convention-on-climate-change> (30 November 2022, date last accessed)
- <sup>13</sup> IPCC. *Climate Change 2021: The Physical Science Basis [Masson-Delmotte V, Zhai P, Pirani A *et al.* (eds)]*. Cambridge and New York: Cambridge University Press, 2021
- <sup>14</sup> Hansen J, Sato M, Hearty P *et al.* [Ice melt, sea level rise and superstorms: evidence from paleoclimate data, climate modeling, and modern observations that 2 C global warming could be dangerous](#). *Atmos Chem Phys* 2016;**16**:3761-812
- <sup>15</sup> Hansen J. [Foreword: uncensored science is crucial for global conservation](#). In: DellaSala DA (ed). *Conservation Science and Advocacy for a Planet in Peril*. Amsterdam: Elsevier, 2021,451
- <sup>16</sup> The working title of the paper is "Sea level rise in the pipeline."
- <sup>17</sup> Bode HW. *Network Analysis and Feedback Amplifier Design*. New York: Van Nostrand, 1945.
- <sup>18</sup> Lacis A, Hansen J, Lee P *et al.* [Greenhouse effect of trace gases, 1970-1980](#). *Geophys Res Lett* 1981;**8**:1035-8
- <sup>19</sup> CLIMAP project members: [Seasonal reconstruction of the Earth's surface at the last glacial maximum](#). Geol Soc Amer, Map and Chart Series, No. 36, 1981
- <sup>20</sup> Manabe, S, Stouffer, RJ. [Sensitivity of a global climate model to an increase of CO<sub>2</sub> concentration in the atmosphere](#). *J Geophys Res* 1980;**85**:5529-54
- <sup>21</sup> Manabe, S [Carbon dioxide and climate change](#). *Adv Geophys* 1983;**25**:39-82
- <sup>22</sup> Klein SA, Hall A, Norris JR *et al.* [Low-cloud feedbacks from cloud-controlling factors: A review](#). *Surv Geophys* 2017;**38**:1307-29
- <sup>23</sup> Sherwood SC, Webb MJ, Annan JD *et al.* [An assessment of Earth's climate sensitivity using multiple lines of evidence](#). *Rev Geophys* 2020;**58**:e2019RG000678
- <sup>24</sup> Zelinka MD, Zhou C, Klein SA. [Insights from a refined decomposition of cloud feedbacks](#). *Geophys Res Lett* 2016;**43**:9259-69
- <sup>25</sup> Zelinka M, Tan I, Oreopoulos L *et al.* [Detailing cloud property feedbacks with a regime-based decomposition](#). *Clim Dyn* 2022: on-line, doi:10.1007/s00382-022-06488-7
- <sup>26</sup> Rind D, Peteet D. [Terrestrial conditions at the last glacial maximum and CLIMAP sea-surface temperature estimates: Are they consistent?](#). *Quat Res* 1985;**24**:1-22
- <sup>27</sup> Rohling EJ, Marino G, Foster GL *et al.* [Comparing climate sensitivity, past and present](#). *Ann Rev Mar Sci* 2018;**10**:261-88

- 
- <sup>28</sup> IPCC. *Climate Change 2014: Synthesis Report. Contribution of Working Groups I, II and III to the Fifth Assessment Report of the Intergovernmental Panel on Climate Change* [Core Writing Team, Pachauri RK, Meyer LA (eds)]. Geneva, 2014
- <sup>29</sup> Andrews T, Gregory JM, Paynter D *et al.* [Accounting for changing temperature patterns increases historical estimates of climate sensitivity](#). *Geophys Res Lett* 2018;**45**:8490-9
- <sup>30</sup> Rugenstein M, Bloch-Johnson J, Abe-Ouchi A *et al.* [LongRunMIP: motivation and design for a large collection of millennial-length AOGCM simulations](#). *Bull Amer Meteorol Soc* 2019;**100**(12):2551-70
- <sup>31</sup> Myhre G, Shindell D, Bréon F-M *et al.* Anthropogenic and Natural Radiative Forcing. In: Stocker TF, Qin D, Plattner G-K *et al.* (eds). *Climate Change 2013: The Physical Science Basis. Contribution of Working Group I to the Fifth Assessment Report of the Intergovernmental Panel on Climate Change*. Cambridge and New York: Cambridge University Press, 2013
- <sup>32</sup> Hansen J, Sato M, Ruedy R *et al.* [Efficacy of climate forcings](#). *J Geophys Res* 2005;**110**:D18104
- <sup>33</sup> Lohmann U, Rotstajn L, Storelvino T *et al.* [Total aerosol effect: radiative forcing or radiative flux perturbation?](#). *Atmos Chem Phys* 2010;**10**:3235-46
- <sup>34</sup> Kelley M, Schmidt GA, Nazarenko L *et al.* [GISS-E2.1: Configurations and climatology](#). *J Adv Model Earth Syst* 2020;**12**(8):e2019MS002025
- <sup>35</sup> Miller RL, Schmidt GA, Nazarenko L *et al.* [CMIP6 historical simulations \(1850-2014\) with GISS-E2.1](#). *J Adv Model Earth Syst* 2021;**13**(1):e2019MS002034
- <sup>36</sup> Eyring V, Bony S, Meehl GA *et al.* [Overview of the Coupled Model Intercomparison Project Phase 6 \(CMIP6\) experimental design and organization](#). *Geoscientific Model Devel* 2016;**9**(5):1937–58
- <sup>37</sup> GISS (2020) model is described as GISS-E2.1-G-NINT in published papers; NINT (noninteractive) signifies that the models use specified GHG and aerosol amounts
- <sup>38</sup> Lacis AA, Oinas V. [A description of the correlated k distributed method for modeling nongray gaseous absorption, thermal emission, and multiple scattering in vertically inhomogeneous atmospheres](#). *J Geophys R* 1991;**96**:9027-63
- <sup>39</sup> Rothman L, Rinsland C, Goldman A *et al.* [The HITRAN molecular spectroscopic database and HAWKS \(HITRAN Atmospheric Workshation\) 1996 edition](#). *J Quan Spec Rad Trans* 1998;**60**:665–710
- <sup>40</sup> Prather M, Ehhalt D. Chapter 4 Atmospheric chemistry and greenhouse gases. In: Houghton JT (ed). *Climate Change 2001: The Scientific Basis*. New York: Cambridge Univ, 2001;239-87
- <sup>41</sup> Hansen J, Sato M. [Greenhouse gas growth rates](#). *Proc Natl Acad Sci* 2004;**101**:16109-14
- <sup>42</sup> Columbia University. [MPTG and OTG data: www.columbia.edu/~mhs119/GHG/TG\\_F.1900-1990.txt and www.columbia.edu/~mhs119/GHG/TG\\_F.1992-2020.txt 3 December 2022](#) (date last accessed)
- <sup>43</sup> Jouzel J, Masson-Delmotte V, Cattani O *et al.* [Orbital and millennial Antarctic climate variability over the past 800,000 years](#). *Science* 2007;**317**:793-6
- <sup>44</sup> Luthi D, Le Floch M, Bereiter B *et al.* [High-resolution carbon dioxide concentration record 650,000-800,000 years before present](#). *Nature* 2008;**453**:379-82
- <sup>45</sup> Hays JD, Imbrie J, Shackleton NJ. [Variation in the Earth's orbit: pacemaker of the ice ages](#), *Science* 1976;**194**:1121-32
- <sup>46</sup> Lorius C, Jouzel J, Raynaud D *et al.* [The ice-core record: Climate sensitivity and future greenhouse warming](#). *Nature* 1990;**347**:139-45
- <sup>47</sup> Zachos J, Pagani M, Sloan L *et al.* [Trends, rhythms, and aberrations in global climate 65 Ma to present](#). *Science* 2001;**292**:686-93
- <sup>48</sup> Hansen J, Sato M, Kharecha P *et al.* [Climate change and trace gases](#). *Phil Trans Roy Soc A* 2007;**365**:1925-54
- <sup>49</sup> It is often said that glacial terminations (at intervals ~100,000 years in Fig. 2) occur when Earth orbital parameters produce maximum summer insolation at the latitudes of Northern Hemisphere ice sheets (e.g., Cheng H, Edwards RL, Broecker WS *et al.* [Ice age terminations](#). *Science* 2009;**326**:248-52. However, close examination of termination dates shows that they occur at times of late Spring (mid-May) maximum radiation anomalies [55]. Maximum insolation anomaly in late Spring causes meltwater induced darkening of the ice to occur as early in the year as possible, thus lengthening the melt season.
- <sup>50</sup> Ruddiman WF, Fuller DQ, Kutzbach JE *et al.* [Late Holocene climate: natural or anthropogenic?](#) *Rev Geophys* 2016;**54**:93-118
- <sup>51</sup> Schilt A, Baumgartner M, Schwander J *et al.* [Atmospheric nitrous oxide during the last 140,000 years](#). *Earth Planet Sci Lett* 2010;**300**:33-43
- <sup>52</sup> Hansen J, Nazarenko L, Ruedy R *et al.* [Earth's energy imbalance: Confirmation and implications](#). *Science* 2005;**308**:1431-5 An imbalance of 1 W/m<sup>2</sup> for a millennium is enough energy to melt ice raising sea level 110 m or to raise the temperature of the ocean's upper kilometer by 11°C
- <sup>53</sup> Tierney JE, Zhu J, King J *et al.* [Glacial cooling and climate sensitivity revisited](#). *Nature* 2020;**584**:569-73

- 
- <sup>54</sup> Osman MB, Tierney JE, Zhu J *et al.* [Globally resolved surface temperatures since the Last Glacial Maximum](#). *Nature* 2021;**599**:239-44
- <sup>55</sup> At maximum LGM cooling, i.e., at 18 ky BP, the cooling is  $\sim 7^{\circ}\text{C}$  (Osman *et al.* [ref 24]; Tierney, priv. comm.)
- <sup>56</sup> Seltzer AM, Ng J, Aeschbach W *et al.* [Widespread six degrees Celsius cooling on land during the Last Glacial Maximum](#). *Nature* 2021;**593**:228-32
- <sup>57</sup> Schneider T, Teixeira J, Bretherton CS *et al.* [Climate goals and computing the future of clouds](#). *Nature Clim Chan* 2017;**7**:3-5
- <sup>58</sup> Pincus R, Forster PM, Stevens B. [The radiative forcing model intercomparison project \(RFMIP\): experimental protocol for CMIP6](#). *Geoscientific Model Devel* 2016;**9**:3447-3460
- <sup>59</sup> Kagiyama M, Braconnot P, Harrison SP *et al.* [The PMIP4 contribution to CMIP6 – Part 1: overview and overarching analysis plan](#). *Geosci Model Dev* 2018;**11**:1033-1057
- <sup>60</sup> Hegerl GC, Zwiers FW, Braconnot P *et al.* Chapter 9: Understanding and attributing climate change. In: Solomon SD (ed). *Climate change 2007: The physical science basis*. New York: Cambridge Univ, 2007,663-745
- <sup>61</sup> Yoshimori M, Yokohata T, Abe-Ouchi A. [A comparison of climate feedback strength between CO<sub>2</sub> doubling and LGM experiments](#). *J Clim* 2009;**22**:3374-95
- <sup>62</sup> Stap LB, Kohler P, Lohmann G. [Including the efficacy of land ice changes in deriving climate sensitivity from paleodata](#). *Earth Syst Dynam* 2019;**10**:333-45
- <sup>63</sup> Koppen W. Das geographische system der climate. In Koppen W, Geiger G (eds) *Handbuch der Klimatologie I(C)*. Berlin: Boentraeger, 1936.
- <sup>64</sup> Kohler P, Bintanja R, Fischer H *et al.* [What caused Earth's temperature variations during the last 800,000 years? Data-based evidence on radiative forcing and constraints on climate sensitivity](#). *Quat Sci Rev* 2010;**29**:129-45
- <sup>65</sup> Hansen J, Sato M, Kharecha P *et al.* [Target atmospheric CO<sub>2</sub>: Where should humanity aim?](#) *Open Atmos Sci J* 2008;**2**:217-231
- <sup>66</sup> Rabineau M, Berne S, Oliver JL *et al.* [Paleo sea levels reconsidered from direct observation of paleoshoreline position during Glacial Maxima \(for the last 500,000 yr\)](#). *Earth Planet Sci Lett* 2006;**252**:119-37
- <sup>67</sup> Rohling EJ, Hibbert FD, Williams FH *et al.* [Differences between the last two glacial maxima and implications for ice-sheet,  \$\delta^{18}\text{O}\$ , and sea-level reconstructions](#). *Quat Sci Rev* 2017;**176**:1-28
- <sup>68</sup> Hansen J, Sato M, Kharecha P *et al.* [Young people's burden: requirement of negative CO<sub>2</sub> emissions](#). *Earth Syst Dyn* 2017;**8**:577-616
- <sup>69</sup> Hoffman JS, Clark PU, Parnell AC *et al.* [Regional and global sea-surface temperatures during the last interglaciation](#). *Science* 2017;**355**(6322):276-279
- <sup>70</sup> Ruth U, Barnola JM, Beer J *et al.* [EDML1: a chronology for the EPICA deep ice core from Dronning Maud Land, Antarctica, over the last 150 000 years](#). *Clim Past* 2007;**3**:475-485
- <sup>71</sup> Hansen J, Sato M, Russell G *et al.* [Climate sensitivity, sea level, and atmospheric carbon dioxide](#). *Phil Trans R Soc A* 2013;**371**:20120294
- <sup>72</sup> Russell GL, Miller JR, Rind D. [A coupled atmosphere-ocean model for transient climate change studies](#). *Atmos Ocean* 1995;**33**:683-730
- <sup>73</sup> Hoffman PF, Schrag DP. [The snowball Earth hypothesis: testing the limits of global change](#). *Terra Nova* 2002;**14**:129-55
- <sup>74</sup> Sackmann J, Boothroyd AI, Kraemer KE. [Our Sun. III. Present and future](#). *Astrophys J* 1993;**418**:457-68
- <sup>75</sup> Meraner K, Mauritsen T, Voight A. [Robust increase in equilibrium climate sensitivity under global warming](#). *Geophys Res Lett* 2013;**40**:5944-8
- <sup>76</sup> Beerling DJ, Fox A, Stevenson DS *et al.* [Enhanced chemistry-climate feedbacks in past greenhouse worlds](#). *Proc Natl Acad. Sci. USA* 2011;**108**:9770–5
- <sup>77</sup> Bryan K, Komro FG, Manabe S *et al.* [Transient climate response to increasing atmospheric carbon dioxide](#). *Science* 1982;**215**:56-8
- <sup>78</sup> Hansen J, Russell G, Lacis A *et al.* [Climate response times: dependence on climate sensitivity and ocean mixing](#). *Science* 1985;**229**:857-9
- <sup>79</sup> Hansen J [Climate Threat to the Planet](#), American Geophysical Union, San Francisco, California, 17 December 2008, <http://www.columbia.edu/~jeh1/2008/AGUBjerknes20081217.pdf>. (3 December 2022, date last accessed)
- <sup>80</sup> Tom Delworth (NOAA Geophysical Fluid Dynamics Laboratory), Gokhan Danabasoglu (National Center for Atmospheric Research), and Jonathan Gregory (UK Hadley Centre) provided long  $2\times\text{CO}_2$  runs of GCMs of these leading modeling groups. All three models had response time as slow or slower than the GISS GCM.
- <sup>81</sup> Yr 1 (no smoothing), yr 2 (3-yr mean), yr 3-12 (5-yr mean), yr 13-300 (25-yr mean), yr 301-5000 (101-yr mean).
- <sup>82</sup> Good P, Gregory JM, Lowe JA. [A step-response simple climate model to reconstruct and interpret AOGCM projections](#). *Geophys Res Lett* 2011;**38**:e2010GL0452008

- <sup>83</sup> Schmidt GA, Kelley M, Nazarenko L *et al.* [Configuration and assessment of the GISS ModelE2 contributions to the CMIP5 archive](#). *J Adv Model Earth Syst* 2014;**6**:141-84
- <sup>84</sup> The GISS (2014) model is labeled as GISS-E2-R-NINT and GISS (2020) as GISS-E2.1-G-NINT in published papers, where NINT (noninteractive) signifies that the models use specified GHG and aerosol amounts.
- <sup>85</sup> Prather MJ. [Numerical advection by conservation of second order moments](#). *J Geophys Res* 1986;**91**:6671-81
- <sup>86</sup> Romanou A, Marshall J, Kelley M *et al.* [Role of the ocean's AMOC in setting the uptake efficiency of transient tracers](#). *Geophys Res Lett* 2017;**44**:5590-8
- <sup>87</sup> von Schuckmann K, Cheng L, Palmer MD *et al.* [Heat stored in the Earth system: where does the energy go?](#), *Earth System Science Data* 2020;**12**:2013-41
- <sup>88</sup> Loeb NG, Johnson GC, Thorsen, TJ *et al.* [Satellite and ocean data reveal marked increase in Earth's heating rate](#). *Geophys Res Lett* 2021;**48**:e2021GL093047
- <sup>89</sup> Hansen J, Johnson D, Lacis A *et al.* [Climate impact of increasing atmospheric carbon dioxide](#). *Science* 1981;**213**:957-966
- <sup>90</sup> Kamae Y, Watanabe M, Ogura T *et al.* [Rapid adjustments of cloud and hydrological cycle to increasing CO<sub>2</sub>: a review](#). *Curr Clim Chan Rep* 2015;**1**:103-13
- <sup>91</sup> Zelinka MD, Myers TA, McCoy DT *et al.* [Causes of higher climate sensitivity in CMIP6 models](#). *Geophys Res Lett* 2020;**47**:e2019GL085782
- <sup>92</sup> DeConto RM, Pollard D. [Rapid Cenozoic glaciation of Antarctica induced by declining atmospheric CO<sub>2</sub>](#). *Nature* 2003;**421**:245-9
- <sup>93</sup> Crowley TJ. [Pliocene climates: the nature of the problem](#). *Marine Micropaleontology* 1996;**27**:3-12
- <sup>94</sup> Lacis AA, Schmidt GA, Rind D *et al.* [Atmospheric CO<sub>2</sub>: principal control knob governing Earth's temperature](#). *Science* 2010;**330**:356-9
- <sup>95</sup> Rae JWB, Zhang YG, Liu X *et al.* [Atmospheric CO<sub>2</sub> over the past 66 million years from marine archives](#). *Ann Rev Earth Plan Sci* 2021;**49**:609-41
- <sup>96</sup> Steinthorsdottir M, Vajda V, Pole M *et al.* [Moderate levels of Eocene pCO<sub>2</sub> indicated by Southern Hemisphere fossil plant stomata](#). *Geology* 2019;**47**:914-8
- <sup>97</sup> Pearson PN. [Oxygen isotopes in foraminifera: an overview and historical review](#). In: Ivany LC, Huber BT (eds). *Reconstructing Earth's Deep-Time Climate – The State of the Art in 2012*, Paleontolog Soc Pap, 2012;**18**:1-38
- <sup>98</sup> Westerhold T, Marwan N, Drury AJ *et al.* [An astronomically dated record of Earth's climate and its predictability over the last 66 million years](#). *Science* 2020;**369**:1383-7
- <sup>99</sup> Cutler KB, Edwards RL, Taylor FW *et al.* [Rapid sea-level fall and deep-ocean temperature change since the last interglacial period](#). *Earth Planet Sci Lett* 2003;**206**:253-71
- <sup>100</sup> Meckler AN, Sexton PF, Piasecki AM *et al.* [Cenozoic evolution of deep ocean temperature from clumped isotope thermometry](#). *Science* 2022;**377**:86-90
- <sup>101</sup> Yatheesh V, Dymant J., Bhattacharya GC *et al.* [Detailed structure and plate reconstructions of the central Indian Ocean between 83.0 and 42.5 Ma \(chrons 34 and 20\)](#). *J Geophys Res: Solid Earth* 2020,**124**:4303-4322
- <sup>102</sup> Siddall M, Honisch B, Waelbroeck C *et al.* [Changes in deep Pacific temperature during the mid-Pleistocene transition and Quaternary](#). *Quatern Sci Rev* 2010;**29**:170-81
- <sup>103</sup> Rohling EJ, Grant K, Bolshaw M *et al.* [Antarctic temperature and global sea level closely coupled over the past five glacial cycles](#). *Nature Geosci* 2009;**2**:500-4
- <sup>104</sup> Seltzer, AM, Blard, P-H, Sherwood, SC *et al.* [Terrestrial amplification of past, present, and future climate change](#). *Sci Advan* 2023(8 Feb);**9**:eadf8119
- <sup>105</sup> Zhu J, Poulsen CJ, Tierney JE. [Simulation of Eocene extreme warmth and high climate sensitivity through cloud feedbacks](#). *Sci Advan* 2019;**5**:eaax1874
- <sup>106</sup> Hansen J. [Storms of My Grandchildren](#). ISBN 978-1-60819-502-2. New York: Bloomsbury, 2009
- <sup>107</sup> Berner RA. [The Phanerozoic Carbon Cycle: CO<sub>2</sub> and O<sub>2</sub>](#). New York: Oxford Univ Press, 2004
- <sup>108</sup> Rohling EJ. [The climate question: natural cycles, human impact, future outlook](#). Oxford Univ Press, 2019
- <sup>109</sup> Merdith AS, Williams SE, Brune S *et al.* [Rift and plate boundary evolution across two supercontinent cycles](#). *Global Plan Chan* 2019;**173**:1-14
- <sup>110</sup> Peace AL, Phethean JJJ, Franke D *et al.* [A review of Pangea dispersal and large igneous provinces – in search of a causative mechanism](#). *Earth-Science Rev* 2020;**206**:102902
- <sup>111</sup> In Swedish, traps are stairs. Basalt formations are commonly in layers from multiple extrusions.
- <sup>112</sup> Baksi AK. [Comment on “40Ar/39Ar dating of the Rajahmundry Traps, eastern India and their relationship to the Deccan Traps” by Knight \*et al.\* \[Earth Planet Sci. Lett. 208 \(2003\) 85-99\]](#). *Earth Planet Sci Lett* 2005;**239**:368-373
- <sup>113</sup> Guo Z, Wilson M, Dingwell D *et al.* [India-Asia collision as a driver of atmospheric CO<sub>2</sub> in the Cenozoic](#). *Nature Comm* 2021;**12**:3891
- <sup>114</sup> Raymo ME, Ruddiman WF. [Tectonic forcing of late Cenozoic climate](#). *Nature* 1992;**359**:117-22

- 
- <sup>115</sup> Ramos EJ, Lackey JS, Barnes JD *et al.* [Remnants and rates of metamorphic decarbonation in continental arcs](#). *GSA Today* 2020;**30**:doi.org/10.1130/GSATG432A.1
- <sup>116</sup> Bufe A, Hovius N, Emberson R *et al.* [Co-variation of silicate, carbonate and sulfide weathering drives CO<sub>2</sub> release with erosion](#). *Nature Geosci* 2021;**14**:211-6
- <sup>117</sup> Scotese C. [PALEOMAP PaleoAtlas for GPLates](#), <https://www.earthbyte.org/paleomap-paleoatlas-for-gplates/>
- <sup>118</sup> Lee CTA, Shen B, Slotnick BS *et al.* [Continental arc-island arc fluctuations, growth of crustal carbonates, and long-term climate change](#). *Geosphere* 2013;**9**(1):21-36
- <sup>119</sup> McKenzie NR, Horton BK, Loomis SE *et al.* [Continental arc volcanism as the principal driver of icehouse-greenhouse variability](#). *Science* 2016;**352**:444-7
- <sup>120</sup> Petersen KD, Schiffer C, Nagel T. [LIP formation and protracted lower mantle upwelling induced by rifting and delamination](#). *Scientific Rep* 2018;**8**:16578
- <sup>121</sup> Eldholm E, Grue K. [North Atlantic volcanic margins: dimensions and production rates](#). *J Geophys Res* 1994;**99**(B2):2955-68
- <sup>122</sup> Ji S, Nie J, Lechler A *et al.* [A symmetrical CO<sub>2</sub> peak and asymmetrical climate change during the middle Miocene](#). *Earth Plan Sci Lett* 2019;**499**:134-44
- <sup>123</sup> Babila TL, Foster GL. [The Monterey Event and the Paleocene-Eocene Thermal Maximum: two contrasting oceanic carbonate system responses to LIP emplacement and eruption](#). In: Ernst RE, Dickson A, Bekker A (eds).
- <sup>124</sup> Storey M, Duncan RA, Tegner C. [Timing and duration of volcanism in the North Atlantic Igneous Province: implications for geodynamics and links to the Iceland hotspot](#). *Chem Geol* 2007;**241**:264-81
- <sup>125</sup> Svensen H, Planke S, Malthé-Sorensen A *et al.* [Release of methane from a volcanic basin as a mechanism for initial Eocene global warming](#). *Nature* 2004;**429**:542-5
- <sup>126</sup> Gutjahr M, Ridgwell A, Sexton PF *et al.* [Very large release of mostly volcanic carbon during the Palaeocene Thermal Maximum](#). *Nature* 2017;**548**:573-7
- <sup>127</sup> Frieling J, Peterse F, Lunt DJ *et al.* [Widespread warming before and elevated barium burial during the Paleocene-Eocene thermal maximum: evidence for methane hydrate release?](#) *Paleocean Paleoclim* 2019;**34**:546-66
- <sup>128</sup> Small apparent discrepancy is roundoff. CO<sub>2</sub> forcing is 9.13 W/m<sup>2</sup> and solar forcing is – 1.16 W/m<sup>2</sup> at 50MyBP.
- <sup>129</sup> Forcing = 4.6 W/m<sup>2</sup> assumes that the increase of non-CO<sub>2</sub> GHGs is human-made. This is true for CFCs and most trace gases, but a small part of CH<sub>4</sub> and N<sub>2</sub>O growth could be a slow feedback, slightly reducing the GHG forcing.
- <sup>130</sup> 9.9°C for ECS = 1.2°C per W/m<sup>2</sup>; 10.1°C for ECS = 1.22°C per W/m<sup>2</sup> (the precise ECS for 7°C LGM cooling)
- <sup>131</sup> Walker JCG, Hays PB, Kasting JF. [A negative feedback mechanism for the long-term stabilization of Earth's surface temperature](#). *J Geophys Res* 1981;**86**(C10):9776-82
- <sup>132</sup> Foster GL, Hull P, Lunt DJ *et al.* [Placing our current 'hyperthermal' in the context of rapid climate change in our geological past](#). *Phil Trans Roy Soc A* 2018;**376**:200170086
- <sup>133</sup> Tierney JE, Zhu J, Li M [Spatial patterns of climate change across the Paleocene-Eocene thermal maximum](#). *Proc Natl Acad Sci* 2022;**119**(42):e2205326119
- <sup>134</sup> Nunes F, Norris RD. [Abrupt reversal in ocean overturning during the Palaeocene/Eocene warm period](#). *Nature* 2006;**439**:60-63
- <sup>135</sup> Hopcroft PO, Ramstein G, Pugh TAM *et al.* [Polar amplification of Pliocene climate by elevated trace gas radiative forcing](#). *Proc Natl Acad Sci USA* 2020;**117**:23401-7
- <sup>136</sup> Schaller MF, Fung MK. [The extraterrestrial impact evidence at the Palaeocene-Eocene boundary and sequence of environmental change on the continental shelf](#). *Phil Trans Roy Soc A* 2018;**376**:20170081
- <sup>137</sup> Kirkland Turner S. [Constraints on the onset duration of the Paleocene-Eocene Thermal Maximum](#). *Phil Trans Roy Soc A* 2018;**376**:20170082
- <sup>138</sup> Zachos JC, McCarren H, Murphy B *et al.* [Tempo and scale of late Paleocene and early Eocene carbon isotope cycles: implications for the origin of hyperthermals](#). *Earth Plan Sci Lett* 2010;**299**:242-9
- <sup>139</sup> Nichols JE, Peteet DM. [Rapid expansion of northern peatlands and doubled estimate of carbon storage](#). *Nat Geosci* 2019;**12**:917-21
- <sup>140</sup> Hanson PJ, Griffiths NA, Iverson CM *et al.* [Rapid net carbon loss from a whole-ecosystem warmed peatland](#). *AGU Advan* 2020;**1**: e2020AV000163
- <sup>141</sup> Bowen GJ, Maibauer BJ, Kraus MJ *et al.* [Two massive, rapid releases of carbon during the onset of the Palaeocene-Eocene thermal maximum](#). *Nature Geosci* 2015;**8**:44-7
- <sup>142</sup> Archer D, Buffett B, Brovkin V. [Ocean methane hydrates as a slow tipping point in the global carbon cycle](#). *Proc Natl Acad Sci USA* 2009;**106**:20596-601
- <sup>143</sup> Archer D, Eby M, Brovkin V *et al.* Atmospheric lifetime of fossil fuel carbon dioxide. *Annual Rev Earth Planet Sci* 2009;**37**:117-34
- <sup>144</sup> World Health Organization, *Ambient (outdoor) air pollution*, [https://www.who.int/en/news-room/fact-sheets/detail/ambient-\(outdoor\)-air-quality-and-health](https://www.who.int/en/news-room/fact-sheets/detail/ambient-(outdoor)-air-quality-and-health) (23 June 2022, date last accessed)

- 
- <sup>145</sup> Marcott SA, Shakun JD, Clark PU *et al.* [A reconstruction of regional and global temperature for the last 11,300](#). *Science* 2013;**339**:1198-201
- <sup>146</sup> Tardiff R, Hakim GJ, Perkins WA *et al.* [Last Millenium Reanalysis with an expanded proxy database and seasonal proxy modeling](#). *Clim Past* 2019;**15**:1251-73
- <sup>147</sup> Watson AJ, Garabato ACN. [The role of Southern Ocean mixing and upwelling in glacial-interglacial atmospheric CO<sub>2</sub> change](#). *Tellus* 2006;**58B**:73–87
- <sup>148</sup> Wikipedia. [File:Post-Glacial Sea Level.png](#) [https://commons.wikimedia.org/wiki/File:Post-Glacial\\_Sea\\_Level.png](https://commons.wikimedia.org/wiki/File:Post-Glacial_Sea_Level.png) (3 December 2022, date last accessed)
- <sup>149</sup> Barber B. [Resistance by scientists to scientific discovery](#). *Science* 1961;**134**:596-602
- <sup>150</sup> Hoffman PF, Kaufman AJ, Halverson GP *et al.* [A Neoproterozoic Snowball Earth](#). *Science* 1998;**281**:1342-1346
- <sup>151</sup> Alvarez L, Alvarez W, Asaro F *et al.* [Extraterrestrial Cause for the Cretaceous-Tertiary Extinction](#). *Science* 1980;**208**:1095-1108
- <sup>152</sup> Mishchenko MI, Cairns B, Kopp G *et al.* [Accurate monitoring of terrestrial aerosols and total solar irradiance: Introducing the Glory mission](#). *Bull Amer Meteorol Soc* 2007;**88**:677-691
- <sup>153</sup> Hansen J, Rossow W, Fung I. *Long-term monitoring of global climate forcings and feedbacks*. Washington: [NASA Conference Publication 3234](#), 1993
- <sup>154</sup> Bellouin N, Quaas J, Gryspeerdt E *et al.* [Bounding global aerosol radiative forcing of climate change](#). *Rev Geophys* 2020;**58**:e2019RG000660
- <sup>155</sup> Kruzman D. [Wood-burning stoves raise new health concerns](#). *Undark Magazine* 2022,02 March (accessed 06 February 2023).
- <sup>156</sup> Glojek K, Mocnik G, Alas HDC *et al.* [The impact of temperature inversions on black carbon and particle mass concentrations in a mountainous area](#). *Atmos Chem Phys* 2022;**22**:5577-601
- <sup>157</sup> Rutgard O. [Why is Britain taking the axe to wood-burning stoves?](#) Bloomberg Green, 4 February 2023.
- <sup>158</sup> Day JW, Gunn JD, Folan WJ *et al.* [Emergence of complex societies after sea level stabilized](#). *EOS Trans Amer Geophys Union* 2007;**88(15)**:169-70
- <sup>159</sup> VanCuren RA. [Asian aerosols in North America: extracting the chemical composition and mass concentration of the Asian continental aerosol plume from long-term aerosol records in the western United States](#). *J Geophys Res Atmos* 2003;**108**:D20,4623
- <sup>160</sup> Knutti R. [Why are climate models reproducing the observed global surface warming so well?](#) *Geophys Res Lett* 2008;**35**:L18704
- <sup>161</sup> Hansen J, Sato M, Kharecha P *et al.* [Earth's energy imbalance and implications](#). *Atmos Chem Phys* 2011;**11**:13421-49
- <sup>162</sup> Koch D, Bauer SE, Del Genio A *et al.* [Coupled aerosol-chemistry-climate twentieth-century model investigation: trends in short-lived species and climate responses](#). *J Clim* 2011;**24**:2693-714
- <sup>163</sup> Novakov T, Ramanathan V, Hansen JE *et al.* [Large historical changes of fossil-fuel black carbon aerosols](#). *Geophys Res Lett* 2003;**30**:1324
- <sup>164</sup> Two significant flaws in the derivation of this “alternative aerosol scenario” were largely offsetting: (1) the intermediate climate response function employed (Fig. 5 of Hansen J, Sato M, Kharecha P *et al.* [Earth's energy imbalance and implications](#). *Atmos Chem Phys* 2011;**11**:13421-49) was too “fast,” but (2) this was compensated by use of a low climate sensitivity of 3°C for 2×CO<sub>2</sub>.
- <sup>165</sup> Bauer SE, Tsigaridis K, Faluvegi G *et al.* [Historical \(1850-2014\) aerosol evolution and role on climate forcing using the GISS ModelE2.1 contribution to CMIP6](#). *J Adv Model Earth Syst*, 2020;**12(8)**:e2019MS001978.
- <sup>166</sup> In the absence of a response function from a GCM with ECS = 4°C, we use the normalized response function of the GISS (2020) model and put  $\lambda = 1^\circ\text{C per W/m}^2$  in equation (5).
- <sup>167</sup> Hansen J, Ruedy R, Sato M *et al.* [Global surface temperature change](#). *Rev Geophys* 2010;**48**:RG4004
- <sup>168</sup> Lenssen NJL, Schmidt GA, Hansen JE *et al.* [Improvements in the GISTEMP uncertainty model](#). *J Geophys Res Atmos* 2019;**124(12)**:6307-26
- <sup>169</sup> Jin Q, Grandey BS, Rothenberg D *et al.* [Impacts on cloud radiative effects induced by coexisting aerosols converted from international shipping and maritime DMS emissions](#). *Atmos Chem Phys* 2018;**18**:16793-16808
- <sup>170</sup> Hansen J, Rossow W, Carlson B *et al.* [Low-cost long-term monitoring of global climate forcings and feedbacks](#). *Clim Chan* 1995;**31**:247-271
- <sup>171</sup> Bellouin N, Quaas J, Gryspeerdt E *et al.* [Bounding global aerosol radiative forcing of climate change](#). *Rev Geophys* 2020;**58**:e2019RG000660
- <sup>172</sup> Glassmeier F, Hoffmann F, Johnson JS *et al.* [Aerosol-cloud-climate cooling overestimated by ship-track data](#). *Science* 2021;**371**:485-9
- <sup>173</sup> Manshausen P, Watson-Parris D, Christensen MW *et al.* [Invisible ship tracks show large cloud sensitivity to aerosol](#). *Nature* 2022;**610**:101-6

- <sup>174</sup> Wall CJ, Norris JR, Possner A *et al.*: [Assessing effective radiative forcing from aerosol-cloud interactions over the global ocean](#). *Proc Natl Acad Sci USA* 2022;**119**:e2210481119
- <sup>175</sup> Forster P, Storelvmo T, Armour K, *et al.* The Earth's Energy Budget, Climate Feedbacks, and Climate Sensitivity. In: Masson-Delmotte V (ed). *Climate Change 2021: The Physical Science Basis*. New York: Cambridge University Press, 2021, Cambridge, 923–1054
- <sup>176</sup> International Maritime Organization (IMO), MEPC.176(58), Amendments to the annex of the protocol of 1997 to amend the international convention for the prevention of pollution from ships, 1973, as modified by the protocol of 1978 relating thereto (Revised MARPOL, Annex VI), 2008
- <sup>177</sup> Gryspeerd E, Smith TWP, O'Keeffe E *et al.* [The impact of ship emission controls recorded by cloud properties](#). *Geophys Res Lett* 2019;**46**:12,547-55
- <sup>178</sup> International Maritime Organization. [IMO 2020 – cutting sulphur oxide emissions](#), lowers limit on sulfur content of marine fuels from 3.5% to 0.5%. <https://www.imo.org/en/MediaCentre/HotTopics/Pages/Sulphur-2020.aspx> (5 December 2022, date last accessed)
- <sup>179</sup> Yuan T, Song H, Wood R *et al.* [Global reduction in ship-tracks from sulfur regulations for shipping fuel](#). *Sci Adv* 2022;**8**(29):eabn7988
- <sup>180</sup> Data sources, graphs available <http://www.columbia.edu/~mhs119/Solar/>. (23 October 2022, last accessed)
- <sup>181</sup> Loeb NG, Thorsen TJ, Rose FG *et al.* [Recent variations in EEI, SST & clouds](#). ERB Workshop, Hamburg, Germany, 12-14 October, 2022 (3 December 2022, date last accessed).
- <sup>182</sup> Sato M. [Sea ice area](#). Columbia University webpage (05 November 2022, date last accessed).
- <sup>183</sup> McCoy DT, Burrows SM, Wood R *et al.* [Natural aerosols explain seasonal and spatial patterns of Southern Ocean cloud albedo](#). *Sci Adv* 2015;**1**:e1500157
- <sup>184</sup> Section 7.4.2.4 Cloud Feedbacks, in IPCC, 2021: Climate Change 2021 (reference 13).
- <sup>185</sup> Feynman RP. Surely You're Joking, Mr. Feynman! ISBN 0-553-34668-7. New York: WW Norton, 1985.
- <sup>186</sup> Barber B. [Resistance by scientists to scientific discovery](#). *Science* 1961;**134**:596-602
- <sup>187</sup> Hariri AR, Brown SM, Williamson DE *et al.* [Preference for immediate over delayed rewards is associated with magnitude of ventral striatal activity](#). *J Neurosci* 2006;**26**(51):13213-7
- <sup>188</sup> Hansen JE. [Scientific reticence and sea level rise](#). *Environ Res Lett* 2007;**2**:er1246875
- <sup>189</sup> Dunne JP, Winton M, Bacmeister J *et al.* [Comparison of equilibrium climate sensitivity estimates from slab ocean, 150-year, and longer simulations](#). *Geo Res Lett* 2020;**47**:e2020GL088852
- <sup>190</sup> Forster PM, Maycock AC, McKenna CM *et al.* [Latest climate models confirm need for urgent mitigation](#). *Nat Clim Chan* 2020;**10**:7-10
- <sup>191</sup> Liu Z, Zhu J, Rosenthal Y *et al.* [The Holocene temperature conundrum](#). *Proc Natl Acad Sci USA* 2014; 1407229111:E3501-E3505
- <sup>192</sup> Glojek K, Mocnik G, Alas HDC *et al.* [The impact of temperature inversions on black carbon and particle mass concentrations in a mountainous area](#). *Atmos Chem Phys* 2022;**22**:5577-601
- <sup>193</sup> Diamond MS. [Detection of large-scale cloud microphysical changes and evidence for decreasing cloud brightness within a major shipping corridor after implementation of the International Maritime Organization 2020 fuel sulfur regulations](#). *EGUsphere* 2023;doi.org/10.5194/egusphere-2023-971
- <sup>194</sup> Hansen, JE. [A slippery slope: how much global warming constitutes “dangerous anthropogenic interference?”](#) *Clim Change* 2005;**68**:269-79
- <sup>195</sup> Jay Zwally, Eric Rignot, Konrad Steffen, and Roger Braithwaite.
- <sup>196</sup> Braithwaite, RJ. Cover photo for Science 2002;297(5579). Reprinted in Hansen, J. [Defusing the global warming time bomb](#). *Sci Amer* 2004;**290**(3):68-77
- <sup>197</sup> Rignot E, Jacobs S, Mouginot J *et al.* [Ice shelf melting around Antarctica](#). *Science* 2013;**341**:266-70
- <sup>198</sup> Rye CD, Naveira Garabato AC, Holland PR *et al.* [Rapid sea-level rise along the Antarctic margins in response to increased glacial discharge](#). *Nature Geosci* 2014;**7**:732-5
- <sup>199</sup> Hefner M, Marland G, Boden T *et al.* [Global, Regional, and National Fossil-Fuel CO<sub>2</sub> Emissions](#), Research Institute for Environment, Energy, and Economics, Appalachian State University, Boone, NC, USA. <https://energy.appstate.edu/cdiac-appstate/data-products> (4 December 2022, date last accessed)
- <sup>200</sup> Boden TA, Marland G, Andres R J, Carbon Dioxide Information Analysis Center, Oak Ridge National Laboratory, Oak Ridge, Tennessee, USA. [Global, Regional, and National Fossil-Fuel CO<sub>2</sub> Emissions](#), [https://doi.org/10.3334/CDIAC/00001\\_V2017](https://doi.org/10.3334/CDIAC/00001_V2017) (4 December 2022, date last accessed)
- <sup>201</sup> Hansen J, Kharecha P, Sato M *et al.* [Assessing “dangerous climate change”: Required reduction of carbon emissions to protect young people, future generations and nature](#). *Plos One* 2013;**8**:e81648
- <sup>202</sup> Keith DW, Holmes G, Angelo D *et al.* [A process for capturing CO<sub>2</sub> from the atmosphere](#). *Joule* 2018;**2**:1573-94
- <sup>203</sup> Hansen J, Kharecha P: [Cost of carbon capture: Can young people bear the burden?](#). *Joule* 2018;**2**:1405-7
- <sup>204</sup> Prins G, Rayner S [Time to ditch Kyoto](#). *Nature* 2007;**449**:973-5

- 
- <sup>205</sup> Hansen J, Sato M, Ruedy R *et al.* [Dangerous human-made interference with climate: A GISS modelE study](#). *Atmos Chem Phys* 2007;**7**:2287-312
- <sup>206</sup> Matthews HD, Gillett NP, Stott PA *et al.* [The proportionality of global warming to cumulative carbon emissions](#). *Nature* 2009;**459**:829-832
- <sup>207</sup> Hansen J, Sato M [Regional Climate Change and National Responsibilities](#). *Environ Res Lett* 2016;**11**:034009
- <sup>208</sup> [Economists' statement on carbon dividends](#) (28 November 2022, date last accessed)
- <sup>209</sup> Hansen J. Columbia University. [Can Young People Save Democracy and the Planet?](#) (28 November 2022, date last accessed)
- <sup>210</sup> Hayes RB [Nuclear energy myths versus facts support it's expanded use – a review](#). *Cleaner Ener. Sys.* 2022;**2**:100009
- <sup>211</sup> Cao J, Cohen A, Hansen J *et al.* [China-U.S. cooperation to advance nuclear power](#). *Science* 2016;**353**:547-8.
- <sup>212</sup> Ying F. [Cooperative competition is possible between China and the U.S.](#), New York Times, 24 November.
- <sup>213</sup> National Academies of Sciences, Engineering, and Medicine. *Reflecting Sunlight: Recommendations for Solar Geoengineering Research and Research Governance*. <https://doi.org/10.17226/25762> (4 December 2022, date last accessed)
- <sup>214</sup> Hansen J. Columbia University (AGU-CAS meeting, Xi'an, China, 18 October 2018). [Aerosol effects on climate and human health](#) (4 December 2022, date last accessed)
- <sup>215</sup> Tollefson J. [Can artificially altered clouds save the Great Barrier Reef?](#). *Nature* 202;**596**:476-8
- <sup>216</sup> Latham J, Rasch P, Chen CC *et al.* [Global temperature stabilization via controlled albedo enhancement of low-level maritime clouds](#). *Phil Trans R Soc A* 2008;**366**:3969-87
- <sup>217</sup> Patrick SM, Council on Foreign Relations. Special Report No. 93, April 2022 [Reflecting sunlight to reduce climate risk: priorities for research and international cooperation](#) (4 December 2022, date last accessed)
- <sup>218</sup> Hansen J, Sato M, Ruedy R *et al.* [Global warming in the twenty-first century: an alternative scenario](#). *Proc Natl Acad Sci* 2000;**97**:9875-80
- <sup>219</sup> Meckler AN, Sexton PF, Piasecki AM *et al.* [Cenozoic evolution of deep ocean temperature from clumped isotope thermometry](#). *Science* 2022;**377**:86-90